

https://dspace.org/

The role of HIV-1 Rev during allosteric inhibition of integrase

Abrahams, Shaakira

2018

https://hdl.handle.net/10539/27323

Abrahams, Shaakira (2018) The role of HIV-1 Rev during allosteric inhibition of integrase, University of the Witwatersrand, Johannesburg, https://hdl.handle.net/10539/27323

Downloaded from a DSpace repository. https://dspace.org/



The role of HIV-1 Rev during allosteric inhibition of integrase

Shaakira Abrahams

A thesis submitted to the Faculty of Health Sciences, University of the Witwatersrand, Johannesburg, in fulfillment of the requirements for the degree of Doctor of Philosophy in Medicine

DECLARATION

I, *Shaakira Abrahams*, declare that this thesis is my own, unaided work. It is being submitted for the Degree of Doctor of Philosophy in Medicine at the University of the Witwatersrand, Johannesburg. It has not been submitted before for any degree or examination at any other University.

_____

……day of ……., 2018

DEDICATION

To my mother, Jubeida Abrahams

Who instilled in me the importance of education

Your support, strength and courage that you have shown me throughout my life is inspiring

I hope I made you proud

ABSTRACT

The HIV-1 integration step is a pertinent process in the HIV-1 replication cycle that integrates the viral genome into the host chromosome. HIV-1 integrase is crucial in facilitating the integration step. Integration is dependent on many co-factors and viral- as well as host accessory proteins. Lens epithelium-derived growth factor (LEDGF/p75) is a host protein that binds to the hydrophobic pocket of integrase formed by a dimer of integrase. The function of LEDGF/p75 is to tether integrase to the host chromosome for successful integration, and consequently provides a drug target for a novel class of HIV-1 inhibitors. The latest studies on the HIV-1 integration process revealed that the HIV-1 regulatory factor, Rev, plays a cardinal role in the regulation of the integration step. Previous studies have demonstrated that Rev and LEDGF/p75 compete for the hydrophobic pocket located on integrase where Rev is able to dissociate the integrase-LEDGF/p75 complex and subsequently form integrase-Rev complexes and LEDGF/p75-Rev complexes. Interestingly, the latest class of HIV-1 inhibitors known as allosteric integrase inhibitors (ALLINIs), compete with LEDGF/p75 and Rev for the same hydrophobic site located on integrase. Further to this, ALLINIs and Rev inhibit the integration step in the early phase of the replication cycle by inducing an integrase oligomerization shift. Consequently, inactive multimers of integrase are formed that are unable to bind to the host chromosome thus preventing integration. Due to the similarities between Rev and ALLINIs in the mechanism of inhibiting integration and the shared binding site on integrase, this study postulated that ALLINIs interfere with the interaction between Rev and integrase. The first objective was to determine whether ALLINIs, Mut 101 and CX05168, had an effect on HIV-1 subtype C Rev and integrase through *in vitro* selection resistant studies followed by genotypic- as well as phenotypic analysis. This study reports the first mutations against Mut 101 within the HIV-1 subtype C *IN* gene. The integrase mutations identified include: H171L for the 05ZAFV3 (FV 3) isolate and Q164L, L172I, and L172I/H171Q for the 05ZAFV26 (FV 26) isolate. *In vitro* phenotypic inhibition studies demonstrated the phenotypic significance of the mutations through a shift in EC_{50} values (0.53 ± 0.01µM for drug naive; 0.21 ± 0.11µM for Q164L mutated isolate; 2.67 ± 0.95µM for L172I mutated isolate) and the infectious ability of the isolates (FV 3 H171L and FV 26 L172I/H171Q). Molecular docking studies further confirmed the effects of the mutations by predicting the interaction between integrase harbouring the mutations and Mut 101. An increase in the binding energies of the predicted models suggests that the presence of mutations are responsible for weaker interactions between integrase harbouring the identified mutations and Mut 101. Data for *in vitro* resistance studies selected by CX05168 could not be generated as CX05168 failed to inhibit viral replication of the FV 3 and FV 26 isolates at its reported EC_{50} for HIV-1 subtype B isolates. This prompted *in vitro* phenotypic inhibition studies to determine the EC_{50} values of

CX05168 against subtype C isolates (FV 3 = 4.3 ± 0.4μM and FV 26 = 40.1 ± 0.8μM) which was significantly higher than the reported EC_{50} of CX05168 against HIV-1 subtype B (2.35 ± 0.28μM). Furthermore, genotypic analysis of the *rev* gene was not achieved as the amplification thereof faced continuous challenges. The second objective was to delineate how Rev affect the oligomerization of integrase in the presence of Mut 101 and CX05168. AlphaScreen dimerization assays, BS^3 crosslinking studies and dynamic light scattering experiments confirmed the multimerization of integrase in the presence of Rev, Mut 101 and CX05168. However, the aberrant multimerization of integrase induced by the ALLINIs was significantly reduced in the presence of Rev. This finding suggests that Rev and the ALLINIs have distinct pathways to induce integrase multimerization and that Rev indeed modulates the multimerization mechanism of integrase induced by ALLINIs. The third objective aimed to investigate the integrase-Rev interaction in the presence of Mut 101 and CX05168. Through an ELISA method, the dissociation constant (K_d) of integrase-Rev was calculated at 461 ± 5.65nM. Order of addition ELISA experiments demonstrated that ALLINIs do not interfere with the integrase-Rev interaction once Rev is already bound to integrase. However, when ALLINIs are added to integrase before the addition of Rev, a significant shift in K_d was observed. The K_d increased to 850 ± 70.71nM in the presence of Mut 101 and 1010 ± 127.27nM in the presence of CX05168. The integrase-Rev interaction was confirmed through isothermal titration calorimetry where the K_d (419nM) obtained significantly correlated with the K_d calculated through ELISA studies. This study is the first to report the thermodynamic properties of the integrase-Rev interaction. The interaction elicited an exothermic reaction with an enthalphy change (ΔH) = -5350J/mol, a temperature entropy change ($T\Delta S$) = 103.9J/mol.K, stoichiometry of 1 and free energy (ΔG) = -5453.9J/mol which indicated that the reaction was enthalpically driven. Thermodynamics of the integrase-Rev interaction could not be established in the presence of Mut 101 and CX05168 suggesting that multimerization of integrase could have intercepted the reaction. Overall, this study reports novel data and provides insight on the hypothesis of the study which establishes that ALLINIs distort the interaction between Rev and integrase and has downstream effects on integrase multimerization. The data presented in this study may lead to a better understanding of ALLINIs in the replication process, especially in HIV-1 subtype C isolates, and may add value to the development process of future ALLINIs.

PUBLICATIONS

S Abrahams, Qasim Fish, Irene Ketseoglou, Raymond Hewer, Maria Papathanasopoulos, Salerwe Mosebi. *In vitro* selection studies revealing mutations that induce a shift in efficacy of HIV-1 allosteric integrase inhibitor, Mut 101, against primary subtype C isolates. *Manuscript*

S Abrahams, Qasim Fish, Raymond Hewer, Maria Papathanasopoulos, Salerwe Mosebi. HIV-1 allosteric integrase inhibitors may influence the regulatory role of HIV-1 Rev in HIV-1 integration. *Manuscript*

ORAL AND POSTER PRESENTATIONS

S. Abrahams, M. Papathanasopoulos, R. Hewer and S. Mosebi. Determining the interaction between HIV-1 Rev and integrase in the presence of an allosteric integrase inhibitor (Poster). The 25th Congress of the South African Society of Biochemistry and Molecular Biology, 10 – 13 July 2016, East London, RSA

S.Abrahams, Q.Fish, M.Papathanasopoulos, R.Hewer and S.Mosebi. ALLINIs modulate the interaction between HIV-1 Rev and integrase (Oral). 8th SA AIDS conference, 12 – 15 June 2017, Durban, RSA

ACKNOWLEDGMENTS

I would like to express my overwhelming gratitude to the individuals who provided their support, advice and expertise throughout this journey

Thank you to my excellent supervisors who provided me with an opportunity to do a PhD:

A depth of gratitude to Dr Salerwe Mosebi. Thank you for supporting me in my quest to reach this audacious goal. This study could not have been completed without your unwavering guidance, motivation and expertise.

Professor Maria Papathanasopoulos, thank you for always making the impossible possible and for contributing your excellence towards this study.

Dr Raymond Hewer, I will always be grateful for the opportunities that you have given me and for introducing me to the world of HIV research. Your constant motivation and belief in me has made this journey easier.

My colleagues and friends at the Centre of metal based drug discovery group at Mintek: Dr Morore Maphahlele, Dr Denise Le Noury and Ms Zikhona Njengele. A special thank you to Dr Qasim Fish, Dr Thompo Rashamuse and Ms Angela Harrison for their technical support in the laboratory. I couldn't have done this without you guys.

Thank you to the staff and students in the HIV pathogenesis research unit (Department of haematology and molecular medicine) at the University of the Witwatersrand, who were always willing to assist me.

Thank you to Dr Irene Ketseoglou in the HIV genotyping lab, NHLS, for sharing her technical abilities, expertise and time with me

I would like to extend my gratitude to the National Research Foundation for awarding me the professional development program fellowship that allowed me to complete my PhD degree. A huge thank you to Mintek for the financial support provided throughout this study

Lastly, thank you to my family – Chad, Nazlie, Imraan, Raabia, Asaad, Zayaan, Rayyaan, Tatum, Maliha and Cayden. Thank you for the support, love and joy you have given me during the tough times.

2D	Two dimensional
3TC	Lamivudine
aa	Amino acid
ABC	Abacavir sulphate
AIDS	Acquired immunodeficiency syndrome
AMP	Ampicillin
APOBEC	Apolipoprotein B mRNA editing enzyme catalytic polypeptide-like
APS	Ammonium persulfate
Arm	Arginine rich motif
ATP	Adenosine triphosphate
ATV	Atazanavir
BIC	Bictegravir
B-Me	β- Mercaptoethanol
bp	Basepairs
BS^3	Bis(sulfosuccinimidyl)suberate
BSA	Bovine serum albumin
CA	Capsid protein
CCD	Catalytic core domain
CCR5	C-C chemokine receptor 5
cDNA	Complimentary DNA
CTD	C-terminal domain
CXR4	C-X-C chemokine receptor 4

DC	Dendritic cells
ddI-EC	Enteric coated didanosine
DOR	Doravirine
dH_2O	Distilled water
DLS	Dynamic light scattering
DTG	Dolutegravir
DTT	Dithiothreitol
E.Coli	*Escherichia Coli*
EC_{50}	Half maximal effective concentration
EDTA	Ethelynediaminetetraacetic acid
EFV	Efavirenz
ELISA	Enzyme linked immunosorbent assay
ER	Endoplasmic reticulum
ETR	Etravine
EVG	Elvitegravir
$FCIC_{50}$	Fold-change IC_{50}
FDA	Food and Drug Administration
FI	Fusion inhibitor
FPV	Fosamprenavir Calcium
FTC	Emtricitabine
GFP	Green fluorescent protein
gp	Glycoprotein
GRAVY	Grand average of hydrophobicity

HAART	Highly Active Antiretroviral Therapy
HIV	Human immunodeficiency virus
HRP	Horseradish peroxidase
IBD	Integrase binding domain
IC_{50}	half maximal inhibitory concentration
IDV	Indinavir
IN	Integrase
INI	Integrase inhibitor
INSTI	Integrase strand transfer inhibitor
IL-2	Interleukin-2
ITC	Isothermal titration calorimeter
IPTG	Isopropyl β-D-1-thiogalactopyranoside
LEDGF	Lens epithelium-derived growth factor/p75
LTR	Long terminal repeat
Luria Bertani	LB
Mg^{2+}	Magnesium
$MgSO_4$	Magnesium Sulphate
Mr	Molecular weight marker
MVC	Maraviroc
NES	Nuclear export signal
NVF	Nelfinavir
NVP	Nevirapine
NIH	National Institute of Health

Ni^{2+}	Nickel
NLS	Nuclear localization signal
NNRTI	Non-nucleoside reverse transcriptase inhibitor
NRTI	Nucleoside reverse transcriptase inhibitor
NTD	N-terminal domain
NtRTI	Nucleotide reverse transcriptase inhibitor
OD	Optical density
P	Passage
PBMC	Peripheral blood mononuclear cells
PBS	Phosphate buffered saline
PCR	Polymerase chain reaction
PFV	Prototype foamy virus
PHA-P	Phytohemagglutinin
PI	Protease inhibitor
PIC	Pre-integration complex
PMSF	Phenylmethanesulfonylfluoride
PR	Protease
PVDF	Polyvinylidene difluoride
RAL	Raltegravir
RC	Replication capacity
Rev	Regulatory factor
RNA	Ribonucleic acid
RRE	Rev Response Element

RPV	Rilpivirine
RT	Reverse transcriptase
RTV	Ritonavir
SANBS	South African national blood service
SDS-PAGE	Sodium Dodecyl Sulfate Polyacrylamide Gel electrophoresis
SP1	Spacer linker 1
SP2	Spacer linker 2
SPR	Surface plasmon resonance
SQV	Saquinavir
ST	Strand transfer
T20	Enfuvirtide
TAF	Tenofovir alafenamide
TAM	Thymidine analogue mutations
TAR	Transactivation response element
Tat	Transcription transactivator
$TCID_{50}$	50% tissue culture infective dose
TDF	Tenofovir disoproxil fumarate
TEMED	Tetramethylethylenediamine
TMB	Tetramethylbenzidine
TNF	Tenofovir
TPV	Tipranavir
vDNA	Viral DNA
vRNA	Viral RNA

vRNP	Viral RNA nucleocapsid
ZDV	Zidovudine
Zn^{2+}	Zinc
α	Alpha
β	Beta
ΔH	Enthalpy change
ΔS	Entropy change
ΔG	Gibbs free energy

Units of measurement

%	Percent
°C	Degree Celsius
µg	Microgram
µm	Micro molar
d.nm	Diameter.nanometre
J	Joules
K_d	Dissociation constant
Kda	Kilodalton
K	Kelvin
L	Litre
M	Molar
Mg	Milligram
ml	Millilitre
mM	Millimolar

nm	Nanometre
nM	Nanomolar
Rpm	Revolutions per minute
X g	Gravitational force

Amino acid residues are abbreviated to its IUPAC single- and three letter code

LIST OF FIGURES

CHAPTER 1: Introduction

Figure 1.1: The structure and constituents of the HIV virus particle (virion) 1

Figure 1.2: The genomic organization of HIV-1 and the essential proteins expressed by the viral genome 4

Figure 1.3: Schematic representation of each step of the HIV-1 lifecycle 6

Figure 1.4: The schematic representation of the HIV-1 integrase (IN) structural domains: .. 15

Figure 1.5: A depiction of the essential HIV-1 integration step catalyzed by integrase (IN).. 16

Figure 1.6: Crystal structure of an IN tetramer interacting with vDNA where the reactive DNA is depicted in magenta and the non-transferable DNA is depicted in orange 18

Figure 1.7: The two-dimensional structure of raltegravir (RAL) interacting with the Magnesium (Mg^{2+}) groups located in the active site of HIV-1 integrase (IN). 19

Figure 1.8: The structural basis of the integrase (IN)-LEDGF interaction extracted from Cherapanov et al, 2005 (Protein databank accession code: 2B4J) 22

Figure 1.9: Molecular docking demonstrating the binding mode of LEDGIN, CX05168, to HIV-1 integrase (IN) 25

Figure 1.10: Representations of the allosteric integrase (IN) inhibitor, Mut 101 A) Chemical structure of the 3-(quinolin-yl)-2 acetic acid derivative, Mut 101 B) Cartoon representation of the two interacting catalytic core domains (CCD, orange and blue) of an IN dimer forming the LEDGF binding pocket. 26

Figure 1.11: The crystal structure demonstrating the interaction between allosteric integrase (IN) inhibitor, BI-D, and A) H171T mutated IN and B) wild type IN..... 28

Figure 1.12: Structural model of the HIV-1 integrase (IN)-Rev complex 30

Figure 1.13: A schematic model of the LEDGF, integrase (IN) and Rev interaction..... 31

CHAPTER 3: Results

Figure 3.1: Representation of A) FV 26 and B) FV 3 viral growth kinetics in drug pressure studies selected by Mut 101 and CX05168 53

Figure 3.2: Sigmoidal curves depicting the EC_{50} values of CX0516 against primary subtype C A) FV 3 and B) FV 26 in PBMCs. 54

Figure 3.3: Dose escalating curves of Mut 101 monitored at every second subculture passage (p) against primary HIV-1 subtype C A) FV 26 and B) FV 3..... 56

Figure 3.4: Sigmoidal curves demonstrating the dose response of Mut 101 against A) FV 26 drug naïve and B) FV 26 p20 in in vitro phenotypic inhibition assays.. 57

Figure 3.5: Amino acid (aa) sequence alignment of HIV-1 integrase (IN) primary subtype C FV 3 and FV 26 isolates selected by Mut 101. 60

Figure 3.6: Molecular docking of integrase (IN) mutants with Mut 101. Representation of the interaction between Mut 101 and A) wild type IN B) IN mutant Q164L C) IN mutant L172I and D) IN H171Q/L172I. 63

Figure 3.7: SDS-PAGE analysis of the expression and purification processes of recombinant HIV-1 His-tagged proteins, A) His-tagged integrase B) His-tagged Rev C) His-tagged-FLAG integrase.. 66

Figure 3.8: Western blot analysis detecting recombinant A) HIV-1 integrase (IN) B) HIV-1 Rev and C) HIV-1 FLAG-tagged IN.. 68

Figure 3.9: Western blot analysis depicting the crosslinking reactions of integrase (IN) multimerization induced by Mut 101, CX05168 and HIV-1 Rev alongside Precision Plus Protein™ marker (Bio-Rad, USA)..... 70

Figure 3.10: Graphs depicting the normalized fluorescence intensity of the interaction between integrase (IN) molecules induced by A) Mut 101 B) CX05168 and C) HIV-1 Rev at a concentration gradient:). 71

Figure 3.11: Comparing the percentage integrase (IN) multimerization induced by 1µM Mut 101, CX05168 and HIV-1 Rev quantified using an AlphaScreen multimerization assay. 72

Figure 3.12: Quantification of integrase (IN) multimerization in the presence of both HIV-1 Rev and Mut 101 or CX05168 using an AlphaScreen multimerization assay..... 73

Figure 3.13: Evaluating the effect of A) Mut 101 and B) CX05168 on integrase (IN) multimerization in the absence and presence of HIV-1 Rev through dynamic light scattering analysis (DLS)..... 74

Figure 3.14: The dissociation constant (K_d) plots representing the order of addition interactions between A) integrase (IN) and Rev B: IN-CX05168-Rev C) IN-Rev-CX05168 D) IN-Mut 101-Rev and E) IN-Rev-Mut 101. 76

Figure 3.15: Representation of the dissociation constant (K_d) of integrase (IN) and HIV-1 Rev in the absence and presence of Mut 101 and CX05168.. 77

Figure 3.16: A) Bar graphs representing the interaction between IN and Rev in the absence and presence of Mut 101 and CX05168 at a concentration gradient. 79

Figure 3.17: Evaluating the effect of Mut 101 and CX05168 on the integrase (IN)-Rev interaction in a dose dependant manner 80

Figure 3.18: The isothermal titration calorimeter (ITC) thermograms of the HIV-1 integrase (IN) and Rev interaction. 82

Figure 3.19: The raw heat graphs of the interaction between HIV-1 integrase (IN) and Rev in the presence of A) Mut 101 and B) CX05168.. 83

Figure 3.20: The fluorescence intensity peaks obtained when analysing HIV-1 integrase (IN) samples containing injected Rev in the absence and presence of ALLINIs. 84

LIST OF TABLES

Table 1.1: The HIV-1 genome and its corresponding proteins encoded 2

Table 1.2: Summary of the major HIV-1 reverse transcriptase resistant mutation pathways 12

Table 1.3: Summary of the major HIV-1 protease inhibitor resistant pathways 13

Table 1.4: Summary of resistant mutations against integrase inhibitors 20

Table 2.1: RT-PCR thermocycling conditions used for cDNA synthesis 36

Table 2.2: Cycling conditions for amplification using the Platinum Taq DNA Polymerase High Fidelity 37

Table 2.3: List of primers for sequencing of the pol gene integrase region 39

Table 2.4: List of primary- and secondary antibodies used in Western blot analysis to confirm the presence of recombinant proteins. 46

Table 3.1: polymorphism mutations present in drug naïve FV 3 and FV 26 isolates when compared to HIV-1 subtype B- and C consensus sequences 58

Table 3.2: Displaying the correlation between the genotype and phenotype of Mut 101 selected FV 3 and FV 26 isolates 61

Table 3.3: The molecular docking binding energies for each mutant identified in FV 26 isolates selected by Mut 101 68

TABLE OF CONTENTS

DECLARATION……I

DEDICATION……II

ABSTRACT……..……..…III

CONFERENCE PROCEEDINGS……..……V

ACKNOWLEDGEMENTS……VI

ABBREVIATIONS……..……...VII

LIST OF FIGURES……XIII

LIST OF TABLES……..……...XVI

CHAPTER 1: Introduction

1.1 OVERVIEW OF THE HUMAN IMMUNODEFICIENCY VIRUS 1

1.1.1 The biological structure of HIV 1

1.1.2 HIV-1 genomic organisation and viral proteins 2

1.1.3 The HIV-1 replication cycle 4

1.2 ANTIVIRAL THERAPY FOR HIV-1 6

1.2.1 Brief overview of the current antiretrovirals therapy against HIV-1 7

1.2.1.1 Reverse transcriptase inhibitors 7

1.2.1.2 Protease inhibitors 8

1.2.1.3 Entry inhibitors 8

1.2.1.4 Fusion inhibitors 9

1.2.1.5 Integrase inhibitors 9

1.2.2 Resistant mutations against HIV-1 antiretroviral drugs 9

1.2.2.1 Brief description of the major HIV-1 resistance mutations within antiretroviral drug classes 10

1.3 THE ROLE OF INTEGRASE IN THE HIV-1 REPLICATION CYCLE 14

1.3.1 HIV-1 integrase enzyme structure and domain organization 14

1.3.2 The mechanism of DNA integration in the HIV-1 replication cycle 15

1.3.3 The HIV-1 integrase intasome 17

..... 18

1.3.4 HIV-1 integrase inhibitors 18

1.3.4.1 Antiretroviral drug resistance mutations in the integrase enzyme 19

1.3.5 The interaction of LEDGF and integrase during HIV-1 integration 21

1.3.6 Allosteric integrase inhibitors targeting the LEDGF-integrase interaction 22

1.3.6.1 Characterization of LEDGIN, CX05168 23

1.3.6.2 Characterization of Mut 101 25

1.3.6.3 Resistance mutations in the integrase enzyme against ALLINIs 27

1.3.7 The regulatory role of Rev in HIV-1 integration 29

1.3.7.1 Structure and the function of Rev 29

1.3.7.2 The interaction between HIV-1 integrase and Rev 29

_Toc501666865

1.4 SIMILARITIES BETWEEN THE ROLE OF ALLINIs AND REV IN THE HIV-1 INTEGRATION STEP 32

1.5 HYPOTHESIS 32

1.6 OBJECTIVES 32

CHAPTER 2: Methods

2.1 IN VITRO SELECTION STUDIES 33

2.1.1 Isolation of peripheral blood mononuclear cells 33

2.1.2 50% Tissue culture infective dose ($TCID_{50}$) determination and HIV-1 subtype C expansion 33

2.1.3 Classical in vitro selection experiments 34

2.1.4 Genotyping 35

2.1.4.1 RNA extraction using the EasyMAG NucliSens automated system 35

2.1.4.2 Complimentary DNA synthesis from extracted viral RNA 36

2.1.4.3 Amplification of the HIV-1 rev gene 38

2.1.4.4 Purification of the PCR product 38

2.1.5 Genotypic analysis of the pol gene extracted from Mut 101 selected FV isolates ... 39

2.1.6 Molecular docking of Mut 101 with mutant integrase proteins 39

2.1.7 In vitro phenotypic inhibition studies of viral isolates collected in in vitro selection studies 40

2.2 HIV-1 RECOMBINANT PROTEIN EXPRESSION AND PURIFICATION 41

2.2.1 HIV-1 His-tagged integrase and HIV-1 His-tagged-FLAG integrase expression and pol gene induction 41

2.2.2 Eschericia (E) coli BL 21 DE3 cell lysis 42

2.2.3 Purification of HIV-1 His-tagged proteins using Nickel affinity chromatography 42

2.2.4 Buffer exchange of purified protein using a PD-10 Sephadex column 43

2.2.5 HIV-1 His-tagged Rev plasmid construction and transformation 43

2.2.6 Expression and purification of His-tagged Rev 44

2.2.7 Purification of HIV-1 His-tagged Rev using Nickel affinity chromatography 44

2.2.8 Confirmation of protein expression and purification 45

2.2.9 Determining the Tryptophan fluorescence spectra of purified HIV-1 integrase and Rev 50

2.3 MULTIMERZATION STUDIES 46

2.3.1 Determining multimerization of HIV-1 integrase using an AlphaScreen multimerization assay 46

2.3.2 Multimerization of HIV-1 integrase through crosslinking experiments 47

2.3.3 Analysing integrase multimerization using Dynamic Light Scattering 48

2.4 ELISA STUDIES 48

2.5 CHARACTERIZING THE INTERACTION BETWEEN HIV-1 INTEGRASE AND REV THROUGH ISOTHERMAL TITRATION CALORIMETRY. 50

2.6 DATA ANALYSIS 50

CHAPTER 3: Results

3.1 IN VITRO SELECTION STUDIES TO SELECT HIV-1 DRUG RESISTANCE MUTATIONS 52

3.1.1 Classical in vitro selection of CX05168 and Mut 101 selected viruses 52

3.1.2 In vitro phenotypic inhibition assays of CX05168 and Mut 101 54

3.1.2.1 EC_{50} values of CX05168 against FV 26 and FV 3 54

3.1.2.2 Determining the phenotypic resistance of FV 26 and FV 3 viruses selected by Mut 101 55

3.1.3 Genotypic analysis of the Mut 101 resistant selected FV viral isolates 57

3.1.4 In Silico effects of the identified mutants on the ALLINI – integrase interaction 61

3.2 PURIFICATION OF RECOMBINANT HIV-1 VIRAL PROTEINS 65

3.3 EFFECT OF MUT 101, CX05168 AND HIV-1 REV ON IN MULTIMERIZATION 68

3.3.1 Crosslinking studies evaluate the multimerization of IN induced by ALLINIs and HIV-1 Rev 68

3.3.2 Determining integrase multimerization through an AlphaScreen multimerization assay 70

3.3.3 Evaluating the size of integrase molecules using dynamic light scattering experiments 73

3.4 DETERMINING THE INTERACTION BETWEEN HIV-1 REV AND INTEGRASE 75

3.4.1 Calculating the dissociation constant (K_d) of the integrase–Rev interaction in the presence of ALLINIs using an ELISA based method 75

3.4.2 Comparing the percentage reduction of the integrase and Rev interaction between two order of addition reactions 77

3.4.3 Characterization of the HIV-1 integrase interaction with Rev through isothermal titration calorimetry 81

3.4.3.1 The thermodynamic properties of the HIV-1 integrase-Rev interaction 81

3.4.3.2 The effect of Mut 101 and CX05168 on the HIV-1 integrase and Rev interaction 82

CHAPTER 4: Discussion

4.1 CX05168 IS LESS ACTIVE AGAINST HIV-1 SUBTYPE C PRIMARY FV ISOLATE 86

4.2 THE CORRELATION BETWEEN THE GENOTYPIC- AND PHENOTYPIC ANALYSIS OF MUT 101 SELECTED ISOLATES 88

4.2.1 Non-infectious virions produced in the presence of Mut 101 88

4.2.2 Substitution at integrase H171 plays a role during the production of defective HIV-1 virions 89

4.2.3 Integrase double mutation H171Q/L172I in HIV-1 isolate FV 26 could attribute to the decrease in viral replication 90

4.2.4 Baseline polymorphisms detected in HIV-1 FV drug naïve isolates do not affect the efficacy of Mut 101 90

4.2.5 Integrase Q164L mutation decreases the EC_{50} of Mut 101 against in vitro selected isolates 91

4.2.6 L172I located on integrase is attributed to an increase in EC_{50} of Mut 101 against in vitro selected isolates 92

4.3 HIV-1 REV REVERSES THE MULTIMERIZATION OF INTEGRASE INDUCED BY ALLINIS 92

4.4 The order of addition of ALLINIs impact the integrase-Rev interaction 93

4.4.1 ALLINIs do not interfere with the integrase-Rev interaction once the protein complex has formed 93

4.4.2 ALLINIs are unable to dissociate the IN-Rev complex 94

4.4.3 The immobilization of integrase and Rev to a solid-phase influence the interaction between integrase and Rev 95

4.4.4 Isothermal titration calorimetry studies confirm the interaction between HIV-1 integrase and Rev 97

4.4.5 ALLINIs affect the interaction between HIV-IN and Rev 98

CHAPTER 5: Future work and Conclusion

5.1 FUTURE WORK 99

5.2 CONCLUSION 100

REFERENCES……99

APPENDIX: Ethics waiver……113

CHAPTER 1

Introduction

1.1 OVERVIEW OF THE HUMAN IMMUNODEFICIENCY VIRUS

1.1.1 The biological structure of HIV

Human immunodeficiency virus (HIV) is the causative agent of the acquired immunodeficiency syndrome, (AIDS).[1–3] HIV is a member of the Lentivirus genus belonging to the *Retroviridae* family, with HIV type 1 (HIV-1) responsible for the global pandemic.[4,5] The 100-120 nanometre (nm) spherical shaped HIV particle (virion) is comprised of the viral envelope, the matrix and viral capsid (Figure 1.1). The envelope is the phospholipid membrane formed upon budding of the virion from the host cell during HIV replication.[3,6] The envelope is surrounded by approximately 72 spike-like protrusions comprised of a trimeric glycoprotein (gp) 41 non-covalently attached to a trimeric gp120.[4,7,8] The viral matrix consists of protein 17 (p17) that links the viral envelope to the viral core thus maintaining the integrity of the virion.[9,10] The viral core consists of p24 and encapsulates two non-covalently linked single stranded ribonucleic acid (RNA), and viral enzymes such as integrase (IN), protease (PR) and reverse transcriptase (RT).[4,11]

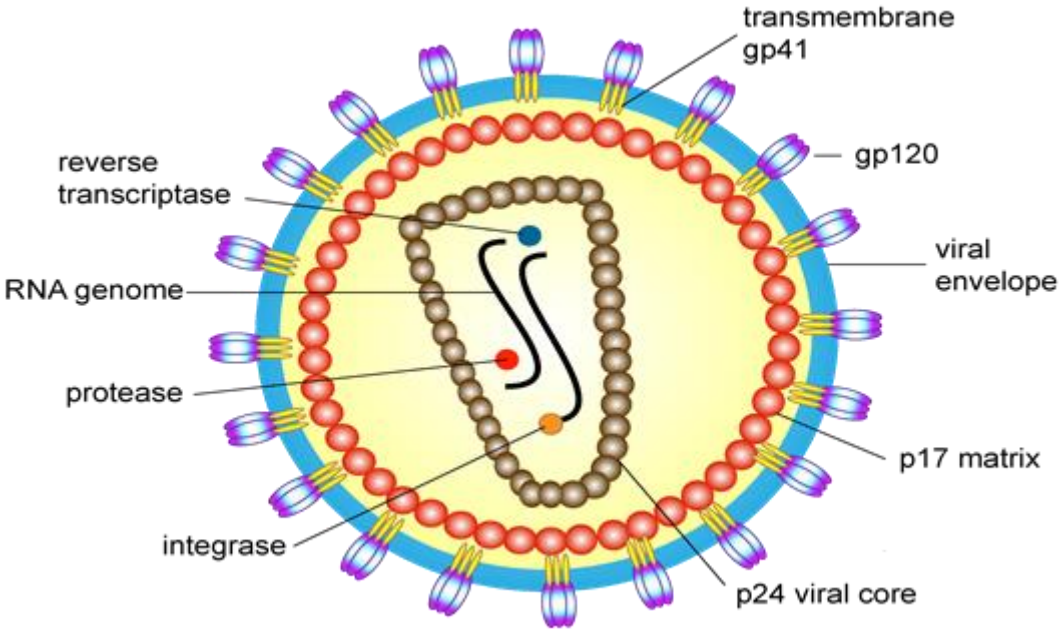


Figure 1.1: The structure and constituents of the HIV virus particle (virion). *The illustration depicts the HIV viral RNA genome and essential enzymes contained within an HIV viral particle. The viral envelope surrounds the p17 matrix and the inner p24 viral core. Spike like protrusions comprising a trimeric gp41, are located within the viral envelope and attached to a trimeric gp120. The p24 viral core possess the viral RNA genome and enzymes such as reverse transcriptase, protease and integrase. Image adapted from Abrahams, 2014.*[12]

1.1.2 HIV-1 genomic organisation and viral proteins

The HIV-1 genome is encoded on a single RNA plus strand that encodes nine genes. Table 1.1 lists the genes that comprise HIV-1 as well as the viral proteins encoded by these genes.

Table 1.1: The HIV-1 genome and its corresponding proteins encoded

Class of gene	**Gene**	**Precursor polyprotein encoded**	**Functional protein encoded**
Structurally related proteins	*gag*	Gag polyprotein	Matrix p17, capsid p24 and the nucleocapsid (p9), p6, SP1, SP2
	pol	Pol polyprotein	RT, RNase H, IN, PR
	env	gp160	gp120, gp41
Regulatory proteins	*tat*	Tat	
	rev	Regulatory factor (Rev)	
Accessory proteins	*nef*	Nef	
	vpr	Vpr	
	vif	Vif	
	Vpu	Vpu	

Figure 1.2 Illustrates the HIV-1 genome and the proteins it expresses. HIV-1 long terminal repeats (LTR) regulate the expression of HIV genes. The HIV-1 LRT comprise the U3, R and U5 regions which contains a plethora of host- and viral transcription factors. These transcription factors interact and regulate the LTR activity specific to cell types, cycle regulation, cell- differentiation and activation. The *gag, env and pol* genes encode structurally

related proteins. The *gag* gene encodes a 55 kilo Dalton (kDa) precursor protein, p55. Viral PR cleaves p55 into smaller structural proteins such as p17 (matrix), p24 (viral capsid), p6 and p9 (nucleocapsid) which are the building blocks of the viral core.[13] The *env* gene encodes a precursor glycoprotein, gp160, which is processed by cellular PR into the transmembrane gp41 and the surface gp120. Together, gp41 and gp120 make up the outer membrane envelope proteins.[14] The *pol* gene encodes a Gag-Pol precursor polyprotein that is ultimately cleaved by the virally encoded PR to detach the Pol polypeptide from the Gag-Pol fusion protein. The Pol polypeptide is subsequently cleaved further into essential enzymes RT, RNase H, IN and PR. RT is responsible for cDNA synthesis, IN facilitates viral DNA (vDNA) integration into host DNA and PR mediates the cleavage of Gag-Pol polyproteins during maturation of virions, respectively.[15–17] HIV-1 has two viral regulatory genes known as *tat* and *rev.* The regulatory genes *tat* and *rev* encode the transcription transactivator (Tat) and regulatory factor (Rev), respectively, and are essential in HIV-1 gene expression. Tat is an RNA binding protein that binds to the transactivation response element (TAR) at the 5' terminal end of HIV RNA thereby activating transcription.[18] Rev is a sequence based RNA binding protein that regulates HIV gene expression by binding to a complex RNA secondary structure, termed the Rev Response Element (RRE).The interaction between Rev and the RRE facilitates the migration of unspliced or incomplete spliced viral RNA (vRNA) from the nucleus to the cytoplasm which can also lead to the suppression of HIV regulatory factors.[19–21] In addition, Rev plays a vital role in regulating DNA integration during HIV-1 replication (discussed further in section 1.3.7.3).[22] Accessory genes *nef, vif, vpr* and *vpu* encode the accessory proteins that are not essential for viral replication *in vitro* however they are vital for viral replication *in vivo*. The negative replication factor (Nef) is the most immunogenic accessory protein and ensures HIV infection by perturbing T-cell activation, it also increases virulence by down regulating CD4+ lymphocytes through post-translational modification as well as increasing virulence of HIV virions.[23–25] Viral infectivity factor (Vif) activates infectivity of the HIV virion and prevents the antiviral host protein apolipoprotein B mRNA editing enzyme catalytic polypeptide-like (APOBEC) from entering the HIV virion by targeting it for cellular degradation.[26] HIV replication does not rely on Vif in most cells suggesting that these cells host a protein similar in function to Vif.[15] However, HIV virions produced in the absence of Vif are defective. Viral protein R (Vpr) play several roles in HIV-1 replication. Vpr forms part of the HIV-1 pre-integration complex (PIC) where it mediates nuclear localization of the HIV PIC resulting in HIV infection in non-dividing cells such as macrophages.[27] In addition, Vpr regulates apoptosis in infected cells and transactivates HIV-1 long terminal repeats (LTR) as well as host cell genes. Vpu is a phosphoprotein integrated in the cell membrane and plays a

role in CD4+ down regulation through ubiquitination. Vpu also overcomes the host restriction factor tetherin and assists in the release of HIV progeny virions from the infected cell surface.[28,29]

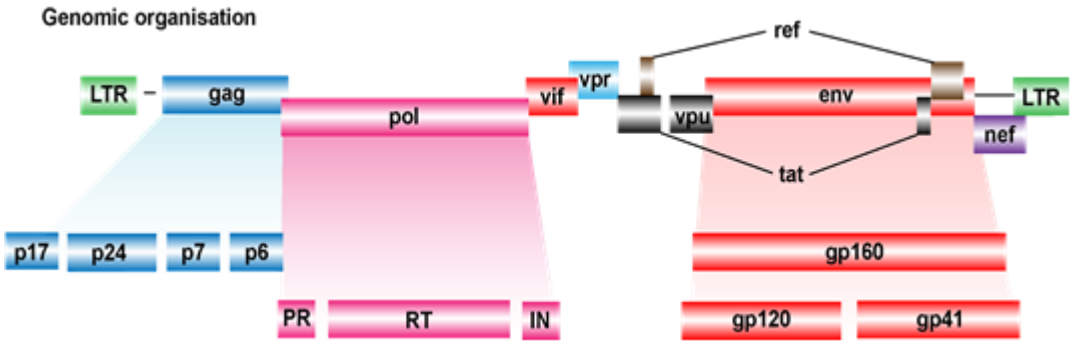


Figure 1.2: The genomic organization of HIV-1 and the essential proteins expressed by the viral genome. *Image obtained from Abrahams, 2014.*[12]

1.1.3 The HIV-1 replication cycle

HIV mainly targets T-helper lymphocytes, macrophages and dendritic cells (DC) that express cell surface receptors such as CD4+, and co-receptors C-C chemokine receptor 5 (CCR5) or the C-X-C chemokine receptor 4 (CXCR4).[30] CCR5 is an essential co-receptor for HIV-1 transmission and replication of the virus. HIV isolates using CXCR4 is often a result of viral evolution in infected individuals where the isolates have altered pathogenic properties and tropism.[3,31] Other co-receptors such as mannose binding protein located on macrophages and DC-SIGN co-receptors located on dendritic cells have the ability to interact with gp120 but is not able to promote fusion and virus entry.[30] Since CD4+ T-lymphocytes are the major target for HIV infection, Figure 1. briefly describes the HIV-1 life cycle in CD4+ lymphocytes. A single HIV-1 replication cycle is completed in approximately 24 hours after infection and consists of several steps including fusion, viral entry, uncoating and reverse transcription, integration, viral protein expression, virion budding and maturation. These replication steps constitute the early phase replication cycle and the late phase replication cycle. The early phase replication cycle is initiated when the trimeric gp (gp120 and gp41) is activated and consequently induces conformational changes that lead to the fusion of the viral and host membrane. Upon binding of gp120 to the CD4 receptor, a bridged sheet is formed between the inner and outer domain of gp120. The formation of this sheet subsequently exposes a site where gp120 interacts with CD4, CCR5 or CXCR4 on the surface of the host cell.[32,33] After binding of gp120 to the CD4 receptors and co-receptors, a fusion peptide, located on the hydrophobic terminus of gp41 is inserted into the host cell membrane subsequently inducing a conformational change.[34,35] This

conformational change rearranges the trimerized amino- and carboxyl terminal heptad repeat sequences within gp41, assists in the formation of a six-helix hairpin structure and ultimately facilitates the fusion of the viral- and host cell membranes. Fusion subsequently propels the viral capsid into the cytoplasm of the host cell.[36–38] Following fusion of the viral- and host cell membrane, dissolution/uncoating of the p24 capsid ensues subsequently releasing the viral genetic material, viral replication enzymes and associated proteins into the cytoplasm of the host cell.[39] The viral genetic material, two single RNA positive strands, are reverse transcribed to viral complimentary DNA (cDNA) by error-prone RT. Following the completion of the reverse transcription step, the resultant viral cDNA is then further used to assemble the PIC required for the integration step. The PIC comprise a tetramer of IN that assembles with Vpr, p6, p7 matrix, and host proteins such as BAF, Gemin2, HAT p300, HMGA1, HSP 60, Human EED protein, Importin 7, IN interactor 1, lens epithelium-derived growth factor/p75 (LEDGF) and UNG2.[40–49] The PIC translocates into the nucleus of the host cell where IN catalyses the irreversible integration of the pro-vDNA into the host DNA forming the provirus.[50] IN facilitates integration through a two-step transesterification reaction consisting of 3' endonucleolytic processing of the vDNA in the cytoplasm and the strand transfer (ST) step in the nucleus (further discussed in section 1.3.2). During the late phase of the HIV-1 replication cycle, Tat binds to the HIV-1 RNA element (TAR) consequently initiating transcription.[51] The integrated DNA is transcribed and the resulting mRNA is exported to the cytoplasm. The exported mRNA is translated to polypeptide chains and hence commencing the viral assembly step.[25] The polypeptide chains are cleaved by viral or host proteases to synthesize viral proteins in the endoplasmic reticulum (ER) which are ultimately transported to the cell surface. HIV-1 PR is responsible for the cleavage of Gag polyprotein at nine cleavage sites that results in the formation of the viral capsid, matrix and other structural proteins. Host protease, Furin, is responsible for the cleavage of gp160 into viral envelope proteins.[52] The viral proteins are embedded in the cell membrane and cluster together with essential host proteins thereby forming an immature virion. The host proteins present in the immature virion include Actin, Cyclophilin A, Ezrin, and Moesin.[53,54] It is estimated that the immature virion consists of approximately 2400 Gag monomers and 120 Gag-Pro-Pol molecules.[54] The immature virion subsequently buds off from the cell surface and together with a portion of the host cell membrane forms the viral envelope. Virion maturation is achieved when the Gag polyprotein chains of the immature virion are fully cleaved by PR. The capsid protein (CA) is a resultant protein from the proteolytic cleavage of Gag polyproteins. It has been shown that the CA plays an essential role in the assembly and maturation of virions. The capsid forms a conical core

which subsequently encases the cleaved viral enzymes as well as genomic DNA.[55] The newly produced infectious virion is now ready to infect new host cells.[56]

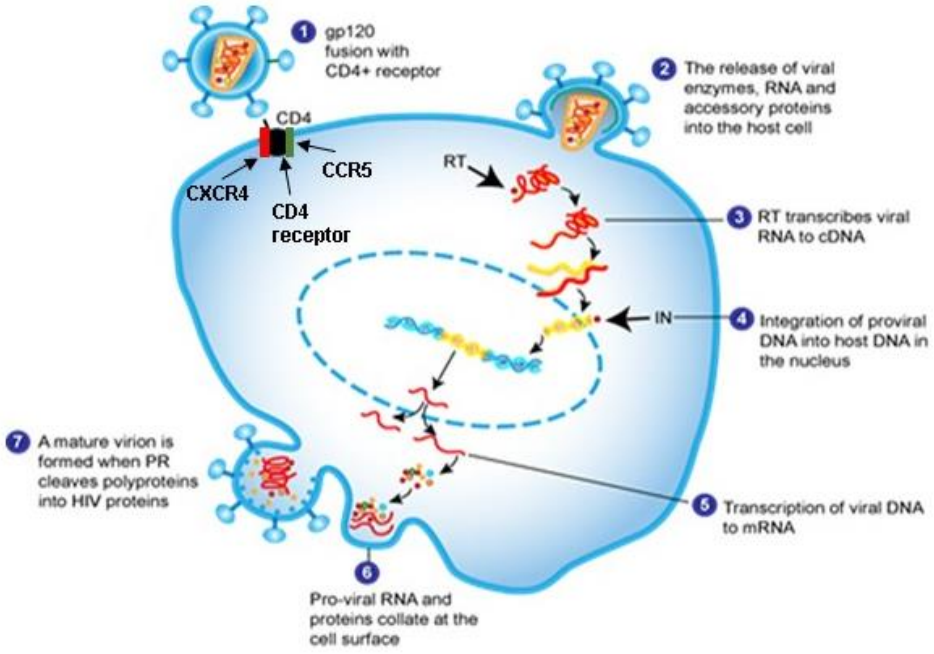


Figure 1.3: Schematic representation of each step of the HIV-1 lifecycle: 1*: Binding and fusion of the viral gp120 to CD4 receptor and CXCR4 and CCR5 co-receptors* ***2****: Uncoating of the viral capsid resulting in the release of enzymes, RNA and accessory proteins into the host cell.* ***3****: Reverse transcriptase (RT) synthesize complimentary DNA (cDNA) through reverse transcription.* ***4****: Integrase (IN) binds to the cDNA which is subsequently translocated into the nucleus where integration of pro-viral DNA into the host DNA occurs.* ***5****: Transcription of pro-viral DNA to mRNA and subsequent expression of viral proteins.* ***6****: Viral proteins as well as host proteins collate at the cell surface forming the resultant immature virions.* ***7****: Protease (PR) cleaves gag polyproteins into individual viral proteins producing mature infectious virions. Illustration extracted from Abrahams, 2014.*[12]

1.2 ANTIVIRAL THERAPY FOR HIV-1

Each step in the HIV-1 replication cycle represents a potential antiviral drug target. There are currently five drug classes approved by the U.S. Food and Drug Administration (FDA) namely; RT inhibitors, IN inhibitors (INI), PR inhibitors (PIs), Fusion inhibitors (FI), and chemokine receptor antagonists (CCR5 antagonists).[57,58] Highly Active Antiretroviral Therapy (HAART) is

a combination of antiretroviral drugs that comprise at least two different drug classes, predominantly RT inhibitors and PIs, that delay disease progression from HIV to AIDS. HAART effectively suppresses viral transmission rates and reduce viral loads of HIV infected patients below the detection limit (< 50 RNA copies/ml).[59] In addition to the success in reduction of mortality and morbidity of HIV infected individuals, HAART plays a vital role in increasing the genetic barrier to the development of antiretroviral drug resistance.[59]

1.2.1 Brief overview of the current antiretrovirals therapy against HIV-1

1.2.1.1 Reverse transcriptase inhibitors

Antiretrovirals targeting RT encompass nucleoside RT inhibitors (NRTI), nucleotide RT inhibitors (NtRTI) and non-nucleoside RT inhibitors (NNRTI). NRTIs were the first class of HIV antivirals approved, however their efficacy is lower than that of NNRTIs, PIs and INIs. Although less potent, NRTIs still play a pivotal role in both HIV-1 and HIV-2 antiretroviral regimens.[60,61] Zidovudine (ZDV) was the first NRTI approved by the FDA in 1985 and functions as faulty DNA blocks that are incorporated into the newly synthesized vDNA resulting in chain termination.[61,62] NRTIs and NtRTIs share a similar mechanism of action in that they are analogues of the naturally occurring DNA nucleosides required for DNA synthesis.[63] At present, seven NRTIs are commercially available that includes lamivudine (3TC), ZDV, abacavir sulphate (ABC), tenofovir disoproxil fumarate (TDF), emtricitabine (FTC) and didanosine (ddI).[64] These NRTIs and NtRTIs analogues differ from the naturally occurring deoxynucleotides as the analogues do not possess a 3'-hydroxyl on the deoxyribose moiety required for the formation of a 5'-phosphodiester bond that facilitates DNA chain extension.[63,65,66] NRTIs and NtRTIs compete and replace the naturally occurring deoxynucleotides thereby impeding vDNA synthesis. Before NRTIs are incorporated into vDNA, they are activated when cellular kinase enzymes phosphorylate the deoxyribose moiety on the NRTIs.[50] TDF and Tenofovir alafenamide (TAF), current NtRTIs, evade the conversion step of nucleosides to nucleotides.[64] TDF has been associated with toxicity in renal function and bone density thus, based on favourable properties, TAF was selected to ultimately replace TDF. TAF, a prodrug of Tenofovir (TNF), demonstrated antiviral efficacy similar to TDF and is 10 times more active than TDF.[67] The first NNRTI, Nevirapine (NVP), was approved and introduced to the HIV antiretroviral therapy regimen in 1996. All first generation NNRTIs, NVP, and efavirenz (EFV) exhibit the same mechanism of action against the activity of RT. NNRTIs inactivate the RT enzyme by binding to a hydrophobic pocket on the p66 subunit of RT

consequently inducing a conformational change that hinders the activity of the enzyme.[59,66] Due to adverse events associated with EFV such as neurological and psychiatric, rash and teratogenacity, secondary generation NNRTIs namely etravirine (ETR) and Rilpivirine (RPV) have been developed.[66,68,69] The flexibility of ETR molecules permits the molecule to rotate effectively thus allowing multiple binding conformations.[60,64] Doravirine (DOR) is the latest NNRTI that is currently in development has demonstrated a high genetic barrier against the other NNRTIs resistant strains.[70] Due to several side effects, EFV has been downgraded as a first line therapy to an alternative therapy. DOR has shown to be an effective alternative to EFV due to its robust activity and good tolerability.

1.2.1.2 Protease inhibitors

The discovery of PIs was pivotal as it prompted the advent of combinational therapy, HAART. PIs are substrate analogues of the HIV aspartyl protease enzyme and therefore function as competitor inhibitors that compete for the active site of protease. Binding of PIs to the PR active site consequently block the activity of the enzyme and thus prevent the cleavage of viral proteins. These uncleaved viral proteins are then considered defective and therefore the virion cannot mature into an infectious particle.[71] FDA approved PIs include nelfinavir (NFV), saquinavir (SQV), darunavir (DRV), ritonavir (RTV), fosamprenavir calcium (FPV), indinavir (IDV), atazanavir (ATV) and tipranavir (TPV).[64] The pharmacodynamics of PIs are improved by low doses of ritonavir (RTV) into the PI regimen. RTV is an attractive pharmacoenhancer as it inhibits two essential stages in metabolism. Firstly, RTV inhibits both CYP3A4 and p-glycoprotein present in the enterocytes located in the intestine. CYP3A4 is a vital cytochrome P450 isoenzyme that plays a key role in drug metabolism while P-glycoprotein, an efflux transporter, transports drugs from the cell cytoplasm to the intestinal lumen for subsequent excretion of the drug. By inhibiting CYP3A4 and P-glycoprotein, the PI concentration increase and therefor a lower dosage of PIs are required. Secondly, RTV functions in the liver where it inhibits CYP3A4 thus maintaining the plasma half-life of the drugs. In addition, RTV may also inhibit P-glycoprotein in CD4+ cells which leads to a decrease in drug transport out of the cell consequently increasing the intracellular half-life of the drug.[72]

1.2.1.3 Entry inhibitors

Viral entry inhibitors are designed to target two distinct viral entry steps: 1 – gp120 attachment to the CD4 T-cell receptor and 2 – gp120 binding to CCR5- and CXCR4 co-receptors. Entry inhibitors such as maraviroc (MVC), a co-receptor antagonist, inhibit viral entry into the host

cell. A cavity is formed by the 2, 3, 6 and 7 α helices comprising CCR5 to which MVC binds to.[73] Consequently, CCR5 on the host cell is blocked from binding to gp120 and subsequently preventing viral fusion required for viral entry. MVC is only active against HIV-1 CCR5-utilizing viruses and inactive against CXCR4-utilizing viruses or dual-tropic viruses.[64,74,75]

1.2.1.4 Fusion inhibitors

FDA approved fusion inhibitor (FI), enfuvirtide (T20), prevents the fusion of the viral envelope and cell membrane by interacting with gp41 extracellularly. T20 inhibits the final step of the fusion process by binding to the HR1 binding region on gp41 and hence perturbing the folding process of HR1 and HR2. The disruption of the folding process averts the necessary conformational change of gp41 and creation of the six helix bundle essential for fusion of the virion and host cell.[76,77]

1.2.1.5 Integrase inhibitors

The latest class of antiretrovirals to obtain FDA approval target IN and inhibit integration of vDNA into the host genome by targeting IN.[78] IN has no known human homologue, and as such, IN is considered to be one of the most favourable antivirals targets in the replication cycle of HIV. Raltegravir (RAL), an IN strand transfer inhibitor (INSTI), was the first INI approved by the FDA in 2007.[79,80] Elvitegravir (EVG) was FDA approved in 2012 followed by dolutegravir (DTG) approved in 2013.[81] INIs are further discussed in section 1.3.4. A single tablet regimen, QUAD pill (Gilead Science, USA), was approved in 2012 that encompasses a fixed dose-combination of EVG, TDF, FTC and cobicistat.[82] EVG, TDF and FTC confers HIV antiretroviral activity by suppressing viral replication whereas cobicistat inhibits the EVG metabolizing enzyme cytochrome P450 3A consequently increasing the concentration of EVG in blood.[64,83,84] Bictegravir (BIC), developed Gilead Science, is the latest INSTI approved by the FDA in February 2018 for combinational therapy with TDF and FTC. BIC demonstrated a markedly improved in vitro resistance profile against RAL and EVG and was comparable to DTG.[85,86]

1.2.2 Resistant mutations against HIV-1 antiretroviral drugs

Despite the successful development of antiretrovirals, obstacles such as the inevitable emergence of antiretroviral drug resistant HIV-1, or transmission of HIV-1 drug resistant

viruses loom. The emergence of viral resistant mutations compromises the efficacy of the antiretroviral agents.[87] Viral resistant mutations in relevant HIV-1 genes may confer cross-resistance to antivirals agents within a drug class and can therefore limit treatment options for treatment experienced patients.[87] To overcome the drug failure concern, novel drug classes or second generation antivirals within a drug class should be developed.[87] Mutations in the viral genome are caused by the error-prone RT as well as drug pressure which results in viral resistance against antivirals. O'Neil[88] described the frequency of mutations caused by RT as 0.85 basepairs (bp)/genome/replication cycle. HIV-1 is known to mutate approximately one nucleotide per replication cycle.[89] In the absence of antiretroviral treatment, it is estimated that 10^{10} virions are produced on a daily basis. The high replication rate is accompanied by a high mutation rate that results in inestimable variants of the virus.[90] These variants are known as quasispecies. As such, individuals who harbour these resistant strains have less antiretroviral treatment options resulting in an increase in mortality.[91] The reason for virological failure in treatment experienced patients is mainly due to poor adherence to antivirals. Low treatment adherence provides the virus with an opportunity to re-emerge and replicate freely at a high rate consequently a high mutation rate.[92] The extent of resistance can be quantified by analysing the properties of the virus such as the degree of resistance through fold-change IC_{50} ($FCIC_{50}$) and the replication capacity (RC) of the antiretroviral drug resistant virus relative to wild type virus.[87] By using drug combinations such as those recommended in HAART, the dosage required for effective treatment decreases, the genetic barrier to developing drug resistance mutations increases, and therefore the emergence of drug resistant HIV-1 viral strains is delayed.[93]

1.2.2.1 Brief description of the major HIV-1 resistance mutations within antiretroviral drug classes

Overall, HIV-1 has developed resistance against all antiretroviral drug classes. Mutations in NRTIs emerge through two mechanisms - either through the impaired incorporation of the nucleotides into the pro-vDNA chain or through the elimination of nucleotides from the pro-vDNA chain producing thymidine analogue mutations (TAMs) through a process called pyrophosphorolysis.[94] Pyrophosphorolysis reverse the action initiated by NRTIs by removing the chain terminating residue thus restoring an extendable primer.[95] Consequently, reverse transcription and DNA synthesis is restored. TAMs responsible for ZDV resistance include M41L, D67N, K70R, L210W, T215Y, T215F, K219Q, and K219E. TAMs are also involved in resistance against ABC (M41L, L210W, and T215F/Y) and TNF (M41L, L210W, T215F/Y, and

K70R). Clinically significant resistance (i.e. an increase in viral load) occurs following the emergence of several mutations (Table 1.2). Non-TAM mutations include M184V,Q151M, and K65R against ABC, 3TC, FTC and ZDV, K70E against ABC and TNF, L74V/I against ABC and Y115F against ABC and TNF. These mutations displace NRTIs on the DNA chain thus inducing a conformational change in the RT domain that attracts adenosine phosphate (ATP) at the terminal end of the DNA chain. The introduction of ATP to the DNA chain disrupts the NRTIs and pro-vDNA consequently elongating the DNA strand.[94] M184V also confers a 1.5 to 3 fold decrease in viral susceptibility against ddI and ABC consequently leading to an increase in viral activity, however, some inhibitory activity is retained.[96,97] Clinical studies have demonstrated that HIV RNA plasma levels are reduced to 0.5 and 0.7 Log_{10} in the presence of ddI and ABC, respectively, in patients harbouring only the M184V mutation.[98] These results suggest that the phenotypic significance of M184V is dependent on the presence of NRTI mutations. Mutations selected by NNRTIs alter the binding efficiency of the NNRTIs to the RT enzyme.[99] Due to first generation NNRTIs low genetic barrier to developing resistance, a single mutation in the RT binding domain can significantly decrease the efficacy of NNRTIs. NVP requires only one primary mutation to confer high-level resistance against the drug. The mutations include V106A/M (two fold resistance), Y188L (50 fold resistance), K103N/S (20 fold resistance), G190A/S/E (six fold resistance) and Y181C/I/V (two fold resistance).[100,100–102] L100I, M230L and K101E/P are secondary mutations and require other primary NNRTI mutations for resistance to occur. ETR has the highest genetic barrier amongst all the NNRTIs and therefore, in some cases, requires an additional mutation for clinical failure to occur.[103] E138K selected by RPV exhibits cross-resistance to ETR, EFV and NVP.[104]

Table 1.2: Summary of the major HIV-1 reverse transcriptase (RT) resistance mutation pathways

RT inhibitor	Drug	Mutant	Phenotypic effects
Nucleoside RT inhibitor (NRTI)	Lamivudine	M184**V/I**; K65**R**; Q151**M**	The **bold underlined** residues indicate that the activity of the drug is reduced against HIV-1 strains harbouring these substitutions. A moderate loss of drug activity against strains harbouring amino acid substitutions, depicted in **bold**. The plain text residues are unable to confer resistance against the drug on its own and requires the presence of a secondary mutation against the same drug class.
	Emtricitabine	M184**V/I**; K65**R**; Q151**M**	
	Abacavir sulphate	M184V/I; K65**R**; Q151M; K70E; L74**VI**; Y115**F**; M41L; L210W; T215F/Y	
	Tenofovir	K65**R**; K70E; Y115F; M41L; K70**R**; L210W; T215F/Y; Q151**M**	
	Zidovudine	M41**L**; D67**N**; K70**R**;L210**W**; T215**F/Y**; K219Q/E	
Non-nucleoside RT inhibitors (NNRTI)	Nevirapine	L100I; K101**E/P**; K103**N/S**; V106**A/M**; Y181**C/I/V**; Y188**L/C/H**; G190**A/S/E/Q**; M230**L**	
	Efavirenz	L100I; K101E/**P**; K103**N/S**; V106**A/M**; Y181C/I/V; Y188**L/C/**H; G190**A/S/E/Q**; M230**L**	
	Etravirine	L100**I**; K101E/**P**; Y181**C/I/V**; Y188L; G190A/S/**E/Q**; M230**L**	
	Rilpivirine	L100**I**; K101**E**/**P**; Y181**C/I/V**; Y188**L**; G190A/S/**E/Q**; M230**L**	

Data was extracted from the Stanford HIV drug resistance database, https://hivdb.stanford.edu/ (Accessed, 29/08/2017)

PI resistant mutations occur in and around the active site of PR consequently causing a conformational change in the PR binding site preventing the interaction between PR and PIs. One or more major mutations are required for resistance to develop against first generation PIs (Table 1.3). The major mutations are selected for SQV (G48V, L90M), IDV (M46I, V82A/L/F, I84V), RTV (V82A/L/F, I84V), NFV (D30N, L90M), ATV (I150l, I84V, N88S) and FPV (I150V, I84V). Secondary mutations increase viral fitness and the enzyme activity of PR. A high genetic barrier is observed between first- and second generation PIs where several

mutations have to emerge before resistance develops against second generation PIs such as LPV/RTV, DRV, and TPV.[105]

Table 1.3: Summary of the major HIV-1 protease inhibitor resistant pathways

Drug Class	Drug	Mutant
Protease inhibitors	Atazanavir	V32I; M46I/L; I47**V**; G48**V/M**; I50**L**; I54V/T/A/L/M; V82A/T/F/S; I84**V**; N88**S**; L90**M**
	Darunavir	V32**I**; I47**V/A**; I50**V**; I54**L/M**; L76**V**; V82F; I84V
	Lopinavir	D24I; V32**I**; M46I/L; I47V**A**; G48**V/M**; I50**V**; I54**V/T/A/L/M**;L76**V**; V82**A/T/F/S**; I84**V**; L90M
The **bold underlined** residues indicate that the activity of the drug is reduced against HIV-1 strains harbouring these substitutions. A moderate loss of drug activity against strains harbouring amino acid substitutions, depicted in **bold**. The plain text residues are unable to confer resistance against the drug on its own and requires the presence of a secondary mutation against other protease inhibitors		

Data was extracted from the Stanford HIV drug resistance database, https://hivdb.stanford.edu/ (Accessed, 29/08/2017)

Resistance against FI, T20, has developed in the HR1 domain of gp41. Amino acid (aa) substitutions in the 36-45 region of HR1 lead to a decrease in T20 efficacy.[106,107] The most common mutations against T20 are G36D/E/V, V38E/A, Q40H, N42T and N43D. The activity of enfuvirtide decreases 10 fold against one primary resistance mutation and 100 fold in the presence of a secondary enfuvirtide resistance mutation.[108] The HAART program assists with the circumvention of resistance mutations by combining T20 with a NNRTI, PI or INSTIs.

Resistance against MVC targeting CCR5 is complex and may occur through aa substitutions in the V3 loop of gp120. Resistant mutations have only been observed in *in vitro* selection

studies and against several viruses in clinical trials. *In vitro* selection studies selecting mutations for vicriviroc (investigational CCR5 antagonist) induced full resistance (>20 000 fold) after 19 passages against HIV-1 subtype B CC1/85. Three mutations emerged sequentially in the V3 loop: K305R, A316V and G321E.[109,110] Although the V3 is cardinal in resistance against CCR5 inhibitors, resistance occur through more than one genetic pathway that does not include the V3 loop.[111] Specific mutations associated with resistance against MVC have not been described yet, however studies have shown that the HIV virion is somehow able to interact with the CCR5 co-receptor in the presence of MVC, without associated mutations in the gp120.[74] Thus, a mechanism of action of resistance against MVC has not been established as yet.

Resistance against INSTIs will be further discussed in section 1.3.4.1.

1.3 THE ROLE OF INTEGRASE IN THE HIV-1 REPLICATION CYCLE

1.3.1 HIV-1 integrase enzyme structure and domain organization

HIV replication is mediated by a retroviral viral enzyme, HIV-1 IN that belongs to the transposase family of DNA transferases. The key function of IN is to mediate the HIV-1 integration step that incorporates the newly synthesized vDNA into the host chromosomal DNA.[78,112] The 3'-terminus of the *gag-pol* gene encode the 32 kDa protein as a polyprotein that is ultimately cleaved by PR during virion maturation in the late phase of the HIV-1 replication cycle.[17] IN is comprised of 288 aa organized into three functional domains demonstrated in figure 1.3: the N-terminal domain (NTD), the catalytic core domain (CCD) and the C-terminal domain (CTD).[113–115] Each domain has been investigated individually due to the solubility complexity in the preparation of the full length IN protein as well as the flexibility of the three domains comprising the enzyme. Therefore, a structurally similar retroviral IN derived from the prototype foamy virus (PFV) has been used in previous studies to mimic the actions of full length IN with vDNA (further discussed in section 1.3.3).[116] The NTD (aa 1-50) consists of a dimeric helix-turn-helix that has a conserved histidine (His) and cysteine (Cis) motif (HHCC) coordinated by zinc (Zn^{2+}).[117] The binding of Zn^{2+} to the HHCC motif induces multimerization of IN thus forming an IN tetramer, which is the functional state of IN required for integration. The highly conserved CCD (aa 51-212) is comprised of six beta (β)-sheets surrounded by six helices and contains a catalytic triad known as the $D_{64}D_{116}E_{152}$ (DDE) motif consisting of Asp-64, Asp-116 and Glu-152 acidic residues. The divalent metal cation magnesium (Mg^{2+}) coordinates Glu-152, Asp-64 and Asp-116 making it a fundamental cofactor in the catalytic domain.[78] D_{64} and D_{116} of the catalytic triad coordinates the metallic

cofactors required for the catalytic IN activities and is essential for polynucleotidyl transfer. These aa residues are conserved throughout the IN CCD domain of retroviral IN and transposases.[118–120] The CTD (aa 213-288) is less conserved and has a SH3-like fold that facilitates non-specific DNA binding thereby maintaining the stability of the IN complex with DNA.[117] Positively charged residues present in the area spanning from the end of the CCD on one monomer to the CTD of the other monomer assists in vDNA stabilization required for subsequent integration. Overall, all three domains of IN are involved in DNA binding, polynucleotidyl transfer and multimerization that are vital for integration.[113]

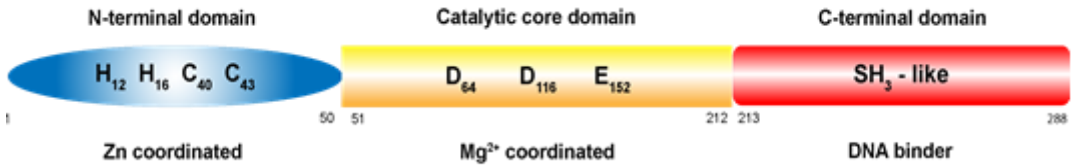


Figure 1.4: The schematic representation of the HIV-1 integrase (IN) structural domains*: the zinc coordinated N-terminal domain, the Mg^{2+} coordinated catalytic core domain and the non-specific DNA binding C-terminal domain. Illustration obtained and modified from McCol and Chen, 2010.*[121]

1.3.2 The mechanism of DNA integration in the HIV-1 replication cycle

HIV-1 integration is a biochemical process exclusive to retroviruses, an obligatory process that ensures the success of HIV-1 replication. Integration involves the insertion of vDNA into the host chromosome consequently leading to the simultaneous replication of vDNA and host DNA during cell division. The entire process is distributed into two steps illustrated in figure 1.5 , the 3'-processing step and the ST step.[122] Following the reverse transcription of vRNA to viral cDNA, IN cleaves conserved dinucleotides, CA, at the linear 3'-vDNA end in the cytoplasm. As a result, GT dinucleotides are released subsequently generating CA overhangs with 3'-CA hydroxyl groups in preparation for the successive ST step. IN and the processed vDNA together with the other components of the PIC migrate to the nucleus where the ST reaction occurs. LEDGF forms part of the PIC that interacts with IN thus enabling tethering of the host vDNA to the PIC (further discussed in section 1.3.5).[123] vDNA binds to one subunit of each dimer that comprise an IN tetramer – this is known as the intasome. The intasome

permits the target DNA to attach to a cleft between the active sites of two IN subunits (further discussed in section 1.3.3). Consequently, the residues in the DDE motif coordinate the Mg^{2+} ions thus exposing the hydroxyl groups of the processed vDNA. This leads to an attack on the phosphodiester bonds on the host DNA at the site of insertion. Integration is completed when the two unpaired nucleotides at the 5'-end of the vDNA are removed, the gaps between the host- and vDNA are filled and the strands are covalently ligated by the host DNA repair proteins.[118,124–126] The host cell genome now contains the viral genetic material, known as the provirus, which is necessary to create progeny viruses.

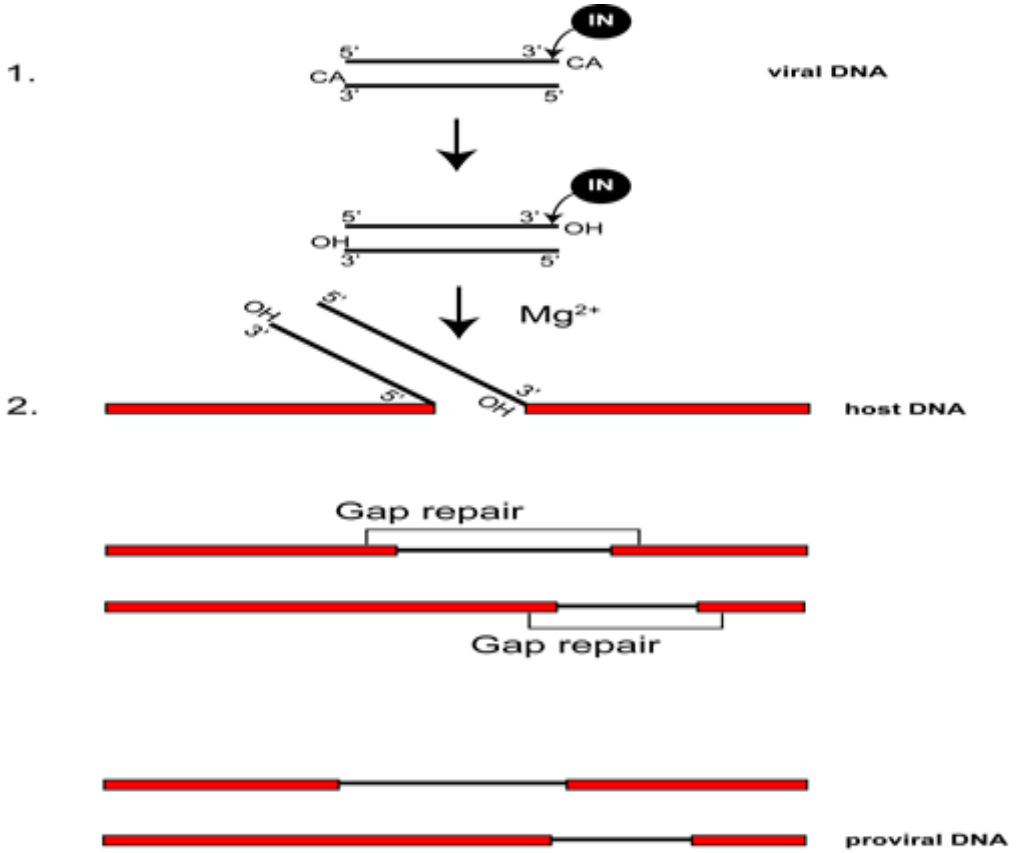


Figure 1.5: A depiction of the essential HIV-1 integration step catalyzed by integrase (IN). *The first step of the integration step involves 3'-end processing. Upon binding of IN to the vDNA, CA dinucleotides are cleaved at the 3'-end consequently exposing hydroxyl groups. In the second step, the exposed hydroxyl groups of the processed vDNA attacks the host DNA resulting in integration. The DNA is ligated using host DNA repair proteins thereby forming a provirus. Illustration obtained from Abrahams, 2014.*[12]

1.3.3 The HIV-1 integrase intasome

As described in the previous sections, resolving the crystal structure of full length HIV-1 IN with vDNA has proven challenging. Although IN sequences of HIV-1 and PFV share a low percentage sequence similarity (>20%), PFV IN is structurally related to the functional state of HIV-1 IN and is able to facilitate DNA integration in a similar manner as HIV-1 IN.[127,128] PFV IN easily forms intasomes using short oligonucleotide substrates required for integration and is highly soluble thus making it biophysically better than HIV IN. Cherepanov and co-workers conducted comparison studies between HIV-1 IN and PFV IN and identified the conserved regions within the IN active site.[129] Based on multiple sequence alignments, HIV IN active residues in the DDE motif were structurally similar to residues Asp-128 and Asp-85 in the PFV IN active site.[116] Furthermore, studies demonstrating the superimposition of HIV-1 IN and PFV IN, revealed that the CCD of both enzymes had a similar RNase H-like fold. The spatial arrangement of the NTD and CTD surrounding the CCD of PFV IN and HIV-1 IN is thought to differ. PFV IN possess longer linkers between domains resulting in an increase in enzyme flexibility.[128] In addition, PFV IN contains two aa insertions located on the N-terminal end of the enzyme as well as between the CCD and CTD. Taken together, it is reason to believe that PFV IN can be used as a template that resembles the functionality of HIV-1 IN.[128] Hare and co-workers resolved the intasome crystal structure using PFV IN and a number of findings were reported:[130] Specifically, for an intasome to form, IN requires a tetrameric state. The dimer of dimers that form an IN tetramer consists of inner and outer subunits per dimer (Figure 1.6). vDNA engage with the inner IN subunits while the outer subunits are positioned sporadically. The IN dimers primarily form when NTD and CTD regions interact. The CTD of each dimer interacts with the phosphate backbone of vDNA consequently crosslinking the subunits. The 3'-end of vDNA interact with the active site of the CCD which subsequently creates an interaction with an opposing NTD.[131]

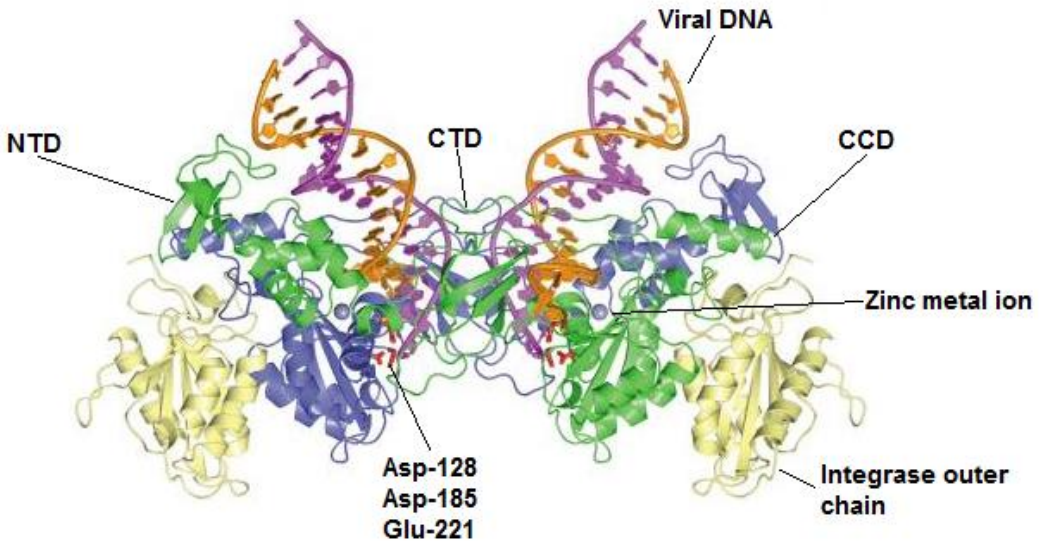


Figure 1.6: Crystal structure of an IN tetramer interacting with vDNA where the reactive DNA is depicted in magenta and the non-transferable DNA is depicted in orange. *The inner blue and green domains (N-terminal domain, catalytic core domain and C-terminal domain) are involved in vDNA binding where the yellow domains are the outer IN chains of the IN tetramer. The red sticks represents residues Asp-128, Asp-185 and Glu-221 located in the active site where the grey spheres represents the Zn^{2+} metal ions. The crystal structures were extracted from Hare et al, 2010.*[131]

1.3.4 HIV-1 integrase inhibitors

There are currently three FDA approved INIs RAL, EVG and DTG which are structural analogues of diketo acid derivatives and share structural moieties. RAL, a pyrimidine carboxamide, is the first FDA approved INI discovered by Merck Research Laboratories in 2007 (Figure 1.7). The aim of INIs, or INSTIs, is to inhibit the ST process in the integration step through chelating the Mg^{2+} cofactors that modulate IN activity. The oxygenated groups of INSTIs such as RAL and EVG, interact with Mg^{2+} in the DDE motif of the CCD and as such, inhibit the ST reaction and consequently HIV-1 replication.[79,80] [81]. A recent advance in the INI drug class involves small molecules that target the interaction between LEDGF/p75 (LEDGF) and IN [132–134]. These small molecules, known as allosteric IN inhibitors (ALLINIs), bind to the LEDGF binding pocket in the CCD of IN subsequently disrupting the interaction between LEDGF and IN. Consequently, the enzyme activity of IN is then allosterically inhibited. [132,133]

LEDGF will be further discussed in section 1.3.5. There are presently no FDA approved ALLINIs however there are several potential drugs currently in clinical trials. ALLINIs are further discussed in section 1.3.6.

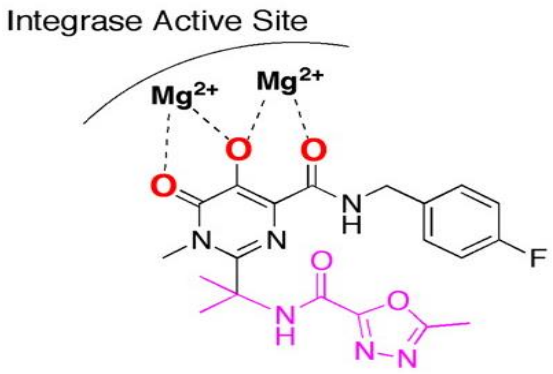


Figure 1.7: The two-dimensional structure of raltegravir (RAL) interacting with the Magnesium (Mg^{2+}) groups located in the active site of HIV-1 integrase (IN). *The coplanar oxygen groups (red), present on RAL, chelate the Mg^{2+} metal ions within the IN active site. Structure obtained from Agrawal and co-workers.*[135]

1.3.4.1 Antiretroviral drug resistance mutations in the integrase enzyme

Recent reports have indicated that virological failure due to RAL treatment is attributed to resistance mutations in the IN catalytic core domain.[136,137] Resistance against RAL is conferred in a stepwise process through mutations in one of three distinct pathways N155H, Q148H/R/K or the uncommon Y143R/C/H (Table 1.4).[138,139] Studies conducted by Malet and co-workers demonstrated that N155H is most likely the initial mutation followed by the emergence of a secondary mutation, Q148H.[140] The Q148 pathway mutations have demonstrated stronger RAL resistance than N155H pathway mutations.[140] However, these primary mutations are often associated with catalytically impaired IN that subsequently reduces the RC of the virus. Q148 is usually associated with G140S and N155H is associated with E92Q.[142] Delelis and co-workers[142] elucidated that Q148H as a single mutation confers RAL resistance but impairs RC. G140S as a single mutation does not confer resistance but restore RC when coupled to Q148H. Therefore, Q148H in combination with G140S produces a virus that has a high RC and is greatly resistant to RAL.[142] Likewise, N155H in combination with E92Q or T97A increase both RC as well as resistance against RAL.[142] The primary

mutation, Y143C/R, reduces RAL susceptibility 5-20 fold, however when coupled with T97A, RAL susceptibility decreases by >100 fold.[143–145] Resistance against EVG is conferred through the E92Q pathway associated with E138K, Q148K/R/H, or N155H resulting in a 150 fold decrease in susceptibility. Resistant mutations against RAL were also observed in patients failing EVG therapy indicating cross resistance mutations between RAL and EVG through the Q148 pathway associated with G140S.[146,147]

Furthermore, DTG conferred the mutations, E92Q and Q148H/R, only in RAL-experienced patients.[148] T124A was observed in treatment-naive patients and conferred low-level resistance against DTG.[148] In addition the primary mutation R263K was observed in treatment-naive patients where viral replication decreased by 20% and a low-level of DTG resistance was observed (2 to 6 fold).[149] Secondary mutations H51Y, E138K or M50I were observed which increased DTG resistance but decreased viral replication.[150]

Table 1.4 Summary of HIV-1 resistance mutations against integrase inhibitors

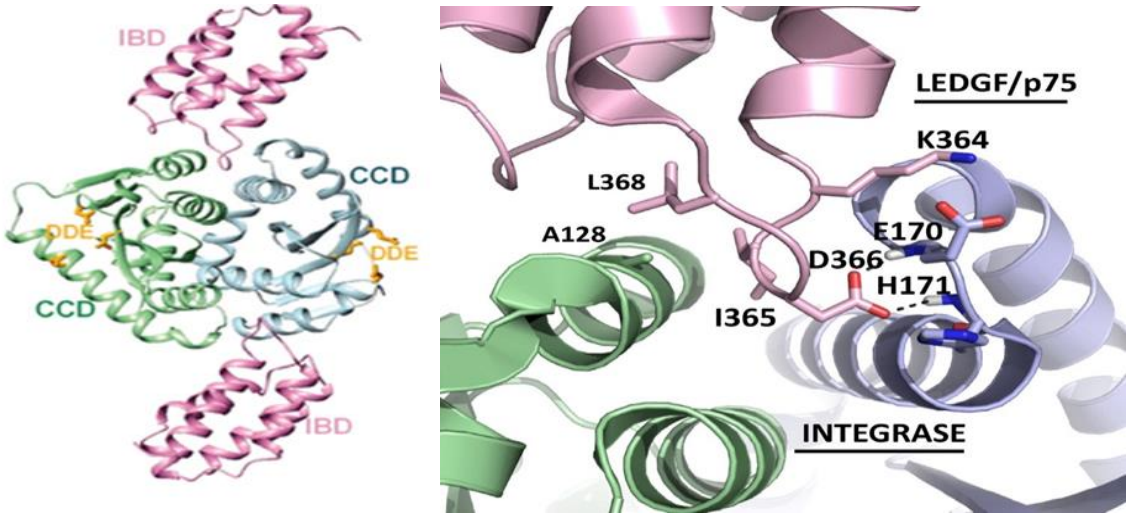
Integrase inhibitor	**Mutant**
Raltegravir	T66A/I/**K**; E92**Q**; E138**K/A/T**; G140**S/A/C**; Y143**R/C/H**; Q148**H/R/K**; N155**H**; R263K
Elvitegravir	T66**A/I/K**; E92**Q**; E138**K/A/T**; G140**S/A/C**; S147**G**; Q148**H/R/K**; N155**H**; R263K
Dolutegravir	T66K; E92Q; E138K/A/T; G140S/A/C; Q148**H/R/K**; N155H; R263K
The **bold underlined** residues indicate that the activity of the drug is reduced against HIV-1 strains harbouring these substitutions. A moderate loss of drug activity against strains harbouring amino acid substitutions, depicted in **bold**. The plain text residues are unable to confer resistance against the drug on its own and requires the presence of a secondary mutation against integrase inhibitors	

Data was extracted from the Stanford HIV drug resistance database, https://hivdb.stanford.edu/ (Accessed, 29/08/2017)

1.3.5 The interaction of LEDGF and integrase during HIV-1 integration

In the HIV-1 replication cycle, the integration step requires the assistance of cellular cofactors, such as LEDGF for successful integration of vDNA into the host chromosome. LEDGF is a ubiquitous cellular chromatin-associated protein that ensures tethering of proteins to DNA. LEDGF contains an N-terminal PWWP motif that is cardinal for chromatin binding. As such, the interaction between IN and LEDGF mediate integration by tethering the PIC to the host chromosome. For ST to occur, a dynamic equilibrium between oligomeric states of IN is required. IN functions as a tetramer and is formed upon the interaction between LEDGF and IN (Figure 1.8). The IN binding domain (IBD) is located on the C-terminal of LEDGF and is comprised of four compacted right handed α-helices. The IBD of LEDGF binds to two regions in the CCD-CCD interface of an IN dimer.[123] The first region includes the region surrounding Trp-131 and Trp-132 whereas the second region extends from Ile-161 to Glu-170.[151,152] X-ray crystallography experiments described the interaction between the CCD of IN and the IDB region of LEDGF.[151] Each subunit of the IN dimer is referred to as IN chain A and IN chain B. A hydrophobic pocket is formed between IN chain A (residues Thr-174 and Met-178) and IN chain B (residues Leu-102, Ala-128, ALA-129, Trp-132). The side chain of LEDGF, Ile-365, makes contact with Thr-174 and Met-178 on IN chain A and Leu-102, Ala-128, Ala-129, Trp-132 on IN chain B. As a result, Trp-131 on the IN chain B is exposed and subsequently interacts with Phe-406 and Val-408. A bidentate hydrogen bond is formed between Asp-366 on LEDGF and the main chain amides on IN that comprise Glu-170 and His-171. Consequently, a salt bridge is formed between Ile-365 on LEDGF and Glu-170 on IN chain A. The backbone amide, Ile-365, which forms part of LEDGF interacts with the carbonyl backbone group, Gln-108, on IN chain A and Thr-125 on IN chain B via a hydrogen bond. Although the CCD on IN comprise most of the total contact between full length IN and LEDGF, the NTD on IN is also involved.[151] The mutation H12N located in the NTD of IN attributed to the reduction in the interaction between IN and LEDGF. Moreover, complete deletion of the Zn^{2+} binding domain results in a decline in IN-LEDGF complexes.[153] The contact between LEDGF and both the CCD and NTD is involved in IN stabilization through multimerization of the protein as well as the formation of the intasome. As such, the IN is in a tetrameric state that is favourable for the ST reaction of integration to occur.[127,154,155] The CCD-CCD interface to which LEDGF binds provides a target for antiviral drugs such as ALLINIs (See section 1.3.6). Small molecules aim to target this interface which mimics the interaction of LEDGF residues Ile-365 and Asp-366 and IN thus promoting IN multimerization. Furthermore, Levin et al, 2009 documented that the IN-LEDGF complex is dissociated by the HIV-1 regulatory

protein, Rev, resulting in the inhibition of the HIV integration step.[22] The interaction between LEDGF and Rev is further discussed in section 1.3.7.3.



A **B**

Figure 1.8: The structural basis of the integrase (IN)-LEDGF interaction extracted from Cherapanov et al, 2005 (Protein databank accession code: 2B4J) A) *Co-crystal structure of the domains involved in the IN-LEDGF complex. The integrase binding domain (IBD) in magenta binds to the hydrophobic pocket formed when the catalytic core domain (CCD) of one IN subunit (green) interacts with the CCD of a second IN subunit (blue) The DDE motif (yellow) comprising the active site of IN indicates that the LEDGF-IBD bind to IN at a site distinct to the catalytic site of IN.* ***B)*** *Cartoon representation of the residues involved in the IN-LEDGF interaction. The CCD molecules from two IN subunits are green and blue while the IBD of LEDGF is magenta. Biochemical characterization and resistance profiles ascertained that residues L368, D366, K364 on the LEDGF-IBD and A128, H171, I365 and E170 located on IN are essential for the IN-LEDGF interaction.*[151,152]

1.3.6 Allosteric integrase inhibitors targeting the LEDGF-integrase interaction

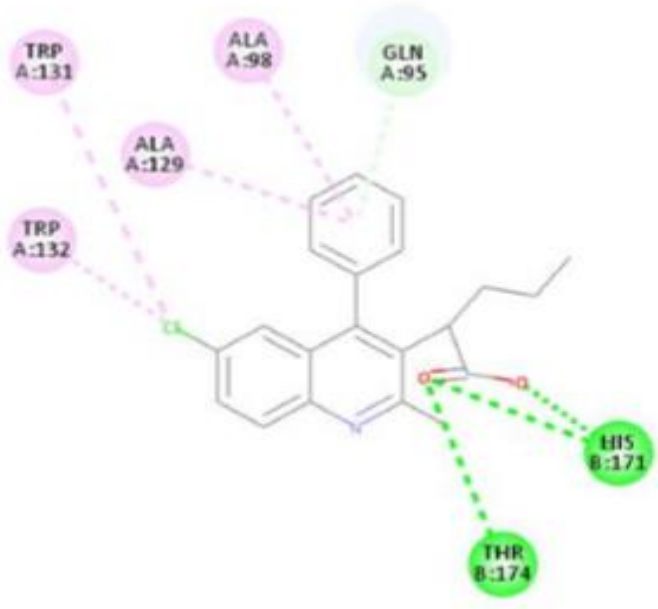
Although HIV-1 antiretrovirals are deemed a clinical success, the efficacy of current INSTIs is compromised due to the emergence of HIV-1 antiretroviral drug resistance in treated patients. The development of ALLINIs is a proposed alternative approach for INSTI-resistant viruses. The challenges of resistance mutations induced by INSTIs can be circumvented by developing small molecules that inhibit IN activity by binding to IN at a site other than the catalytic site. The CCD-CCD interface on an IN dimer is an attractive site for ALLINI binding and the

structural mapping of the interaction between LEDGF and IN provides a novel IN pharmacophore. Studies investigating the activity of HIV-1 in LEDGF knock-down cells demonstrated a reduction in HIV-1 infectivity in the absence of LEDGF.[156–158] Therefore, the hydrophobic pocket can be considered a feasible drug target for small molecules such as ALLINIs. Wang and co-workers revealed that ALLINI potency increased in the absence of LEDGF suggesting that LEDGF and ALLINIs compete for the CCD interface on IN.[159] The mechanism of action of ALLINIs is based on their ability to enhance the interaction between the CCD molecules of IN causing multimerization.[133] Studies by Hayouka and co-workers indicated that the binding of ALLINIs to IN induces multimerization and consequently shifts the IN oligomerization equilibrium in the absence of vDNA resulting in IN inactivity.[160] In addition to the multimerization approach that hinders HIV-1 replication, Jurado and co-workers elucidated that the HIV virions produced in the presence of ALLINIs are defective and thus less infectious.[161] In 2016, a study conducted by Kessl et al, discovered the mechanism of action that ALLINIs exhibit to produce non-infectious and defective virions.[162] The study elucidate that ALLINIs inhibit the interaction between IN and vRNA and as such, defective and non-infectious virions are produced. Moreover, Jurado et al, also demonstrated that ALLINI treatment results in defective viral cDNA for integration and therefore impedes the integration process.[161] Christ et al termed the small molecules that target and perturb the IN-LEDGF interaction as LEDGINs.[163–166] Kessl et al, demonstrated that LEDGINs induced IN multimerization in addition to interfering with the IN-LEDGF interaction. As such, these small molecules are then referred to as ALLINIs.[162,167] These small molecules inhibited the IN-LEDGF interaction at low micro molar (µM) ranges however the most potent inhibitors were quinoline-based acetic acid derivatives. These derivatives are further discussed in section 1.3.6.1.

1.3.6.1 Characterization of LEDGIN, CX05168

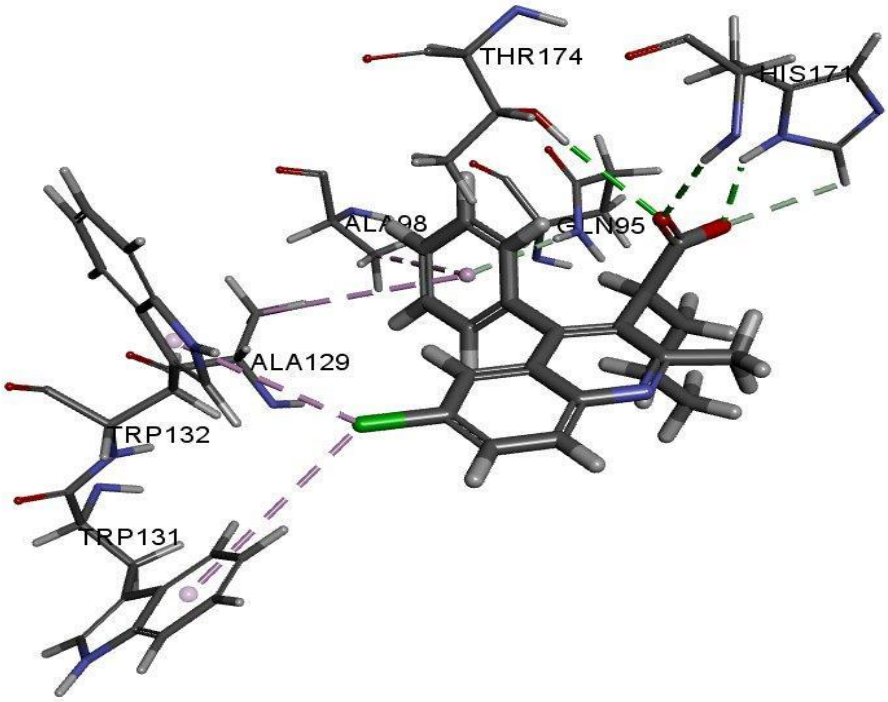
A commercial compound library consisting of 200 000 diverse compounds was screened by Christ et al, using an *in silico* pharmacophore derived from the IBD-CCD co-crystal structure.[165] The best scoring compounds were tested in biological screening assays where four compounds impeded the IN-LEDGF interaction. Structural activity relationship studies were conducted in order to design more active derivatives. Co-crystal structures involving the CCD-IBD regions of IN and LEDGF revealed that the phenyl acid and chlorine groups on the identified compounds mimicked the Ile-365, Asp-366 and Leu-368 residues located on LEDGF. The derivatization process of identified compounds led to the discovery of 2-(6-chloro-

2-oxo-4-phenyl-1,2-dihydroquinolin-3-yl)acetic acid, LEDGIN 3. This compound yielded moderate antiviral activity and was therefore used to derive more potent analogues. As a result, 2-(quinolin-3-yl) acetic acids derivatives, LEDGIN 4, 5 and 6, that are closely related to LEDGIN 3 were synthesised. These LEDGINS demonstrated inhibition of the IN-LEDGF interaction *in vitro* and showed a reduction in HIV replication in *in vitro* HIV phenotypic inhibitions studies.[165] LEDGIN 6 (CX05168), a quinolone derivative identified by Christ et al, exhibited a half maximal inhibitory concentration (IC_{50}) of 2.35 µM and was used in the current study due to the ease of accessibility.[168] Crystal structures of IN CCD with CX05168 confirmed that the compound binds to the cleft formed between the CCDs of two IN monomers. Glu-170 and His-171 were identified as crucial residues where the main chains of these residues interact with the carboxyl groups on CX05168 through hydrogen bonds (Figure 1.9). The side chain of Ala-128 located on IN pack against the compound. Furthermore, no conformational changes of the residues within the hydrophobic pocket occurs in the presence of CX05168.[165] Biological evaluation indicated that CX05168 was active against several HIV-1 subtype B strains (NL4.3, HXB2D, IIIB) as well as INSTI resistant strains.[165] Further investigations and derivatizations identified CX05045 and CX014442 as more potent congeners where CX014442 demonstrated antiviral activity in nanomolar (nM) ranges (46 ± 12nM).[165,168]



A

Figure 1.9 continued on the following page



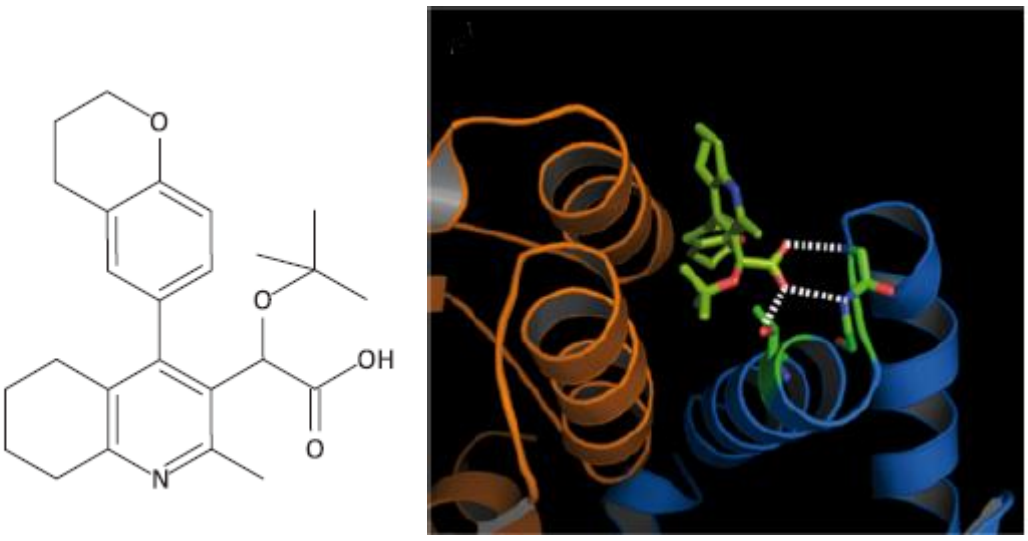
B

Figure 1.9: Molecular docking demonstrating the binding mode of LEDGIN, CX05168, to HIV-1 integrase (IN) A) *Two-dimensional structure exhibiting the interaction between the residues comprising the hydrophobic pocket of an IN dimer and CX05168. Hydrogen bonds connect the carboxyl moeity of CX05168 to the residues near His-171 and Thr-174 denoted by the green dashed line. The pink residues connected by the pink dashed line denote van der Waals bonds* ***B)*** *Ball and stick structure of the amino acid residues involved in the interaction between IN and CX05168. Images obtained from a concurrent study within our laboratory using Discovery Studio software version 3.1 (Accelrys, USA).*

1.3.6.2 Characterization of Mut 101

A series of ALLINIs targeting the 3-(quinolin-yl)-2 acetic acid pharmacophore were identified by the Biodim Mutabilis group.[167] Mut 101 exhibited the highest antiviral activity with a half maximal effective concentration (EC_{50}) value = 540nM against HIV-1 NL4.3. X-ray crystallography studies demonstrated that two Mut 101 molecules bind to the LEDGF hydrophobic pocket on IN to which other quinoline based IN inhibitors, such as CX05168, bind. As such, these compounds exert a similar mechanism when inhibiting HIV-1 replication. The carboxylic acid group of Mut 101 forms hydrogen bonds with the amino groups on the main

chain of Glu-170 and His-171 (Figure 1.10). The hydroxyl group on the side chain of Thr-174 located on IN forms a hydrogen bond between the aa residue and the carboxyl group on the Mut 101. Conformational changes occur within the IN structure in the presence of Mut 101 which has not been observed with other quinolone derivative inhibitors. Firstly, the binding of Mut 101 to IN alter the conformation of three α-helices located in the regions between 115-122, 123-124 and 92-98. The conformational change results in the displacement of the loop containing Ile-90, Pro-91 and Ala-92. Secondly, residues located within the binding pocket, Gln-95 and Glu-170, are displaced upon Mut 101 binding. The conformational changes within the LEDGF binding pocket induce the formation of higher order multimers of IN, a mechanism of action observed in the presence of quinolone based IN inhibitors. Furthermore, the structural changes of IN in the presence of Mut 101 are attributed to the inability of IN to interact with co-factors and DNA required for the integration step. Biochemical analysis demonstrated that Mut 101 moderately reduces the ST step of integration (66%), impedes the IN-LEDGF interaction and yielded EC_{50} values in nM ranges against HIV-1 subtype B NL4.3 and HXB2.[167]



A **B**

Figure 1.10: Representations of the allosteric integrase (IN) inhibitor, Mut 101 A) *Chemical structure of the 3-(quinolin-yl)-2 acetic acid derivative, Mut 101* ***B)*** *Cartoon representation of the two interacting catalytic core domains (CCD, orange and blue) of an IN dimer forming the LEDGF binding pocket. Mut 101 (Green) interacts with amino acid residues, Glu-170, His-171 and Thr-174, within the LEDGF binding pocket via hydrogen bonds. Images extracted from Le Rouzic et al, 2013.*[167]

1.3.6.3 Resistance mutations in the integrase enzyme against ALLINIs

ALLINIs target IN at a site distinct from the active site. As such, ALLINIs exert a high genetic barrier against resistance mutations induced by INSTIs such as RAL, EVG and DTG. Studies have shown that Mut 101 and CX05168 are active against resistant mutations located in the *IN* gene. Mut 101 demonstrated a high genetic barrier against INSTIs resistant mutations G140S and Q148H while CX05168 exhibited a high genetic barrier against IN mutation E92Q, G140S, Q148H and N155H.[167,168] Although no cross resistance between INSTIs and ALLINIs have been reported as yet, new resistance pathways against ALLINIs have emerged. The A128T mutation was discovered through *in vitro* resistant selection studies and is deemed the primary mechanism of ALLINI resistance.[165,168–170] A128 is a critical residue for the IN-LEDGF interaction and thus renders resistance against ALLINIs upon the substitution of the Ala-128 residue with Thr. The substitution from Ala to Thr induces a change in the positioning of the quinoline core and phenyl ring within the ALLINI that is responsible for the linkage between two IN monomers. The hydrogen bond that forms between the ALLINI and IN remains unaffected, which then imitates the interaction between LEDGF and IN and consequently prevents aberrant multimerization of IN in the presence of ALLINIs. The A128T resistant mechanism relies on the prevention of aberrant multimerization induced by ALLINIs while the mutation does not affect the interaction between ALLINIs and IN.[169] H171T/Q was the second major resistance pathway identified. Slaughter et al, described the mechanism of action of H171T against ALLINIs such as BI-D.[171] The substitution of His-171 with Thr prevents the ALLINI from binding to IN. The hydrogen bond between the side chain of His-171 and the *tert*-butoxy oxygen ether of BI-D is compromised upon the substitution of His with Thr. His-171 interacts with the carboxylic acid of BI-D via electrostatic interactions as well as an interaction with the *tert*-butoxy oxygen group on BI-D through hydrogen bonding. When His is substituted with Thr, the bond interactions are modified where the side chain of Thr-171 interacts with the carboxylic acid group of BI-D through a newly formed hydrogen bond. However, the hydrogen bond formed between the carboxylic acid of BI-D and His-171 is absent in the presence of the Thr substitution which consequently decrease the affinity of the ALLINI to the IN binding site (Figure 1.11). The reduced interaction between BI-D and IN results in a 67.9 fold change in EC_{50} when compared to wild type IN. Viral replication is restored in the presence of this mutation as LEDGF does not require a *tert*-butoxy moiety to interact with IN.[171] A third, less prominent, resistance pathway was discovered where Glu-170 was substituted with Gly located within the IN-LEDGF hydrophobic pocket. E170 is imperative for the interaction between IN and LEDGF and thus a substitution at this point leads to resistance.[165] The mechanism of resistance includes the disruption between the CCD and CTD that subsequently

affects multimerization of IN.[172] The double mutation, A128T/E170G, had a 17 fold resistance against ALLINIs while retaining activity against all other antivirals.[165] Studies by Christ et al have shown that mutations occur in the *pol* gene when under CX05168 pressure.[165] These mutations include the A128T and E170G which is found in the LEDGF-IN pocket. HIV-1 subtype B NL4.3 harbouring these mutations are fully resistant to CX05168. The mutations emerged after 39 passages and caused a 25 fold increase in CX05168 EC_{50} concentration (2.35µM). Studies by Le Rouzic et al, explicated that Mut 101 is fully active against mutation A128T.[167] In addition, studies have shown that both Mut 101 and CX05168 are active against HIV mutants and Q148H resistant to INSTIs.[165,167]

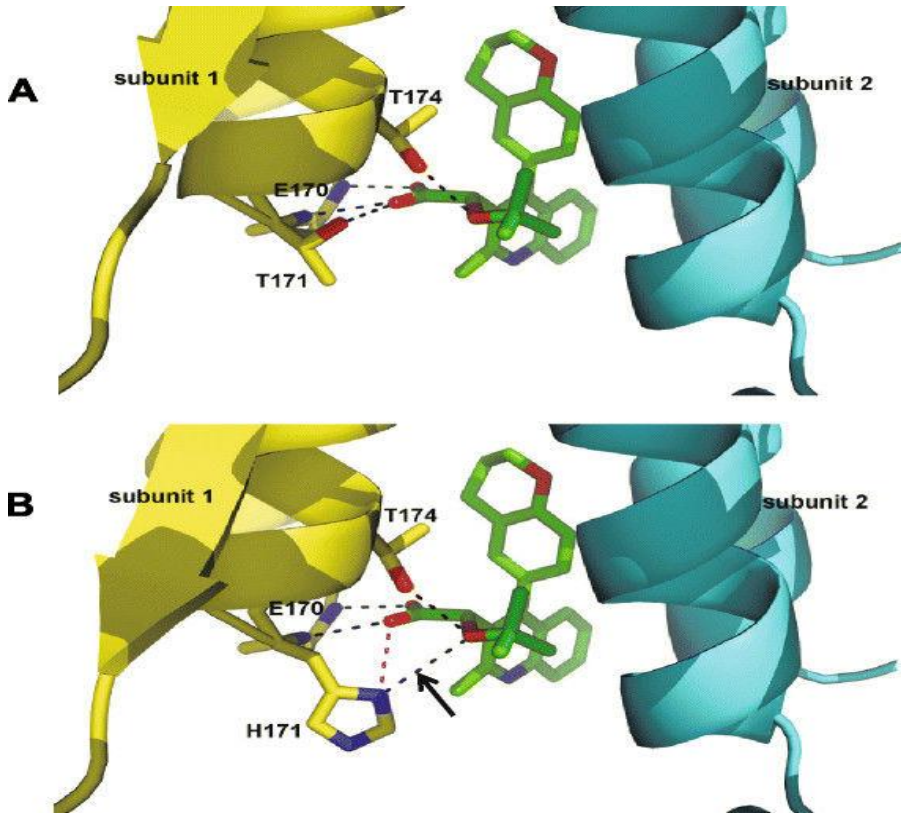


Figure 1.11: The crystal structure demonstrating the interaction between allosteric integrase (IN) inhibitor, BI-D, and A) H171T mutated IN and B) wild type IN. *Subunit 1 (yellow) and 2 (cyan) represents the CCDs of an IN dimer that forms a hydrophobic pocket. BI-D is depicted in green where the red regions represents the oxygen atoms and the blue regions represent the nitrogen atoms. Hydrogen bonds are depicted by the black dashed-lines where the magenta dashed-line depicts the electrostatic interaction between the Nitrogen atom and the carboxylic acid on BI-D. The arrow in* ***B*** *shows the hydrogen bond between His-171 and the tert-butoxy group on BI-D which does not occur in IN harbouring H171T* ***(A).*** *The crystal structures were extracted from Slaughter et al.*[171]

1.3.7 The regulatory role of Rev in HIV-1 integration

1.3.7.1 Structure and the function of Rev

Rev is an 18kDa regulatory transactivation phosphoprotein comprising 118 aa synthesized in the cytoplasm.[173] The conventional function of Rev is that it facilitates the export of mRNA containing the HIV-1 RRE into the cytoplasm. As such, the Rev protein structure contains structural domains that coordinate its function in the late phase of HIV-1 replication. The protein consists of an arginine rich motif (ARM) at the N-terminal and a Rev activation domain at the C-terminal of Rev. The ARM has a highly conserved sequence that spans over aa 38–49 that forms an α-helical secondary structure.[19] Multimerization of Rev is mediated through the ARM region and is required for the binding of Rev to the RRE located on mRNA. The hydrophilic nuclear localization sequence (NLS) is situated in the ARM region which binds to importin thus directing Rev into the nucleus.[19,173] The Rev activation domain is a Leu rich motif that spans residue 71–82 at the C-terminal of Rev and contains the hydrophobic nuclear export signal (NES). The binding of the NLS to mRNA conceals the NLS consequently exposing the NES site.[21] Exportin then binds to the NES site thus allowing the export of mRNA to the cytoplasm. Previous studies have elucidated that mRNA is retained in the nucleus in the absence of Rev and therefore preventing translation of viral proteins.[20] The more recently discovered function of Rev occurs in the early phase of the HIV replication cycle and involves the regulation of integration of viral cDNA into the host chromosome (Further discussed in section 1.3.7.3).[22,173,174]

1.3.7.2 The interaction between HIV-1 integrase and Rev

Peptide mapping was initially used to determine the aa residues responsible for the interaction between IN and Rev.[174] In addition, Benyamini and co-workers constructed the IN-Rev complex through protein docking studies and compared the results with the experimental data in previous reports.[175] The protein docking results and the experimental results correlated and showed that Rev binds IN through the same interface as LEDGF. As such, an interplay is created between IN, LEDGF and Rev. Rev binds to IN at two distinct sites where IN residues 66-80 and 118-128 forms the first site and residues 174-188 comprise the second site (Figure 1.12). Rev residues 13-23 and 23-67 interact with IN 174-188 residues located on IN. Hydrophobic interactions occur between IN residues Leu-68 and Gly-70 and Rev residues Leu-60 and Tyr-63, respectively.[175]

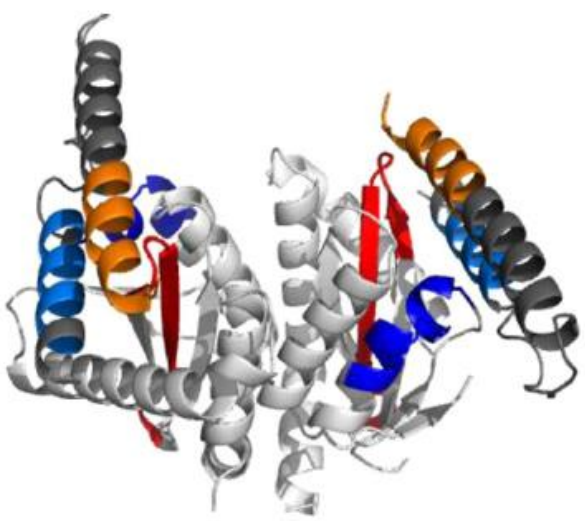


Figure 1.12: Structural model of the HIV-1 integrase (IN)-Rev complex. *The light grey helices denote IN dimer and the dark grey denote a region of the Rev monomer. Rev residues 53-67 (orange) interact with IN residues 66-80. The light blue represents Rev 13-23 that interacts with dark blue IN residues 118-128. Extracted from Benyamini and co-workers, 2011.*[175]

1.3.7.3 HIV-1 Rev regulate the integration step

The novel function of Rev in the HIV integration step was first demonstrated by Levin and co-workers in 2009.[22] The study showed a direct correlation between IN-Rev complex formation and inhibition of integration.[176] During the natural lifecycle of HIV-1, an interplay between Rev, IN, and LEDGF occurs that regulates the irreversible integration of viral cDNA into the host chromosome.[177] Figure 1.13 depicts the interplay between Rev, LEDGF and IN. Rev enhances the dissociation of the IN-LEDGF complex by binding to LEDGF and then to IN.[177] The IBD (aa 361-441) on LEDGF mediates the binding of either Rev (through aa 35-50) or IN (through aa 130-173) to LEDGF. Rev and LEDGF interact with IN through the CCD of IN.[177] In high expression levels of Rev, Rev binds to LEDGF and IN forming LEDGF-Rev and IN-Rev, respectively. The affinity for Rev to LEDGF is similar to the affinity of Rev to IN with dissociation constants (K_d) of 19 nM and 13nM, respectively, suggesting that Rev is a competitive inhibitor of the IN-LEDGF interaction. The affinity of Rev to the IN-LEDGF complex is higher (K_d = 7nM) than the affinity of LEDGF to IN-Rev (K_d = 27nM) indicating that the IN-Rev interaction is more favourable in the absence of LEDGF. A review by Grewe, 2010 proposed a mechanism of action describing the inhibition of integration by Rev.[178] Upon initial infection, cDNA is

synthesized through reverse transcription and subsequently migrates to the nucleus where it forms part of the PIC. Integration ensues followed by transcription and formation of new virions. Rev is then expressed from integrated or non-integrated vDNA that plays a role in secondary infection within the same cell. The replication cycle of HIV upon secondary infection is altered due to the increase in Rev expression. The newly expressed Rev interacts with IN, which entered the cell upon secondary infection, consequently inhibiting the integration process. The subsequent IN-Rev complexes inhibit the enzymatic activity of IN by inducing multimerization of IN.[133] Levin et al demonstrated that one to two integration events/cell occurs in the presence of Rev. When infecting cells with Rev deficient virus, approximately 10 integration events/cell occurs inferring that an interplay between Rev, LEDGF and IN must occur to regulate the number of integration events/cell. By inhibiting IN activity and multi-integration, Rev functions to circumvent superinfection of HIV-1 since viral fitness decreases upon reinfection of an infected cell with virions released by the same cell.[177] In the absence of Rev, multi-integration of vDNA into the host chromosome occurs which leads to genomic instability and apoptosis.[176]

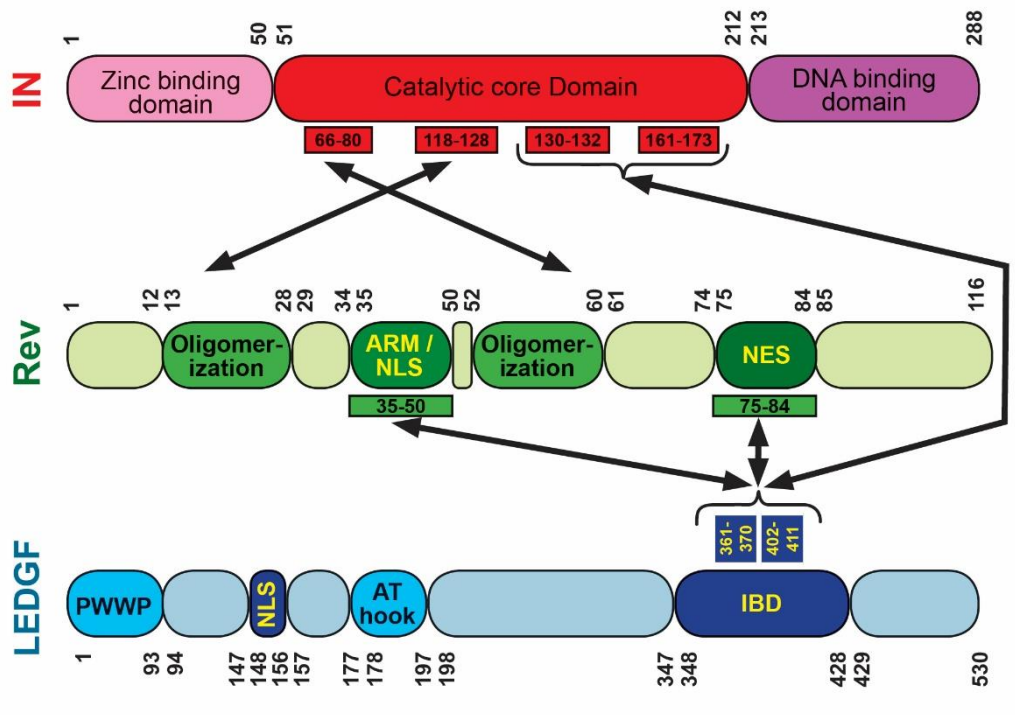


Figure 1.13: A schematic model of the LEDGF, integrase (IN) and Rev interaction: *Both LEDGF and Rev interact with IN through its catalytic core domain. LEDGF interacts with both Rev and IN through the IN binding domain on the C-terminal of LEDGF. Illustration obtained from Levin et al, 2010.*[177]

1.4 SIMILARITIES BETWEEN THE ROLE OF ALLINIs AND REV IN THE HIV-1 INTEGRATION STEP

Taken together, Rev and ALLINIs appear to inhibit the integration step of the HIV-1 replication cycle in a similar manner. Both Rev and ALLINIs interact independently with IN, perturb the integration process and also affects virion particle maturation. The disturbance in the integration process by Rev and ALLINIs is mainly achieved through IN multimerization. In the presence of Rev and ALLINIs, viral cDNA produced that is required for integration is defective (low levels of LTR production) and maturation of the viral core is inhibited. It is therefore apparent that ALLINIs and Rev affect the HIV-1 replication cycle in a similar manner. In addition, studies reveal that Rev is a competitive inhibitor of LEDGF for the IN binding site. Likewise, ALLINIs are also known to be potent competitive inhibitors of the IN-LEDGF interaction. As such, this study aims to investigate the role of Rev in the HIV-1 integration step in the presence of ALLINIs.

1.5 HYPOTHESIS

ALLINIs affect the interaction between Rev and IN.

1.6 OBJECTIVES

The following objectives were attained to elucidate the role of ALLINIs on the IN and Rev interaction:

1. To determine whether drug resistance mutations emerge in HIV-1 genes when under ALLINI drug pressure

2. To investigate whether Rev-driven multimerization is modulated by ALLINIs

3. To determine the binding interaction of Rev to IN in the presence of ALLINIs

CHAPTER 2

Methods

2.1 IN VITRO SELECTION STUDIES

The protocol used for *in vitro* selection studies was extracted and modified from the experimental procedures documented in M.Mphahlele[179], Goethals and co-workers[147] and Margot and co-workers.[180]

2.1.1 Isolation of peripheral blood mononuclear cells

Peripheral blood mononuclear cells (PBMCs) were used to carry out *in vitro* selection studies. Buffy coats were obtained from the South African National Blood Service (SANBS) from which PBMCs were isolated. Each buffy coat was diluted 1:1 in phosphate buffered saline (PBS, 137mM NaCl, 2.7mM KCl, 10mM Na_2HPO_4 and 1.8mM KH_2PO_4). The diluted buffy coat solution was gently layered onto Ficoll Paque (GE Healthcare, UK) at a 4:3 ratio. The layered solution was centrifuged for 40 minutes at 400 x g without breaks and acceleration. The PBMC interface was aspirated and washed twice with 20 ml PBS by centrifugation for 10 minutes at 400 x g. The resulting pellet was resuspended in 10% growth media (Roswell Park Memorial Institute Medium 1640 (RPMI, Gibco, USA) containing 205mM L-glutamine (Thermo Fisher Scientific, USA) and supplemented with 20% inactivated fetal calf serum (FCS, Highveld Biologicals, SA), 20U/ml penicillin-streptomycin (Gibco, USA) and 20µg/µl gentamycin (Gibco, USA)) at 1.5 x 10^6 cells/ml. The cells were stimulated with 5µg/ml phytohemagglutinin (PHA-P, Sigma-Aldrich, USA) then incubated for 72 hours in standard cell culture conditions (37°C with 5% CO_2)

2.1.2 50% Tissue culture infective dose ($TCID_{50}$) determination and HIV-1 subtype C expansion

The 50% tissue culture infective dose ($TCID_{50}$) of HIV-1 subtype C primary isolates from drug naïve patients was determined using the protocol extracted from the ATCG Laboratory Manuel, 2004. Primary HIV-1 subtype C isolates, 05ZAFV3 (FV 3) and 05ZAFV26 (FV 26), were isolated from drug naïve patients at the Charlotte Maxeke Johannesburg Academic Hospital (Johannesburg, South Africa) in a previous study.[181] The viral isolates were diluted 1:12 in 10% growth media including 5% interleukin-2 (IL-2, Sigma-Aldrich, USA). Briefly, the diluted viral isolates were serially diluted six times in a 1:4 ratio with a total of three replicates. Stimulated PBMCs were added to the wells containing virus at a final concentration of 1.5 x 10^6cells/ml to make a total volume of 200µl. The cells treated with virus was incubated for 96

hours in standard cell culture conditions. The cultivated cell suspension was removed and replaced with fresh 10% growth media. The infected cells were then further incubated for 72 hours in standard cell culture conditions. Viral infection PBMCs was monitored using raw absorbance values obtained through the Vironostika HIV Ag/Ab p24 enzyme linked immunosorbent assay (ELISA) kit (Biomerieux, France) according to the kit instructions. These raw absorbance were then further used to quantify the concentration of p24 using a standard curve. Briefly, 100µl of the infected cell suspension was added to wells containing Horseradish peroxidase (HRP)-labelled anti HIV-1 p24. The reaction was made up to 200µl by adding 100µl pre-mixed Specimen Dilution Buffer. The reactions were incubated for one hour at 37°C. The reaction mixture was discarded and the wells were washed seven times with 1x Wash Buffer (25x pre-mixed kit Phosphate Buffer concentrate diluted in PBS) for 30 seconds per wash. A chromogenic substrate, tetramethylbenzidine (TMB) was added to the wells. In the presence of the p24 antigen, the HRP enzyme linked to anti-HIV-1 p24 cleaves the TMB substrate subsequently producing a blue colour. The reactions were terminated with 10% sulphuric acid and measured at 450nm using an Xmark absorbance spectrophotometer (Bio-Rad, USA). The raw absorbance readings obtained from the p24 ELISA were used to calculate the $TCID_{50}$ using the Spearman-Karber equation.

The virus was expanded by adding 1000 $TCID_{50}$ virus to 4.5 x 10^6 stimulated PBMCs in a final volume of 3ml and incubated for 96 hours in standard cell culture conditions. Following the incubation period, 1.5ml of the cell suspension was removed and replaced with fresh 10% growth media. The infected cells were further cultivated for 72 hours in standard cell culture conditions. The p24 concentrations of the infected cells were quantified using the Vironostika HIV Ag/Ab p24 ELISA kit to determine the viral activity of the expanded virus. The assay was conducted as described above. The supernatants with high p24 levels were clarified through centrifugation at 400 x for 10 minutes and subsequently stored in the presence of 20% FCS at -80°C until further use.

2.1.3 Classical in vitro selection experiments

PBMCs were isolated, cultivated at 2 x10^6 cells/ml in 10% growth media and stimulated with 5µg/ml PHA-P followed by a 72 hour incubation in standard cell culture conditions. The harvested PBMCs were subcultured through centrifugation and the resultant cell pellet was infected with 250 $TCID_{50}$ HIV-1 subtype C FV 3 and FV 26 isolates. Infection was achieved by

incubating the virus with the cell pellet for one hour at 37°C with 5% CO_2. Following the incubation period, the cell pellet was resuspended in 3ml growth media containing 5% IL-2. ALLINIs were added to each infected cell suspension at its EC_{50} concentration. CX05168 (Hauyuan chemexpress, China) was added to the cell suspension at 3µM and Mut 101 (Mutabilis group, France) was added at 0.5µM.[165,167] The positive control for both FV 3 and FV 26 isolates contained no compound treatment (drug naïve). The treated cells were incubated for 96 hours in standard cell culture conditions. The cell cultures were continuously maintained up to passage (p) 60. This was achieved through two subcultures per week. Subculture 1 included the following steps: 1.5ml of the cell suspension was replaced with fresh 10% growth media containing 5µg/ml PHA-P. Cells were then further harvested for 72 hours at 37°C with 5% CO_2. The second subculture included the following steps: 1.5ml of the cell suspension was removed and the cell culture was replenished with freshly stimulated PBMCs at a concentration of 1.5 x 10^6 cells/ml. Viral activity of the cultures were monitored through the quantification of its p24 levels using the Vironostika HIV-1 Ab/Ag p24 ELISA kit. ALLINIs were added once weekly and the compound concentration was increased two-fold upon viral breakthrough. The absorbance value to determined viral breakthrough was calculated using the cut-off calculation described by the kit instructions. The cut-off value was calculated at 1.6nm. The ALLINI concentration remained constant when no viral breakthrough was observed. The treated cultures were incubated further for 96 hours in standard cell culture conditions until the following subculture. The supernatants from all subcultured passages were stored at -80°C for further genotypic analysis and *in vitro* phenotypic inhibition studies.

2.1.4 Genotyping

2.1.4.1 RNA extraction using the EasyMAG NucliSens automated system

RNA was extracted from the stored supernatants collected during *in vitro* selection studies. Samples that showed viral breakthrough were used to extract viral RNA for subsequent genotyping analysis. The NucliSENS EasyMAG automated system (BioMerieux, France) was used to extract RNA following the system's instructions. Briefly, 500µl of the samples were loaded into the EasyMAG sample vessels to which 200µl EasyMAG Lysis Buffer was added and incubated for 10 minutes at room temperature. EasyMAG silica beads were added to the lysed samples followed by the elution of RNA from the silica beads using the 25µl EasyMAG

Elution Buffer. The RNA concentration was quantified at 280nm using the NanoDrop 2000 spectrophotometer.

2.1.4.2 Complimentary DNA synthesis from extracted viral RNA

2.1.4.2.1 Reverse transcription polymerase chain reaction of the HIV-1 *IN* gene

The RNA extracted in section 2.1.4.1 was transcribed to cDNA by means of reverse transcription polymerase chain reaction (RT-PCR). The Superscript III One-Step RT PCR System with Platinum *Taq* High Fidelity (Invitrogen, USA) was used to synthesize cDNA in a one-step reaction. Each reaction consisted of the following reagents: 12.5µl 2x reaction mixture, 0.5µl of 10µM forward primer (PR F1, 5'-CCC TCA AAT CAC TCT TTG GCA ACG AC-3'), 0.5µl of 10µM reverse primer (VIF R3, 5'-CTC CTG TAT GCA GAC CCC AAT ATG-3') and 0.5µl SuperScript™ III RT/Platinum™ Taq High Fidelity Enzyme Mix. Additional Magnesium Sulphate ($MgSO_4$) was added to the reaction mixture at a final concentration of 300µM. The reaction mixtures were made up to a final volume of 25µl with distilled water (dH_2O). RT-PCR experiments were carried out using the GeneAmp PCR system 2700 (Applied Biosystems, USA) using the cycling conditions listed in Table 2.1

Table 2.1: RT-PCR thermocycling conditions used for cDNA synthesis

Step	Temperature (°C)	Time	
cDNA synthesis	50	60 minutes	
Pre-denaturation	94	2 minutes	
Denature	92	15 seconds	35 cycles
Anneal	55	30 seconds	
Extend	68	3 minutes 30 seconds	
Final extension	68	10 minutes	

2.1.4.2.2 Amplification of complimentary DNA for the HIV-1 *integrase* gene

The cDNA product yielded from RT-PCR was amplified to increase the yield of the amplicon (approximately 3.5Kb) for subsequent sequencing. The Platinum *Taq* DNA polymerase high fidelity kit (Thermo Fisher Scientific, USA) was used to amplify the first round PCR product. The reactions consisted of 5µl 10 x HiFi reaction buffer, 1µl dNTPs, 2 µl 50mM $MgSO_4$, 1µl 10µM forward primer (PR F3, 5'-GCT CTA TTA GAT ACA GGA GCA GAT G-3'), 1µl 10µM reverse primer (VIF R5, 5'-GGG ATG TGT ACT TCT GAA CTT-3'), 2µl DNA product and 0.2µl Platinum *Taq* DNA polymerase. The reaction mixture was made up to 50µl with dH_2O. The PCR reactions were conducted on the GeneAmp PCR System 9700 (Applied Biosystems, UAS) using the cycling conditions in Table 2.2.

Table 2.2: ***Cycling conditions for second round amplification using the Platinum Taq DNA Polymerase High Fidelity***

Step	Temperature (°C)	Time	
Initial denaturation	94	2 minutes	
Denaturation	94	30 seconds	35 cycles
Anneal	50	30 seconds	
Extension	68	3 minutes	
Final extension	68	10 minutes	

The PCR products were subsequently analysed on a 1% agarose gel. The agarose gel was prepared by adding 1% agarose powder (Sigma Aldrich, USA) to 1 x Sodium Borate Buffer (200mM NaOH, 0.7mM Boric Acid, pH 8) and heated until the powder was dissolved. The solution was cooled and 100 x Sybr gold (Thermo Fisher Scientific, USA) was added. The agarose solution was poured into an agarose gel cassette and allowed to set. The PCR samples were diluted 1:5 in 6x Gel Loading Buffer (New England BioLabs, UK) and loaded onto the agarose gel alongside a DNA ladder (GeneDirex, China). The DNA was separated at 80 volts for approximately one hour and visualised using the ChemiDoc MP (Bio-Rad, USA).

2.1.4.3 Amplification of the HIV-1 rev gene

Forward and reverse primers were designed that targeted exon 1 and exon 2 comprising the consensus sequence of the HIV-1 subtype C *rev* gene. RNA extracted in section 2.1.4.1 was used for RT-PCR using the Superscript III One-Step RT PCR System as described in section 2.1.4.2.1. The PCR product was further used for inner amplification of the *rev* gene using the Platinum *Taq* DNA polymerase high fidelity kit as described I section 2.1.4.2.2. A product was expected at approximately 2.5Kb. However, no amplification product was observed after optimization studies of various PCR parameters were conducted. The following parameters were tested: $MgSO_4$ concentration (100μM to 1mM), DNA template concentrations (0.5μM – 5μM), primers (obtained through primer design and literature[182]) as well as primer concentrations, and annealing temperatures through gradient PCR experiments (45°C - 68°C). Due to the unsuccessful PCR amplification of the *rev* gene, subsequent genotyping could not be conducted to determine if CX05168 and Mut 101 induced resistance mutations within the gene.

2.1.4.4 Purification of the PCR product

Following PCR amplification of *IN*, the amplicon was purified using the QIAgen PCR cleanup kit (QIAgen, Germany). Briefly, the pre-mixed Binding Buffer was added to the PCR product at a 5:1 ratio and applied to a QIAquick spin column. The sample was centrifuged for one minute at 10 000 x g and the flow through was discarded. Pre-mixed Wash Buffer was added to the QIAquick spin column and centrifuged for one minute at 10 000 x g. The flow through was discarded and the spin column was centrifuged for an additional one minute at 10 000 x g. Pre-mixed Elution Buffer was added to the spin column and incubated for one minute at room temperature. The spin column was then centrifuged for one minute at 10 000 x g and the DNA eluate was collected. The DNA concentration was quantified and the purity (A260/A280) was determined using the Nanodrop 2000 spectrophotometer.

2.1.5 Genotypic analysis of the IN gene extracted from Mut 101 selected FV isolates

The purified PCR products obtained in section 2.1.4.3 were sequenced by Inqaba Biotech (South Africa) through automated Sanger sequencing using the primers listed in Table 2.3. Nucleotide chromatograms were analysed using FinchTV software version 1.4.0 (Perkin Elmer, USA) while GeneDoc multiple sequence alignment editor and shading utility version 2.6.002 was used to edit and align DNA sequences. The pairwise alignment setting was used to align all sequences ultimately creating a consensus sequence for HIV-1 subtype C FV 3 and FV 26 isolates. FV 3 and FV 26 drug naïve isolates were blasted against both consensus HIV-1 IN subtype B (Accession number, AIW805917.1) and C (Accession number, AAD17126.1) sequences using the NCBI blastp algorithm (protein–protein BLAST, https://blast.ncbi.nlm.nih.gov/Blast.cgi).

Table 2.3: List of primers for sequencing of the IN gene integrase region

Primer name	**Sequence**
IN_F_4074	5'-CAA CCA GAT AAA AGT GAA TCA G-3'
IN_R_4348	5'-CTC CTT TTA GCT GAC ATT TAT CAC-3'
IN_F_4540	5'-TAG CAG GAA GAT GGC CAG T-3'
VIF_R_5193	5'ATG TGT ACT TCT GAA CTT-3'

2.1.6 Molecular docking of Mut 101 with mutant integrase proteins

Protein docking was conducted to predict the impact of the IN mutants, identified in section 2.1.5, on the interaction between IN and Mut 101. The docking studies were carried out by docking Mut 101 into the IN allosteric site located on the IN-LEDGF interface. The X-ray structure of the IN-LEDGF complex was retrieved from the Protein Databank (PDB code 2B4J) and subsequently used for docking studies. Due to the lack of HIV-1 subtype C IN-LEDGF complex crystal structure availability, an HIV-subtype B model was used. The protein complex was prepared by inserting residues that were missing and removing the LEDGF chain D as

well as the removal of water molecules. The structure was further refined with an OPLS3 force field using the protein preparation wizard in the Schrodinger Maestro suite 11.2. The resultant structure was used for further preparation where the chain C of the IBD located on LEDGF was removed to simulate INI complexes. The energy-minimized structure was optimized until a RMSD of 0.30 Å was reached. The receptor grid generation defined the binding pocket interface between two IN monomer using Ile-365 and Asp-366 as the ligand. The binding site had the following xyz coordinates: -14.33, 3.43 and -5.08.

Mut 101 was minimized to its lowest energy before it was docked into the IN-LEDGF pocket. All possible three dimensional structures (3D) were generated using the default settings in the LigPrep tool. The mutations were incorporated into the structure followed by energy minimization around the mutation. The Ligand docking glide protocol was used to dock Mut 101 into the IN-LEDGF binding pocket.

2.1.7 In vitro phenotypic inhibition studies of viral isolates collected in in vitro selection studies

In vitro phenotypic inhibition studies were conducted using culture supernatants that exhibited viral breakthrough at specific passages as well as the control supernatants. The aim of these experiments was to obtain and compare EC_{50} values of the ALLINIs against drug naïve HIV-1 subtype C FV isolates versus drug treated HIV-1 subtype C FV isolates where viral breakthrough was observed. PBMCs were isolated and stimulated as described in section 2.1.1. After 72 hour incubation at 37°C with 5% CO_2, the cells were subcultured by centrifugation at 400 x g for five minutes. The cells were infected by incubating the pellet with viral supernatants for one hour at 37°C with 5% CO_2. The infected cell pellet was washed two times with 10% growth media by centrifugation at 400 x g for 10 minutes. The cell pellet was resuspended in 10% growth media at a working concentration of 3 x 10^6 cells/ml. The resuspended cells were seeded at a final concentration of 1.5 x 10^6 cells/ml in 96 multiwell plate and incubated for one hour in standard cell culture conditions. ALLINIs were serially diluted two times to a final concentration ranging from 200µM to 1.56µM and added to the seeded cells thus yielding a concentration gradient. The treated cells were incubated for 96 hours in standard cell culture conditions. Viral activity was monitored using the Vironostika HIV-1 Ab/Ag p24 ELISA kit as described above. EC_{50} values were then calculated using the absorbance readings measured at 620nm using the xMark Spectrophotometer.

2.2 HIV-1 RECOMBINANT PROTEIN EXPRESSION AND PURIFICATION

The HIV-1 His-tagged IN and HIV-1 His-tagged-FLAG IN expression and purification protocol was obtained from Marchand and co-workers[210], Bushman and co-workers[211] and Fish[212] , with several parameters modified.

2.2.1 HIV-1 His-tagged integrase and HIV-1 His-tagged-FLAG integrase expression and IN gene induction

HIV-1 His-tagged-FLAG IN plasmid (pHFIN) was cloned and constructed by GenScript (USA) using NdeI and BamHI as the cloning sites. The plasmid was constructed by cloning an HIV-1 subtype B NL4-3 IN coding sequence into a pET-15b vector with a T7 promoter. HIV-1 subtype B wild type His-tagged IN plasmid pINSD.His.Sol (Catalogue number (Cat #) 2957) was obtained from the National Institute of Health (NIH) AIDS Research and Reference Reagents Program. The pINSD.His.Sol plasmid contains an NL4-3 IN coding sequence with an amino-terminal polyhistidine tag inserted into a pET-15b vector. pINSD and pHFIN was previously transformed into *Eschericia (E) coli* express BL 21 (DE3) chemically competent bacterial cells.[183] The transformed expression plasmids were over-expressed and induced using a similar method. Glycerol stocks of the transformants were grown overnight shaking at 37°C in Luria Bertani broth (LB, Laboratorios Conda, Spain) supplemented with 100 µg/ml ampicillin (AMP, Melford, UK) and 25µg/ml chloramphenicol (Dulfecha Biochemie, Spain). The overnight culture was diluted 100 x in LB media supplemented with 100µg/ml AMP and 100µg/ml chloramphenicol and subsequently grown at 37°C in a shaking incubator. The logarithmic growth phase of the bacterial culture was intermittently monitored until it reached an optical density at 600nm (OD_{600}) of 0.6. The bacterial culture was then induced with 1mM isopropyl β-D-1-thiogalactopyranoside (IPTG, Thermo Fisher Scientific, USA) and further incubated for three hours shaking at 37°C. The induced bacterial culture was centrifuged at 3200 x g for 30 minutes at 4°C. The supernatant was discarded and the pellets were stored at -20°C until bacterial lysis.

2.2.2 Eschericia (E) coli BL 21 DE3 cell lysis

The bacterial pellets collected after induction of the bacterial cultures were resuspended in IN Lysis buffer (10mM $MgCl_2$, 0.25% 3-[(3-Cholamidopropyl)-dimethylammonio]-1-propanesulfonate (CHAPS, Sigma Aldrich, USA), 1mM phenylmethanesulfonylfluoride (PMSF, Thermo Fisher Scientific, USA) and 200 µg/µl DNAse (Sigma Aldrich, USA) made up in IN Binding Buffer (1M NaCl, 5mM imidazole, 20mM HEPES, 5% glycerol, 2mM β-Mercapthoethanol (B-Me, Sigma Aldrich, USA, pH 7.2)). The bacterial cell lysate was disrupted using a homogenizer followed by a one hour incubation stirring on ice. The homogenized cell lysate was sonicated for 1 minute at 75Hz and 0.6 cycles using the Labsonic M ultrasonic processor (Sartorius, Germany). The cell lysate was centrifuged at 10 000 x g for 30 minutes at 4°C and the supernatant was collected for protein purification.

2.2.3 Purification of HIV-1 His-tagged proteins using Nickel affinity chromatography

The ÄKTA PrimePlus (GE Healthcare, UK) fast protein liquid chromatography system was used for protein purification of the HIV-1 His-tagged IN and His-tagged-FLAG IN through Nickel (Ni^{2+}) affinity chromatography. The His-trap HP Ni^{2+} affinity column (GE Healthcare, UK) was adapted to the ÄKTA PrimePlus purification system and equilibrated with 10 column volume washes of IN Binding Buffer. The cell lysate was loaded onto the prepared column at 1ml/minute. The column was then washed with 10 column volume washes of IN Binding Buffer at 3ml/minute followed by a 10 column volume wash with IN Wash Buffer 1 (IN Binding buffer with 60mM imidazole, pH 7.2). A final 10 column volume wash was done with IN Wash Buffer 2 (IN Binding buffer with 125mM Imidazole, pH 7.2) at 3ml/minute. The protein was eluted using a 50ml linear gradient on the ÄKTA PrimePlus purification system. The starting buffer was IN Wash Buffer 2 with IN Elution Buffer (IN Binding with 600mM imidazole, pH 7.2) at a final target of 100%. Fractions were collected at 3ml per fraction with a flow rate of 1ml/minute. The fractions where an increase in UV absorbance at 280nm was observed were collected and pooled. The pooled eluate was concentrated through a 10 kDa filter membrane using an ultra-filtration vacuum system (Merck Millipore, USA) under nitrogen gas pressure.

2.2.4 Buffer exchange of purified protein using a PD-10 Sephadex column

A PD-10 Sephadex column (GE Healthcare, UK) was used to buffer exchange the concentrated protein from IN Elution Buffer to IN Storage Buffer 2 (20mM HEPES, 1M NaCl, 4mM EDTA, 2mM dithiothreitol (DTT), Thermo Fisher Scientific, USA, pH7.2). The column resin was equilibrated with IN Storage Buffer followed by the addition of the protein sample. The IN Elution Buffer was then replaced with IN Storage Buffer upon collection of the protein fractions. The protein concentration was quantified using the Nanodrop 2000 spectrophotometer (Thermo Fisher Scientific, USA) using the NanoDrop installation version 1.3.1 software. The Molar (M) concentration of the protein was calculated using the Beer-Lambert equation: $A=\varepsilon.c.l$ where A represents absorbance at 280nm, ε the molar extinction coefficient (mol^{-1} dm^3 cm^{-1}), c the concentration (mol dm^{-3}) and l the path length (cm). The extinction coefficient for HIV-1 IN is 50 460 units and was used to calculate the M concentration of the purified protein.

2.2.5 HIV-1 His-tagged Rev plasmid construction and transformation

The HIV-1 subtype B HXBII *rev* gene was cloned into a pET-15b vector by GenScript (USA). The 360 bp insert was cloned into the pET-15b vector using restriction sites NdeI and BamHI. The cloned plasmid, pRevHXBII, was transformed into *E.Cloni* express BL21 (DE3) pLYSs competent cells (Lucigen, USA). Transformations were achieved through heat shock according to the kit instructions. The competent cells were thawed on ice to which 1µl of the plasmid was added to 40µl cells and incubated for 30 minutes on ice. The cells were heat shocked through incubation at 42°C for 45 seconds then immediately placed on ice for two minutes. The cells were then added to 960µl Express Recovery Medium and incubated shaking at 250 revs per minute (rpm) at 37°C for one hour. While the heat shocked cells were growing, LB-Lennox agar plates were prepared by adding 1g LB-Lennox Agar powder (Sigma-Aldrich, USA) to 1L dH2O. The solution was dissolved and autoclaved. Following autoclaving, the LB-Lennox agar was allowed to cool to 55°C before adding 100µg/ml AMP and 25µg/ml chloramphenicol. The LB-Lennox agar was then poured onto culture plates and allowed to set. The transformant was plated onto the LB-Lennox agar plates at 100µl, 50µl and 10µl and incubated overnight at 37°C. Colonies were picked the following day and was used to inoculate LB media supplemented with 100µg/ml AMP and 25µg/ml chloramphenicol and grown

overnight shaking at 37°C. The resulting bacterial culture was stored in 60% glycerol in a 1:1 ratio at -80°C.

2.2.6 Expression and purification of His-tagged Rev.

The transformed *E.Cloni* BL21 (DE3) glycerol stocks containing pRevHXBII was used to inoculate LB media supplemented with 100µg/ml AMP and 25µg/ml chloramphenicol. The inoculated LB media was incubated shaking overnight at 37°C. The overnight culture was diluted 100 x in LB media containing 100µg/ml AMP and 25µg/ml chloramphenicol. The inoculated culture was incubated at 37°C shaking until the logarithmic growth phase was reached at OD_{600} = 0.6. The cultures were then induced as described in section 2.2.1.

2.2.7 Purification of HIV-1 His-tagged Rev using Nickel affinity chromatography

Stored induced bacterial pellets were thawed and resuspended in Rev Lysis Buffer (50mM Sodium Phosphate (Sigma Aldrich, USA), 500mM NaCl, 0.02% Sodium Azide (NaN_3) 1mM DTT, 10mM MgCl, 0.25% CHAPS, 1mM PMSF,200µg/ml DNase, pH 7.4). The bacterial cells were lysed using the method described in section 2.2.2. The Ni^{2+} affinity column was adapted to the Äkta PrimePlus protein purification system and equilibrated using Rev Binding Buffer (50mM Sodium phosphate (Sigma Aldrich, USA), 500mM NaCl, 0.02% Sodium Azide (NaN_3) 1mM DTT, pH 7.4). The cell lysate was loaded onto the column at 1ml/minute. The column was washed with Rev Binding Buffer at 3ml/minute for 10 column volumes. Rev Wash Buffer 1 (Rev Binding Buffer containing 25mM imidazole, pH 7.4) was used to wash the column at 3ml/minute over 10 column volumes. Rev Wash Buffer 2 (Rev Binding Buffer containing 60mM imidazole, pH 7.4) was used for a final column wash at 3ml/minute over 10 column washes. The protein was eluted with 700mM imidazole using a 50ml linear gradient into Rev Elution Buffer in 3ml fractions. The eluate fractions were pooled and concentrated using the ultra-filtration vacuum system (Merck Millipore, USA) with a 3kDa filter membrane. The concentrated protein sample was buffer exchanged into Rev Storage Buffer (Rev Binding Buffer with 10% glycerol) using a PD-10 Sephadex column as described in section 2.2.4. The protein concentration was quantified by measuring its absorbance at 280nm using the Nanodrop 2000 spectrophotometer and the M concentration was calculated according to the Beer-Lambert equation using the HIV-1 Rev extinction coefficient of 8600 cm^{-1} M^{-1}.

2.2.8 Confirmation of protein expression and purification

The expression and purification of HIV-1 His-tagged IN, His-tagged IN and His-tagged-FLAG IN was verified by its size through Sodium Dodecyl Sulfate Polyacrylamide Gel Electrophoresis (SDS-PAGE). 10% TGX SDS-PAGE gels were prepared using the TGX stain free Fast Cast acrylamide kit solution (Bio-Rad, USA). The gels were prepared using the instructions from the kit. The resolver acrylamide solution was prepared by adding a propriety mix Resolver A solution to Resolver B solution at a 1:1 ratio. A 10% ammonium persulfate (APS) solution and 0.05% Tetramethylethylenediamine (TEMED, Bio-Rad, USA) was added to the resolver mixture. The prepared acrylamide resolver mixture was dispensed into the gel cassette containing 1mm Bio-Rad glass plates. The stacking solution was prepared by adding equal volumes of Stacking solution A and Stacking solution B together with 10% APS and 0.05% TEMED. The prepared stacking solution was added to the top of the cassette containing the Resolving solution. The comb was inserted and the gel was allowed to set at room temperature for 20 minutes. The purified protein samples were added to 2 x Laemmli Buffer (Bio-Rad, USA) at a 1:1 ratio and boiled for two minutes at 100°C. The samples were loaded onto the SDS-PAGE gel alongside a Molecular weight (MW) marker (Precision Plus Protein Marker, Bio-Rad, USA). The SDS-PAGE gels were equilibrated with 1x Tris-Glycine-SDS (TGS) Buffer (25mM Tris, 150mM glycine, and 0.1% SDS) and separated at 250 volts for 25 minutes. The SDS-page gel was visualised on the Chemidoc MP (Life Science Research, Bio-Rad, USA) using the ImageLab Software version 4.1. The SDS-PAGE gel was transferred to a Polyvinylidene difluoride (PVDF) membrane using iBlot transfer stacks (Life Technologies, USA) and the iBlot gel blotting device (Life Technologies, USA) using the pre-programmed P0 setting. The default run was a total of seven minutes consisting of one minute at 20 volts, four minutes at 23 volts and two minutes at 25 volts. The transferred membrane was removed and blocked overnight in Western blot Blocking Buffer (5% Bovine Serum Albumin (BSA) in 1x TBST (420mM Tris pH 7.6, 137mM NaCl, 0.1% Tween 20)) at 4°C. Western blot analysis was conducted by replacing the Western blot Blocking Buffer with primary antibody (Table 2.4) and incubating the membrane for two hours with agitation at room temperature. The membrane was washed three times with 1x TBST for five minutes. Following the wash step, the membrane was incubated with secondary antibody conjugated to HRP (Table 2.4) for two hours at room temperature. The membrane was washed three times for seven minutes with 1x TBST. Clarity ECL Western blotting chemiluminescent substrate (Bio-

Rad, USA) was added to the membrane and incubated for a further 10 minutes at room temperature. The chemiluminescence produced in the presence of the substrate was detected and analysed using the Chemidoc MP.

Table 2.4: List of primary- and secondary antibodies used in Western blot analysis to confirm the presence of purified recombinant proteins.

Recombinant protein	Primary antibody	Secondary antibody
His-tagged integrase; His-tagged- FLAG integrase	7000x diluted anti-IN (NIH Research and Reference Reagents Program, Cat # 756)	10 000x diluted goat anti-rabbit HRP linked IgG
His-tagged Rev	1000x diluted anti-Rev (NIH Research and Reference Reagents Program, Cat # 7376)	10 000x diluted rabbit anti-mouse HRP linked IgG
FLAG-tagged integrase	1000x diluted anit-FLAG (Sigma, USA, Cat# F3165-.2MG)	15 000x diluted rabbit anti-mouse HRP linked IgG

2.3 MULTIMERZATION STUDIES

2.3.1 Determining multimerization of HIV-1 integrase using an AlphaScreen multimerization assay

The AlphaScreen assay is based on chemical-containing hydrogel-coated latex beads known as the acceptor and donor beads that are able to bind tagged molecules such as proteins. Each bead captures one of the two interacting molecules which bring the beads in close proximity upon interaction of the two molecules. This results in a chemical energy transfer from the donor bead to the acceptor bead that produces light emission from the acceptor bead between 520nm and 620nm.[184] The emitted light is detected as the AlphaScreen luminescent signal and is measured in photons counts per second. In this study, Ni-chelate acceptor beads (Perkin Elmer, USA) will capture recombinant His-tagged IN while the anti-FLAG donor beads

(Perkin Elmer, USA) will capture recombinant FLAG-tagged IN. Multimerization of HIV-1 IN was determined and quantified using the AlphaScreen multimerization assay. Anti-FLAG donor beads (Perkin Elmer, USA) and Ni^{2+} chelate acceptor beads (AlphaScreen Histidine detection kit, Perkin Elmer, USA) were prepared by diluting the beads in AlphaScreen Assay Buffer (25mM Tris, 150mM NaCl, 1mM MgCl, 1mM DTT, 0.01% Tween 20, 0.1% BSA, pH 7.4) to a working concentration of 50µg/ml. FLAG-tagged IN was diluted to a working concentration of 1.5µM in AlphaScreen Assay Buffer while His-tagged IN was diluted in AlphaScreen Assay Buffer to a working concentration of 2.5µM. FLAG-tagged IN was incubated with anti-FLAG donor beads at a 1:1 ratio (Further referred to as FLAG-bead-IN mixture). His-tagged IN was incubated with Ni^{2+}chelate acceptor beads at a 1:1 ratio (further referred to as Ni^{2+}-bead-IN mixture) The IN-bead mixtures were incubated for two hours at room temperature. The FLAG-bead-IN mixture and Ni^{2+}-bead-IN mixture were added together at a 1:1 ratio into half area multiwall Optiplates (Perkin Elmer, USA). ALLINIs or Rev was added to the mixtures at 5µl and the reactions were made up to a final volume of 50µl with AlphaScreen Assay Buffer. A concentration gradient for Mut 101, CX05168 and Rev was conducted. The positive control consisted of a reaction where ALLINIs or Rev was substituted with AlphaScreen Assay Buffer. The negative control consisted of AlphaScreen beads only without HIV-1 IN. The fluorescence emission of the interactions were measured using the Enspire Alpha plate reader (Perkin Elmer, USA). The percentage multimerization was calculated using the following equation:

[(Test sample – Positive control)/ (Positive control)] x 100

2.3.2 Multimerization of HIV-1 integrase through crosslinking experiments

Bis(sulfosuccinimidyl)suberate (BS^3) crosslinking studies were used to evaluate the formation of high order IN oligomers. BS^3 is a crosslinker used to covalently link biological molecules. The amine reactive *N*-hydroxysulfosuccinimide esters positioned on the spacer arms of BS^3 react with primary amines located on the side chains of Lys residues consequently forming amide bonds.[185] As such, crosslinking between two molecules is achieved in the presence of BS^3. HIV-1 IN and HIV-1 Rev was diluted in Crosslinking Assay Buffer (25mM HEPES, 200mM NaCl, 1mM DTT, 1mM EDTA, pH 7.2) to a working stock concentration ranging from 3µM to 10µM. HIV-1 IN and HIV-1 Rev were incubated together at room temperature for one hour. BS^3 crosslinking reagent (Thermo Fischer Scientific, USA) was added to the protein complex at a final concentration of 20µM in a total reaction volume of 20µl. The reaction was incubated for 15 minutes at room temperature followed by quenching of the reaction with 50mM Tris

Buffer. The samples were added to 2x Laemmli Buffer and boiled at 100°C for two minutes for subsequent SDS-PAGE analysis. The SDS-PAGE gel was transferred to a PVDF membrane for Western blot analysis as described in section 2.2.8. The oligomerization of HIV-1 IN was detected using 5000x diluted anti-IN (NIH Research and Reference Reagents Program, Cat # 756) and 10 000x diluted HRP-conjugated rabbit anti-mouse.

2.3.3 Analysing integrase multimerization using Dynamic Light Scattering

Recombinant IN was used to analyse the oligomerization shift of IN in the presence of Rev, Mut 101 and CX05168. The principle of dynamic light scattering (DLS) relies on the irradiation of a sample through a laser light causing light scattering. The intensity of the fluctuated light that was scattered is subsequently measured which provides information about the motion of the particles in the samples. As a result, the diffusion coefficient, dependent on the shape and size of the particle, is calculated.[186] As such, DLS provides a useful platform to analyse aggregation of particles. The DLS based multimerization assay was derived and modified from Kessl and co-workers.[187] Recombinant IN was resuspended in DLS Buffer (1M NaCl, 2mM $MgCl_2$, 2mM DTT, 50mM HEPES, pH 7.4) to a final concentration of 200nM in 1ml. The protein solution was incubated for 30 minutes at room temperature. The ALLINIs were added to the protein solution at a final concentration of 10µM and incubated for 30 minutes at room temperature. Rev was added at a final concentration of 50µM with and without ALLINIs. The samples were analysed using the Zetasizer nano-zs DLS instrument (Malvern instruments. UK). The analysis protocol was set up using the Zetasizer software version 7.02. Briefly, a multi parameter analysis setting was used where samples were initially equilibrated for 120 seconds followed by 10 readings with 60 second pauses between each reading. DLS Buffer was recorded as a negative control.

2.4 ELISA STUDIES

ELISA studies were conducted to determine the interaction of HIV-1 IN and HIV-1 Rev in the absence and presence of Mut 101 and CX05168 as well as the K_d of the interaction in the absence and presence of Mut 101 and CX05168. His-tagged IN was coated onto Nunc Maxisorp multiwall ELISA plates (Nunc, Denmark) at a final concentration of 0.3µM in 0.05M Sodium Carbonate Coating Buffer (pH 9.6) overnight at 4°C. The coated plate was blocked for two hours at room temperature with 10% BSA in ELISA Buffer (PBS with 0.02% Tween 20 and 10% BSA). HIV-1 Rev was added to the plate and incubated for two hours at room temperature at a concentration gradient ranging from 10µM to 1µM in ELISA Buffer. Excess

Methods

HIV-1 Rev was removed by washing the wells three times with ELISA Wash Buffer (PBS with 0.02% Tween 20) for five minutes per wash. Primary antibody, anti-Rev (NIH Research and Reference Reagents Program, Cat # 7376), was diluted 200x in ELISA Buffer and subsequently added to the wells. The reactions were incubated for one hour at room temperature. The wells were washed three times for five minutes with ELISA Wash Buffer to remove excess primary antibody. Secondary antibody, HRP conjugated rabbit anti-mouse, was diluted 10 000x in ELISA Buffer and subsequently added to the wells. The reactions were incubated for one hour at room temperature. A final wash step was conducted three times for 10 minutes to remove excess secondary antibody. TMB substrate (Invitrogen, USA) was added to the wells and the reactions were incubated for 30 minutes at 37°C. The colometric changes were quantified by reading the absorbance values of the reactions at 620nm using the SpectraMax Spectrophotometer. The order of addition experiments were conducted to determine the effects of ALLINIs before and after Rev was added to the reaction. The order of addition where ALLINIs were added before Rev was termed IN-ALLINI-Rev. The order of addition where ALLINIs were added after the addition of Rev was termed IN-Rev-ALLINIs. Each compound incubation step was followed by a wash step consisting of three washes with ELISA Wash Buffer for five minutes. An additional order of addition experiment was conducted where 1µM Rev was coated onto the 96 Maxisorp plate in the same manner to which IN was coated as described above. This order of addition was termed Rev-IN + ALLINI. IN at 1-, 5- and 10µM was incubated with the ALLINIs for 15 minutes at room temperature. The IN-ALLINI complex was subsequently added to the Rev coated multiwell plate. The interaction was detected using 500x diluted anti-IN (NIH Research and Reference Reagents Program, Cat # 756) and detected using 10 000x HRP-linked goat anti-rabbit secondary antibody. TMB substrate was added and the colometric change was quantified by reading its absorbance wavelength at 620nm using the SpectraMax Spectrophotometer. The absorbance values quantified for the ELISA reactions described above were used to determine the K_d of each interaction. The K_d were calculated using the Lineweaver-Burke equation:

$1/V = (K_m/V_{max})\ 1/[S] + 1/V_{max}$ where V is the reaction rate, K_m is the Michaelis-Menten constant, V_{max} is the maximum reaction velocity and [S] is the substrate concentration.

2.5 CHARACTERIZING THE INTERACTION BETWEEN HIV-1 INTEGRASE AND REV THROUGH ISOTHERMAL TITRATION CALORIMETRY.

2.5.1 Isothermal titration calorimetry

A direct measure of an interaction between two molecules can be determined by quantifying the heat absorbed or emitted upon the interaction of the two molecules. The heat is measured through a direct method such as Isothermal titration calorimetry (ITC) As such, the interaction between recombinant HIV-1 IN and Rev were analysed using ITC. The Nano ITC (TA Instruments, USA) was used to carry out these experiments in conjunction with the Nano ITC data collection program, ITCRun software version 2.2.5.0. Both proteins were buffer exchanged into ITC Buffer (1M NaCl, 1mM DTT, 2.5mM BME, 20mM HEPES and 5% glycerol) through dialysis for 24 hours at 4°C. The proteins and ITC Buffer were degassed using a vacuum pump and diluted to its working concentration. IN was added to the sample cell while Rev was the titrant. The stirring rate was set at 250 rpm; an injection volume of 8µl for 31 injections was used and a 300 second delay period between injections. When analysing the IN-Rev interaction in the presence of Mut 101 and CX05168, IN was incubated with 100µM Mut 101 or CX05168 for 1 hour at room temperature. IN in the presence of Mut 101 or CX05168 were added to the sample cell while Rev was titrated into the complex as described above. As a control experiment, Rev was titrated into the sample cell containing ITC Buffer. The data collected was analysed using the NanoAnalyze Data Analysis software version 3.3.0 (TA instruments, USA). The Gibbs free energy was calculated using the standard Gibb free energy equation: $\Delta G = \Delta H - T\Delta S$ where ΔH represents the change in enthalpy and $T\Delta S$ represents the change in temperature entropy in Kelvin (K).

2.5.2 Determining the Tryptophan fluorescence spectra of resultant ITC reactions

Tryptophan fluorescence is commonly used to determine the integrity of a protein. The resultant ITC reactions from section 2.5.1 containing IN, Rev and ALLINIs were analysed to evaluate the integrity of the interactions. The prepared samples were added to a 10mm QS micro cuvette and the fluorescence spectra of the proteins were determined using the FF-6300 Spectrafluorometer (Jasco Corporation, USA). The fluorescence spectra were analysed

using the Spectra manager software version 1.06.04 using the spectrum management setting. The following parameters were used: Excitation wavelength at 280nm, emission wavelength from 260nm to 500nm, data pitch at 0.5nm and excitation- and emission bandwidth at 2.5mm or 5mm. The Assay Buffer (1M NaCl, 1mM DTT, 2.5mM BME, 20mM HEPES and 5% glycerol) was used as a blank while the compounds alone were used as negative controls.

2.6 DATA ANALYSIS

All quantitative experiments were conducted in three independent experiments comprising duplicates (n =6). Statistics were calculated using the mean of each experiment. Mean values and standard deviations (SD) were calculated using Microsoft Excel 2013 from which bar graphs and line graphs were generated. Pairwise t-tests were conducted to determine the statistical difference (*p*-value) between protein-ALLINI interactions as well as the difference between EC_{50} values of *in vitro* selected samples. This was calculated using an online calculator, simple interactive statistical analysis (Sisa) tool (www.quantitativeskills.com/sisa/). EC_{50} values were calculated using OriginPro 8 SRO version 8.0724 (OriginLab, USA). Sigmoidal curves and subsequent Hill-slope coefficients were generated using this software.

CHAPTER 3

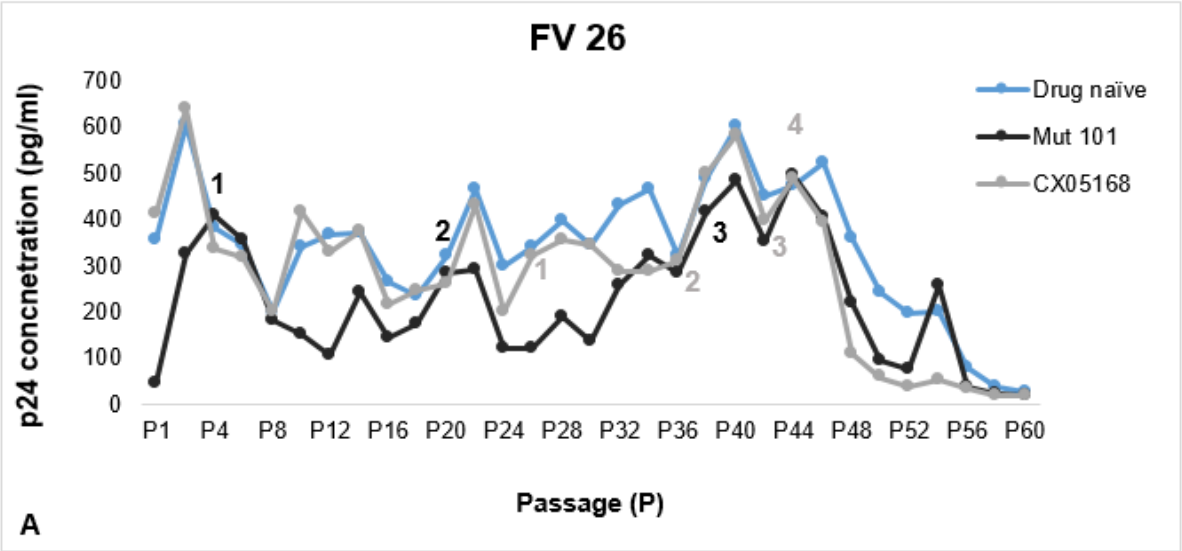
Results

3.1 IN VITRO SELECTION STUDIES TO SELECT HIV-1 DRUG RESISTANCE MUTATIONS

The aim of the first objective (section 1.6) was to select resistant mutations in the HIV-1 *IN and rev* gene with ALLINIs, CX05168 and Mut 101. This was achieved through *in vitro* selection experiments followed by gene sequence analysis to determine possible mutations.

3.1.1 Classical in vitro selection of CX05168 and Mut 101 selected viruses

PMBCs were successfully infected with primary subtype C HIV-1 FV 3 and FV 26 and their respective $TCID_{50}$ was successfully determined. *In vitro* selection studies commenced by treating PBMCs with Mut 101 and CX05168 at its published EC_{50} values of = 0.5µM and 3µM, respectively.[167,168] Untreated cells were used as the positive control. Cells were treated for 26 weeks over 60 passages. Viral growth kinetics of treated and untreated (Drug naïve) FV 26 and FV 3 isolates are represented in figure 3.1. Compound was added weekly and the concentration remained constant until viral breakthrough was observed. The compound concentration was increased two fold upon viral breakthrough. For both FV 3 and FV 26, no inhibition of viral activity was observed when treating the cells with 3µM CX05168. As such, the dose of CX05168 was increased two fold at p26 (6µM) to ultimately 96µM in order to inhibit viral replication. Viral activity appears to have decreased in both FV 3 and FV 26 at p48 at a dose of 96µM. Viral breakthrough was observed three times with FV 26 (Figure 3.1 A) selected by Mut 101 at p6, p20 and p40 where doses were increased to 1µM, 2µM and 4µM. The drug naïve cell controls showed steady viral replication in both FV 3 and FV 26 isolates. For FV 3 (Figure 3.1 B), viral breakthrough was observed twice at p8 and p12 when treated with Mut 101 where doses were subsequently increased to 1µM and 2µM, respectively. However, viral activity decreased extensively from p13 under Mut 101 treatment. PBMCs were then re-infected with supernatant stored at p12 and subsequently treated with 2µM Mut 101.



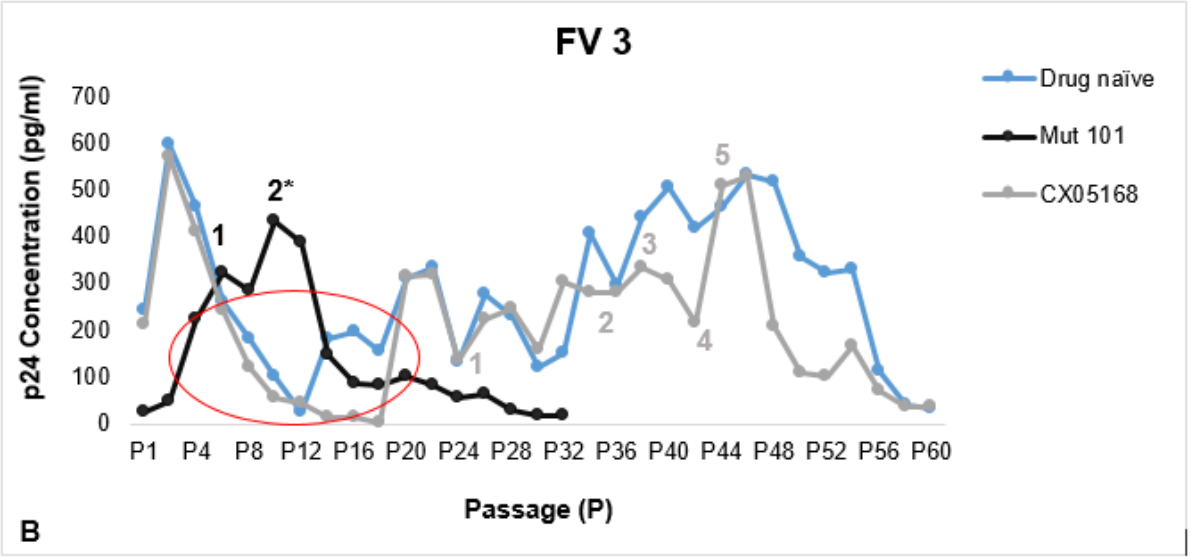


Figure 3.1: Representation of A) FV 26 and B) FV 3 viral growth kinetics in drug pressure studies selected by Mut 101 and CX05168. *p24 levels was expressed in terms of pg/ml obtained through the Vironostika HIV Ag/Ab p24 ELISA kit. The p24 expression levels were monitored at every second passage (p). The numbers in the graph denotes the passage at which the compound concentration, Mut 101 (black) and CX05168 (grey), was increased two fold. The demarcated area shows a rapid decrease in viral activity in the drug naïve cells and CX05168 treated cells.*Indicates the point at which Mut 101 diminished viral activity and PBMCs were re-infected with supernatant from p12*

3.1.2 In vitro phenotypic inhibition assays of CX05168 and Mut 101

3.1.2.1 EC_{50} values of CX05168 against FV 26 and FV 3

Due to the lack of inhibition of primary subtype C FV 3 and FV 26, when treated with CX05168 at concentrations above the EC_{50} (2.3µM), an antiviral assay was conducted to determine the EC_{50} of CX05168 against these primary HIV-1 subtype C isolates (Figure 3.2). The EC_{50} of CX01568 obtained in these experiments were compared to the EC_{50} of CX05168 previously determined against HIV subtype B, NL4 – 3 in MT4- and PBMC cell lines. The EC_{50} for CX05168 against FV 26 was calculated at 40.1 ± 0.8µM, 17 fold higher than the documented EC_{50} of CX05168 at 2.35 ± 0.28µM.[165] Although the EC_{50} of CX05168 against FV 3 (4.3 ± 0.4µM) is not considerably higher than the reported EC_{50}, the difference is considered significant ($p < 0.001$, n = 6).

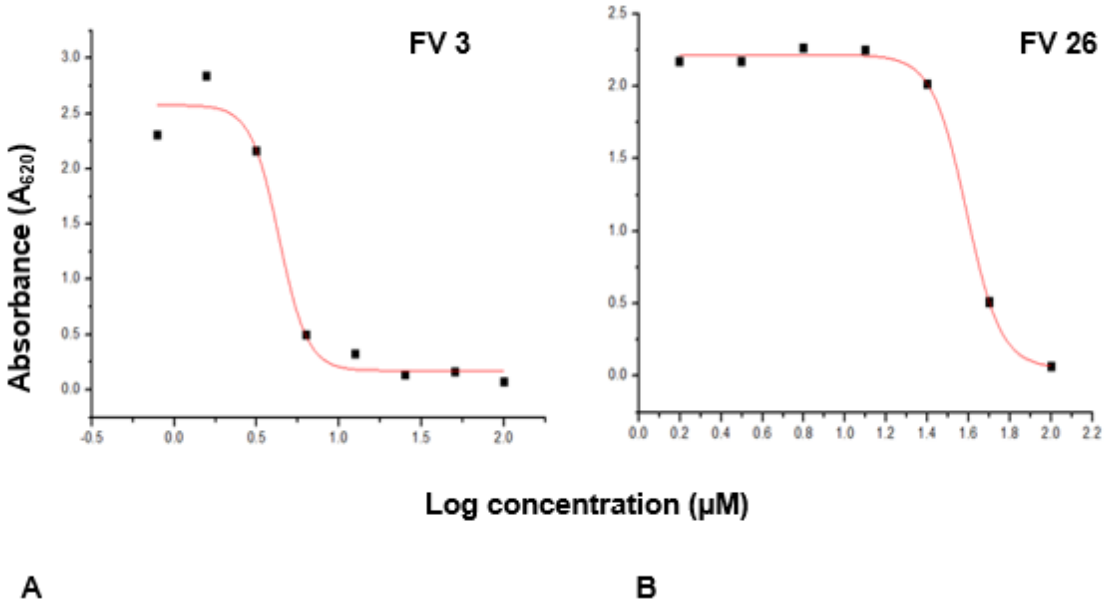


Figure 3.2: Sigmoidal curves depicting the EC_{50} values of CX0516 against primary subtype C A) FV 3 and B) FV 26 in PBMCs. *The Hill-Slope coefficient of FV 26 and FV 3 was calculated at < 1. The steep slopes of the sigmoidal curves typifies the antiviral effect of allosteric integrase inhibitors.*

3.1.2.2 Determining the phenotypic resistance of FV 26 and FV 3 viruses selected by Mut 101

In order to determine whether the passaged primary viruses were in fact resistant to Mut 101, *in vitro* phenotypic inhibition assays were conducted against Mut 101 selected viral strains. The supernatants of viral strains where viral breakthrough was observed (Figure 3.1) were used to infect PBMCs. The infected PBMCs were treated with Mut 101 in a dose response manner to determine the EC_{50} of the selected viral strains. Figure 3.3 depicts the EC_{50} value of Mut 101 against Mut 101 selected FV 26 and FV 3 isolates. The EC_{50} value of Mut 101 against drug naïve FV 3 (0.48 ± 0.15µM) and FV 26 (0.53 ± 0.01µM) isolates correlated with the EC_{50} of Mut 101 documented by Le Rouzic et al, 0.54µM (p > 0.05).[167] Mut 101 demonstrated an EC_{50} value of 0.21 ± 0.11µM against isolate FV 26 p6, 0.38 fold lower than the EC_{50} value of Mut 101 against drug naïve FV 26, however not significant (p > 0.05). Mut 101 against isolate FV p26 demonstrated the highest EC_{50} value with 2.67 ± 0.95µM with an $FCIC_{50}$ of 4.94. Supernatant from FV 3 p8 and FV 26 p41 failed to infect PBMCs and therefore EC_{50} values could not be determined.

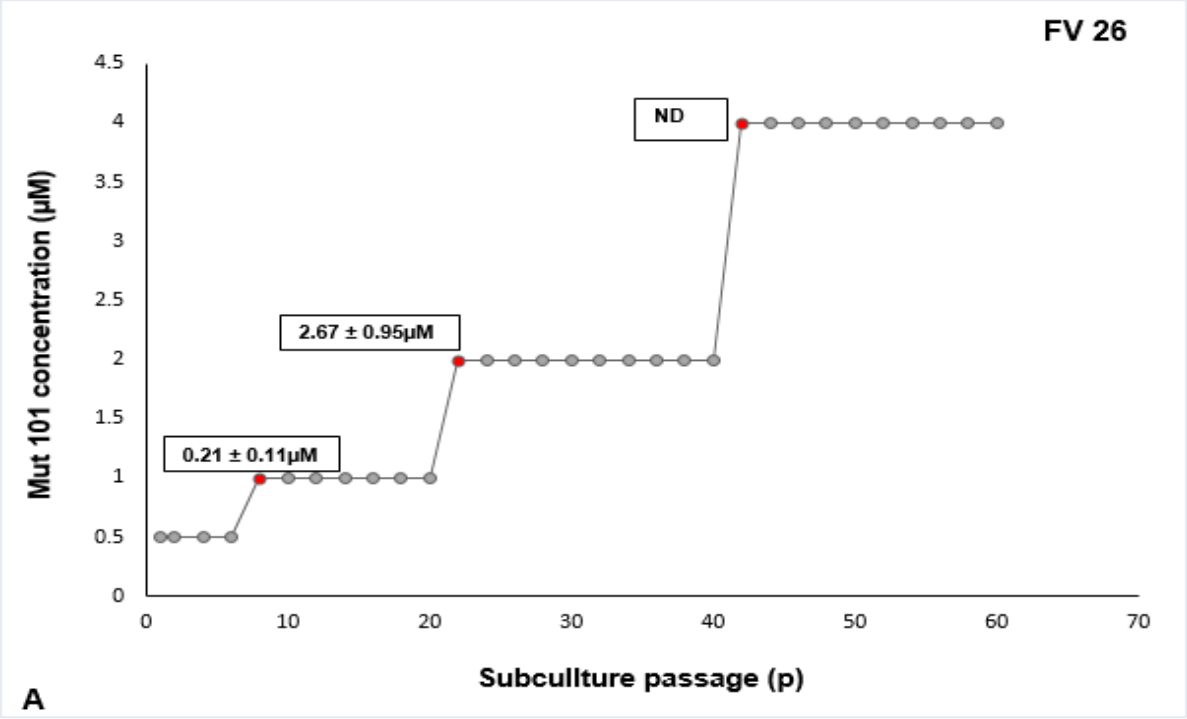


Figure 3.3 continued

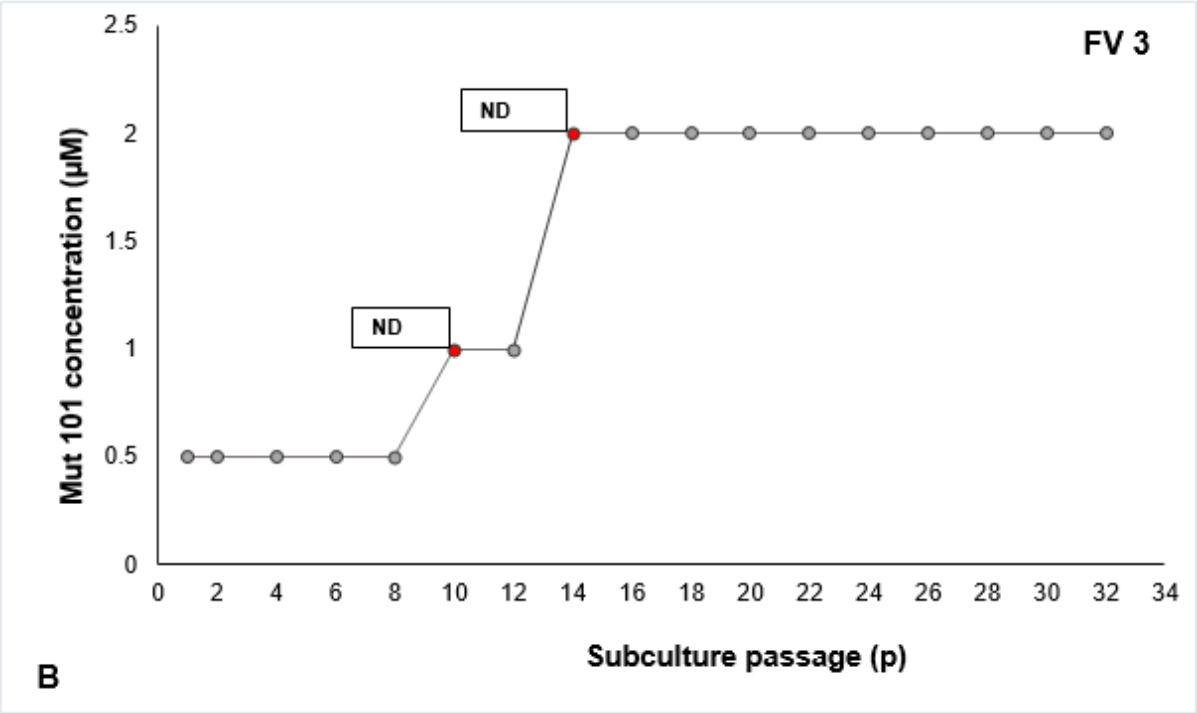


Figure 3.3: Dose escalating curves of Mut 101 monitored at every second subculture passage (p) against primary HIV-1 subtype C A) FV 26 and B) FV 3. *Viral breakthrough is denoted by the red marker where the Mut 101 concentration was increased two fold. The denoted isolates were phenotyped by determining the EC_{50} value of Mut 101 against the isolate (displayed alongside the denoted red marker).*

The dose-response curves exhibiting the EC_{50} value shift from drug naïve FV 26 to selected virus FV 26 p20 is compared and represented in figure 3.4. The EC_{50} curves were plotted using the percentage inhibition versus the log concentration of the compound.

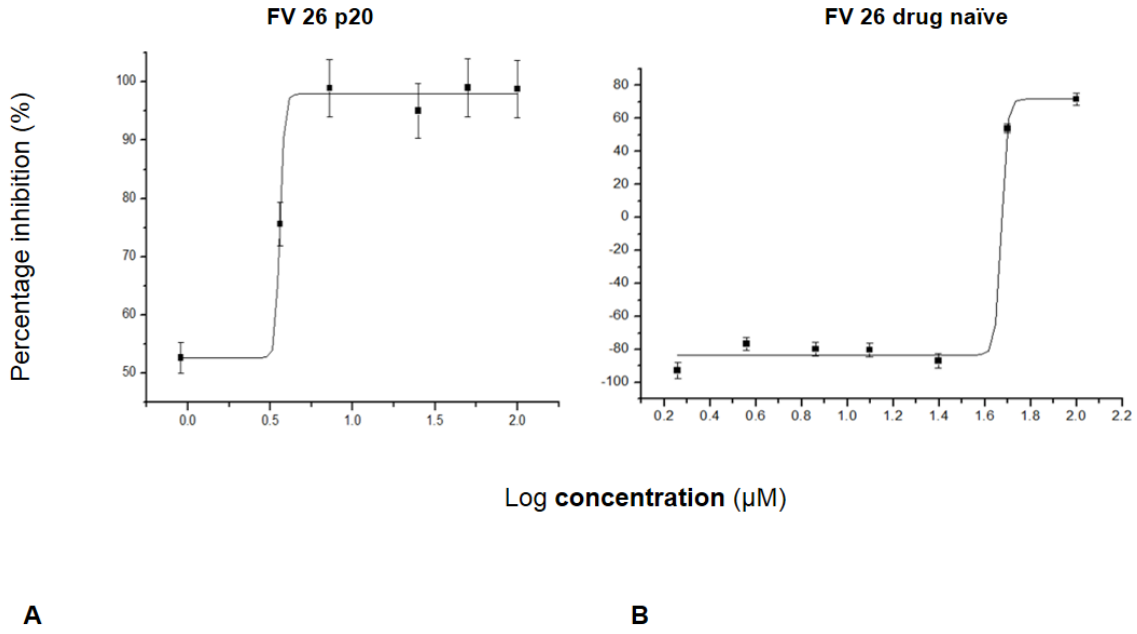


Figure 3.4: Sigmoidal curves demonstrating the dose response of Mut 101 against A) FV 26 drug naïve and B) FV 26 p20 in in vitro phenotypic inhibition assays*. The data is a representation of the average of three independent experiments comprising duplicates per experiment (n = 6).*

3.1.3 Genotypic analysis of the Mut 101 resistant selected FV viral isolates

Genotyping of *in vitro* selected isolates at different passages were conducted through Sanger-based sequencing of the *IN* gene. Figure 3.5 illustrates the aa sequence alignment of the Mut 101 selected FV 3 and FV 26 isolates. This alignment identified the aa substitutions present in each isolate. BLAST results indicated that FV 3 was 98% aligned to IN subtype C and 96% aligned to IN subtype B. FV 26 was less identical to both IN subtype B (94%) and subtype C (97%) compared to the alignment of FV 3. Polymorphisms were found (Table 3.1) in drug naïve FV 3 and FV 26 when compared to a consensus HIV-1 subtype C sequence as well as a consensus subtype B sequence. Polymorphisms differed between FV 3 and FV 26 substantiating the BLAST results. Majority of the aa substitutions identified in FV 3 and FV 26 drug naïve isolates were similar to the reported substitutions for subtype B and subtype C. Aa substitutions such as T218I and A265V identified in isolate FV 3 drug naïve were substituted with residues (Ile and Val) present in consensus subtype C. As such, the substitution differs from subtype B and is aligned with subtype C. However, since FV 3 is a primary subtype C

isolate, the aa substitutions observed when aligning FV 3 drug naïve against IN subtype B, is impertinent. Furthermore, V265 is the consensus residue for IN subtype C whereas A265 is the consensus residue for IN subtype B therefore V265A observed in FV 26 drug naïve could be considered a polymorphism in the subtype C isolate.

Table 3.1: Polymorphism present in drug naïve FV 3 and FV 26 isolates when compared to HIV-1 subtype B- and C consensus sequences

Isolate	**Subtype C consensus substitutions**	**Subtype B consensus substitutions**	
	Amino acid substitution	***Amino acid substitution***	***% subtype B site conservation***
FV3	Y100F	Y100F	98.2
	Q177L	Q177L	97.6
	A124T	A124T	73.5
		T218I	58
		A265V	88.2
FV26	V265A		
	K14R	K14R	56.5
	S255G	S255G	81.2
	G163E	G163E	85.5
	I84M	I84M	82.4
	K215N	K215N	91.8
	A124N	A124N	73.5

The percentage (%) subtype B site conservation data was extracted from The HIV mutation browser (http://hivmut.org/index.php, accessed 5 September 2017).[188]

According to the aa sequence alignment (Figure 3.5), possible resistant mutations emerged in Mut 101 selected FV isolates when compared to the drug naïve isolates, shown in Table

3.2. One of the major ALLINI mutations, H171, was observed in the FV 3 isolate after eight passages (Mut 101 = 1μM). The H171 mutation was also observed in the FV 26 isolate after 41 passages (Mut 101 = 4μM). H171 was substituted with aa L and Q for FV 3 p8 and FV 26 p41 isolates, respectively. The emergence of the H171 mutation is corroborated by the findings by Slaughter *et al*, 2014, that reported the H171 mutation as a major ALLINI resistant pathway.[171] Phenotypic analysis for both these isolates could not be determined through *in vitro* phenotypic inhibition assays due to the lack of infectivity of the viral isolates. In the FV 26 isolate, a Q164L mutation emerged after passage 6 (Mut 101 = 1μM) and disappeared after 20 passages. Interestingly, the EC_{50} value of Mut 101 against isolate FV 26 p6 reduced to 0.21 ± 0.11μM ($p > 0.05$). Mutation, L172I, emerged after 20 passages and was observed in FV 26 p20, FV 26 p21 and FV 26 p41 isolates. A five fold increase in EC_{50} value (2.67 ± 0.95μM) was observed against the FV 26 p20 selected isolate.



Figure 3.5: Amino acid (aa) sequence alignment of HIV-1 integrase (IN) primary subtype C FV 3 and FV 26 isolates selected by Mut 101.

The highlighted residues depict aa substitutions when compared to consensus IN subtype B- and C. Red residues – polymorphisms in both subtype B- and C. Green residues – polymorphisms in subtype B only. Magenta residues –polymorphisms in subtype C only. Blue residues – emerged mutations in drug treated isolate

Table 3.2: Correlation between the genotype and phenotype of Mut 101 selected FV 3 and FV 26 isolates

			Genotype	Phenotype	
FV viral strain	**Passage**	**Mut 101 concentration (µM)**	**Amino acid substitution**	**EC_{50} ± SD (µM)**	**Fold change**
3	Drug naïve	0		0.48 ± 0.15	
3	8	1	H171L	ND*	
26	Drug naïve	0		0.53 ± 0.01	
26	6	1	Q164L	0.21 ± 0.11	2.5 fold reduction
26	20	2	L172I	2.67 ± 0.95	5 fold increase
26	41	4	L172I H171Q	ND	

*Not done

3.1.4 In Silico effects of the identified mutants on the ALLINI – integrase interaction

Molecular docking studies were conducted to determine if the mutations identified in section 3.1.3 impact the interaction between IN and Mut 101. The binding energies (glide emodel) as well as docking scores of wild type IN and mutant IN were compared. Table 3.3 lists and compares the docking scores of each IN mutant. Wild type IN had the lowest docking score (-6.399 Kcal/mol compared to the IN H171Q/L172I mutation that yielded the highest docking score (-5.972 Kcal/mol). A high docking is generally associated with a weak interaction

between two molecules. The docking score of the mutants increased with an increase in passage number. A similar observation was made when comparing the binding energies of wild type IN and the mutant IN isolates. Wild type IN had the lowest Glide emodel score (-70.169Kcal/mol) where L172I/H172Q yielded the highest Glide emodel score (-66.334Kcal/mol). The Glide emodel value increased with an increase in passage number.

Table 3.3: The molecular docking binding energies between integrase mutants and Mut 101

FV 26 isolate	Mutant	Docking Score (Kcal/mol)	Glide emodel (Kcal/mol)
Drug naive	Wild type	-6.399	-70.169
Passage 6	Q164L	-6.129	-68.222
Passage 20	L172I	-6.098	-68.420
Passage 41	L172I H171Q	-5.972	-66.334

When analysing the wild type IN interaction with Mut 101, it is evident that the molecular docking results in this study correlate with the docking studies reported in literature, described in section 1.3.6.2.[167] The two dimensional (2D) structure (Figure 3.6 A) of the interaction between wild type IN and Mut 101 showed that the carboxylic group of Mut 101 forms three hydrogen bonds with aa residues His-171, Glu-170 and Thr-174 on side chain A. The side chain of Thr-174 forms two hydrogen bonds with the ester on the carboxylic group of Mut 101 and an additional hydrogen bond with the carbonyl group on Mut 101. Furthermore, a hydrogen bond connects Gln-95 with the nitrogen atom of the pyridine moiety on Mut 101. Figure 3.6 B represent the interaction between IN mutant Q164L and Mut 101. The 2D structure reveals that IN bearing Q164L exhibited a similar interaction as wild type IN. In the presence of the L172I mutation (Figure 3.6 C), the loss of a hydrogen bond between Gln-95 and the nitrogen atom on the pyridine ring on Mut 101 was observed. This probably results in the weakening of the interaction between Mut 101 and IN in the presence of L172I. Figure 3.6 D depicts the interaction between IN and Mut 101 in the presence of H171Q/L172I. The loss

of two hydrogen bonds were observed in the presence of H171Q/L172I. This includes the hydrogen bond between Thr-174 and the carboxylic group on Mut 101 as well as the hydrogen bond between the nitrogen atom on Mut 101 and Gln-95.

A

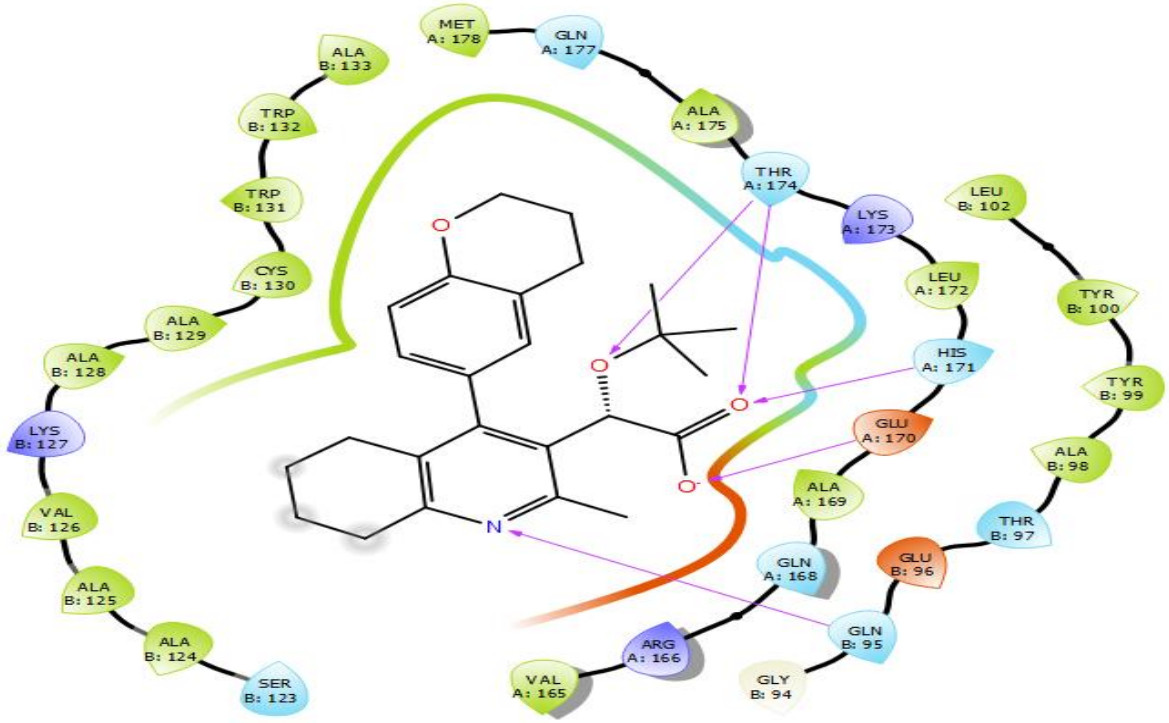
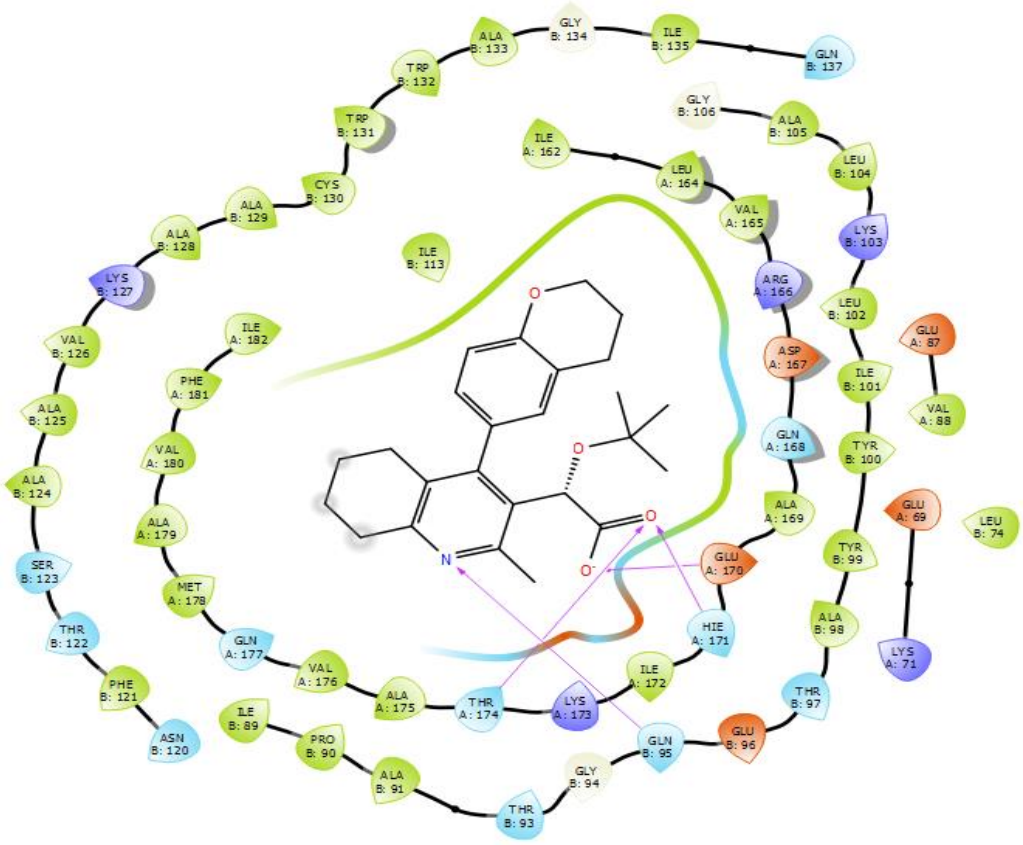
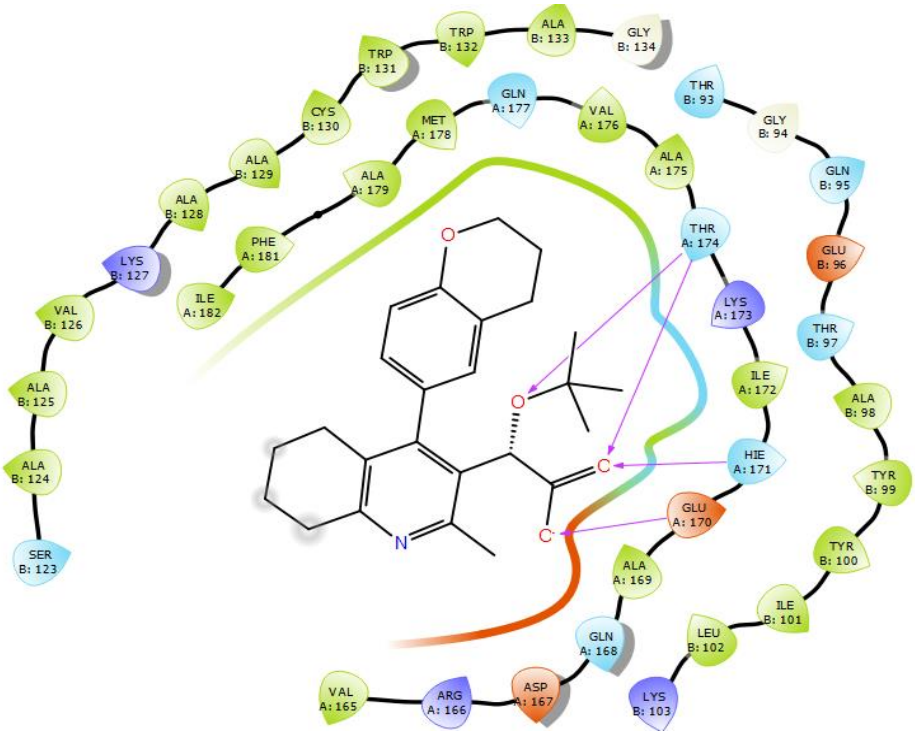


Figure 3.6: Molecular docking of integrase (IN) mutants with Mut 101. *Representation of the interaction between Mut 101 and* ***A)*** *wild type IN* ***B)*** *IN mutant Q164L* ***C)*** *IN mutant L172I and* ***D)*** *IN H171Q/L172I. Schrodinger Maestro suite 11.2 was used to dock Mut 101 into wild type IN as well as IN harbouring mutations selected by Mut 101 during in vitro selection studies. The three letter IUPAC amino acid codes are used to denote the amino acids involved in the interaction between IN and Mut 101 whereas the pink lines depict the hydrogen bonds.*

Figure 3.6 continued

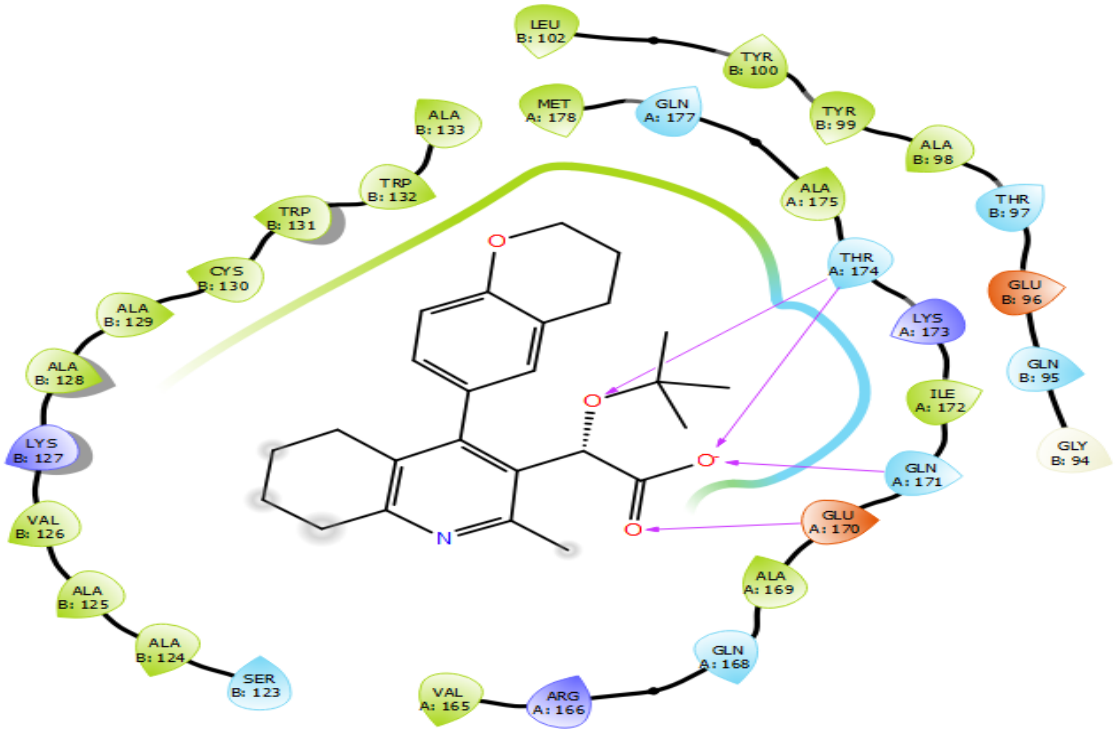


B



C

Figure 3.6 continued



D

Figure 3.6 continued

3.2 PURIFICATION OF RECOMBINANT HIV-1 VIRAL PROTEINS

Recombinant proteins were required for downstream experiments such as ELISAs, AlphaScreen multimerization assays, multimerization crosslinking studies, and DLS analysis. These recombinant HIV-1 proteins include, subtype B His-tagged IN, His-tagged Rev and His-tagged-FLAG IN. The proteins were successfully purified using Ni^{2+}-affinity chromatography after the induction and lysis of BL21 (DE3) bacterial cells. The protein expression and purification steps of His-tagged IN, His-tagged Rev and His-tagged-FLAG IN were analysed using SDS-PAGE illustrated in Figure 3.7. The purified recombinant proteins were observed at their expected sizes of 32 kDa, 19 kDa and 36 kDa for His-tagged IN, His-tagged Rev and His-tagged-FLAG IN, respectively.

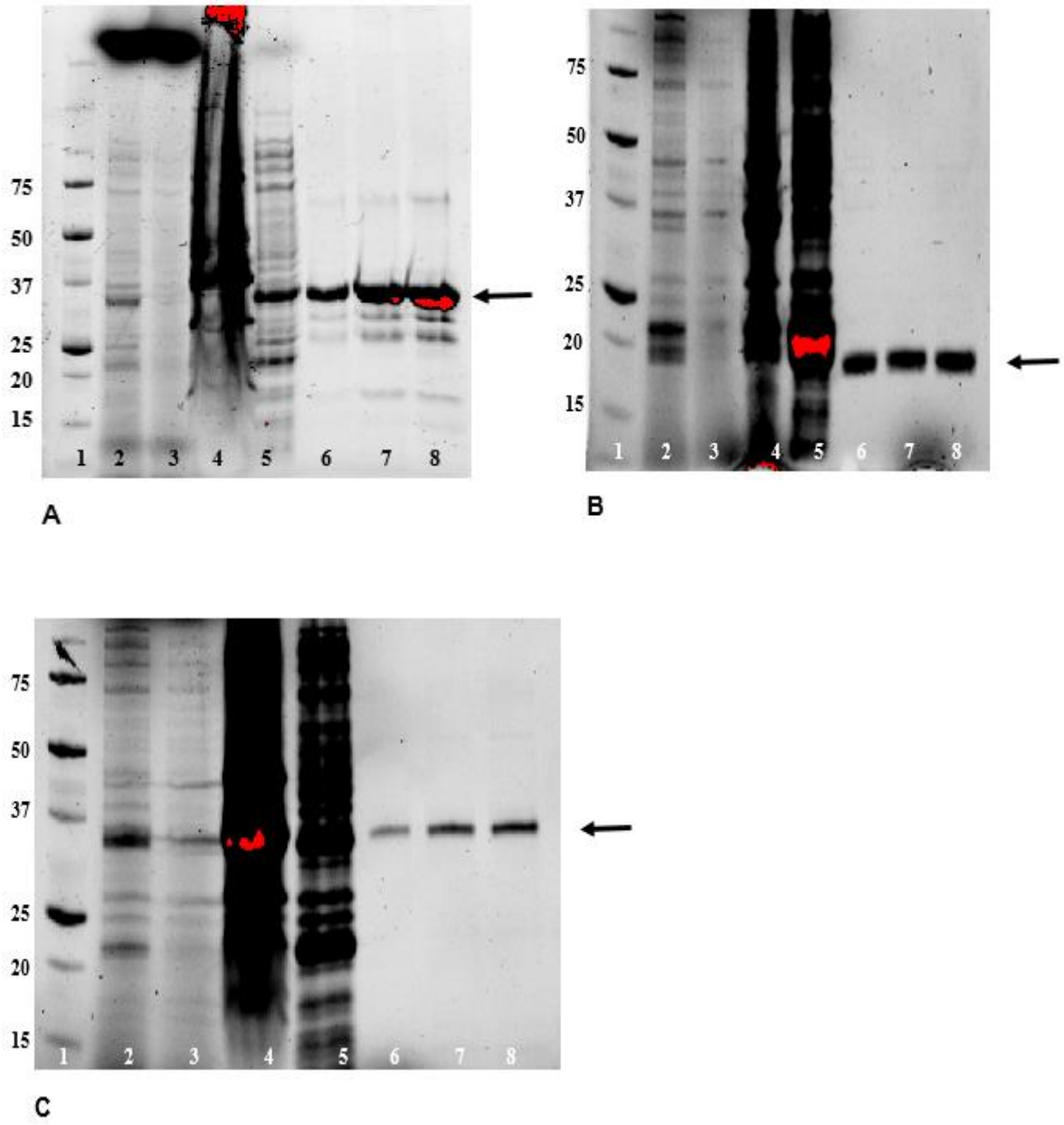


Figure 3.7: SDS-PAGE analysis of the expression and purification processes of recombinant HIV-1 His-tagged proteins, A) His-tagged integrase B) His-tagged Rev C) His-tagged-FLAG integrase*. Lanes 1-8 represent the following steps: 1 - Precision Plus Protein™ marker (Bio-Rad, USA), 2 - IPTG induced BL21 (DE3) cells, 3 - Uninduced BL21 (DE3) cells, 4 - Lysate (Pellet), 5 - Lysate (Supernatant), 6 - Pooled eluate fractions, 7 - Concentrated protein, 8 - Buffer exchanged protein. SDS-PAGE analysis indicates a clear expression of each recombinant protein after induction with IPTG (Lanes 2) and uninduced samples (Lanes 3) at the expected sizes of the proteins demarcated by the arrow. Lanes 4 and 5 compares the pellet and supernatant of the lysate after centrifugation where bulk of the protein was present in the supernatant. Lane 6 represent a pooled sample of the fractions*

eluted with imidazole. A concentrated protein sample was obtained using an ultra-filtration Millipore System which can be observed in Lane 7. The proteins were buffer exchanged into their respective storage buffers using a PD-10 Sephadex column shown in Lane 8. Molecular Weight (in kDa) is indicated on the left.

The purification of the recombinant proteins were successfully validated through Western blot analysis illustrated in Figure 3.8. Positive controls included recombinant proteins received from the NIH Research and Reference Reagents Program. Recombinant His-tagged IN was detected with anti-IN primary antiserum at its expected size of approximately 32 kDa (Figure 3.8 A). The intensity of the band increased with the increase in protein concentration. Rev was used as a negative control and was undetected by the IN antiserum. Recombinant Rev protein was detected in a concentration dependent manner at its expected size of 19 kDa using anti-Rev primary antibody (NIH Research and Reference Reagents Program, Cat # 7376, Figure 3.8 B). Recombinant Rev protein received from the NIH Research and Reference Reagents Program (Cat # 12707) was used as a positive control and was detected at the approximate level of Rev on the Western blot. Anti-FLAG primary antibody detected FLAG-tagged IN at its approximate size of 36 kDa in a dose dependent manner (Figure 3.8 C). His-tagged IN was used as a negative control and was undetected as expected.

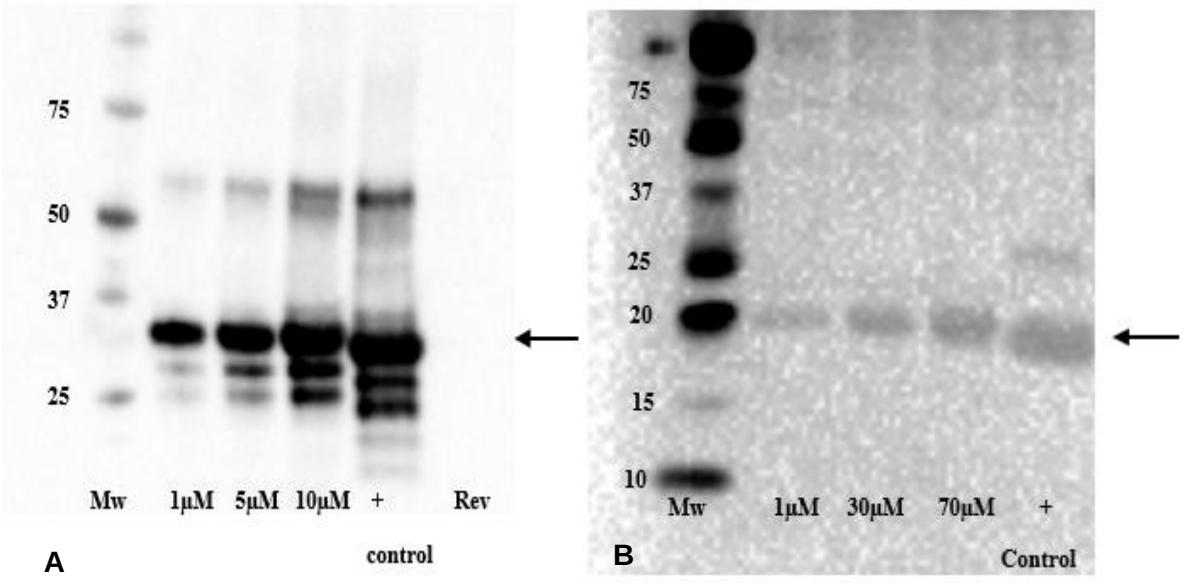


Figure 3.8 continued on the following page

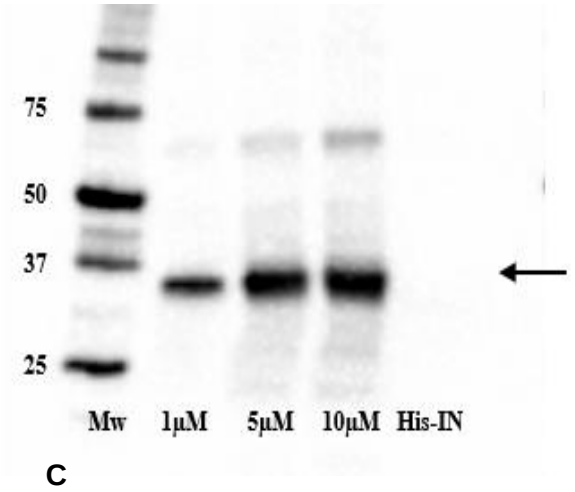


Figure 3.8: Western blot analysis detecting recombinant A) HIV-1 integrase (IN) B) HIV-1 Rev and C) HIV-1 FLAG-tagged IN. A) *IN was detected using polyclonal IN antiserum (NIH Research and Reference Reagents Program, Cat # 756). A concentration gradient of IN at 1-, 5- and 10µM was observed as well as a positive control, HIV-1 NL4-3 IN (NIH Research and Reference Reagents Program, Catalogue (Cat #) number 7274). Recombinant HIV-1 Rev (30µM) was added as a negative control and was undetected. An increase in band intensity was visually observed with an increase in IN concentration at the expected size of approximately 32 kDa.* ***B)*** *Rev was detected using anti-Rev (NIH Research and Reference Reagents Program, Cat # 7376). The arrow depicts the Rev protein at its expected size of approximately 19 kDa. A concentration gradient was observed between 30-, 50-, and 70µM Rev that correlated with the positive control Rev (NIH Research and Reference Reagents Program, Cat # 12707).* ***C)*** *Anti-FLAG antibody detected the recombinant Flag-tagged IN in a concentration gradient manner at its expected size denoted by the arrow. His-tagged IN was used as a negative control and was undetected as expected. Molecular Weight (in kDA) is indicated on the left.*

3.3 EFFECT OF MUT 101, CX05168 AND HIV-1 REV ON IN MULTIMERIZATION

3.3.1 Crosslinking studies evaluate the multimerization of IN induced by ALLINIs and HIV-1 Rev

The ability of IN molecules to interact with each other to form higher order multimers of IN was evaluated through chemically crosslinking proteins. BS^3 crosslinker was used in this study to monitor the multimerization of IN induced by Mut 101, CX05168 and Rev. The multimers of IN

were validated through Western blot analysis detecting IN (Figure 3.9). When analysing the IN sample that does not contain BS^3, a monomeric isoform of IN was detected at approximately 32kDa while a faint band was observed at approximately 72 kDa correlating to the dimeric isoform of IN. With exception of a non-specific band, no bands correlating to IN were detected in the Rev only lane (Negative control). The BS^3 crosslinker in the presence of IN caused a shift in oligomerization of IN from a monomer to a dimer isomer. Rev induced IN multimerization resulting in IN tetramers and dimers. Both Mut 101 and CX05168 at 1µM and 10µM induced aberrant IN multimerization where higher order IN multimers were observed which ultimately lead to the decrease in IN monomers. The IN dimer intensity increased in the presence of 10µM Mut 101 when compared to the multimers formed in the presence of 1µM Mut 101. IN monomers were undetectable in the presence of 10µM CX05168 resulting in an increase in higher order IN isoforms. Rev in the presence of Mut 101 and CX05168 appeared to reduce higher order oligomerization consequently yielding an increase in monomers, dimers and tetramers when compared IN multimers induced by Mut 101 and CX05168. In the presence of both Mut 101 and Rev, a decrease in IN monomers was observed which resulted in an increase in IN tetramer. In the presence of both CX05168 and Rev, the IN monomer isomers were retained when compared to the IN multimers induced by both Rev and Mut 101.

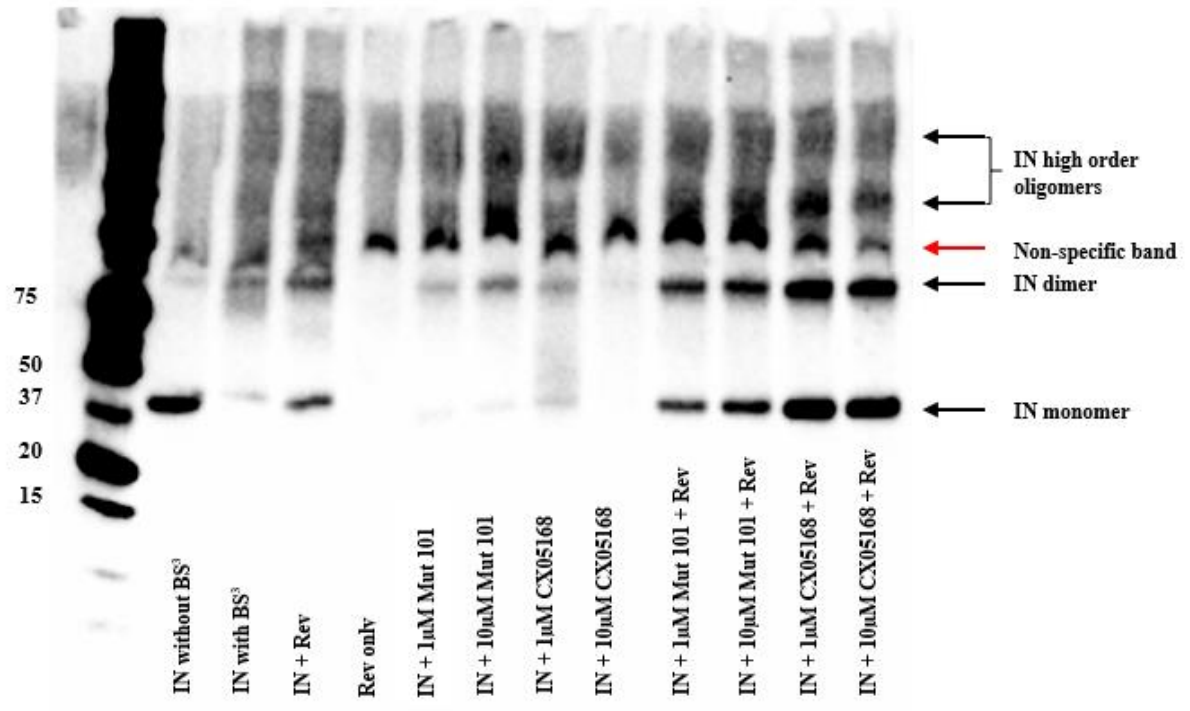


Figure 3.9 continued on the following page

Figure 3.9: Western blot analysis depicting the crosslinking reactions of integrase (IN) multimerization induced by Mut 101, CX05168 and HIV-1 Rev alongside Precision Plus Protein™ marker (Bio-Rad, USA). *IN was detected using IN antiserum (NIH Research and Reference Reagents Program, Catalogue number 7274). High order oligomerization of IN is denoted by the arrows. Rev induced multimers of IN in the form of dimers and tetramers. Aberrant multimerization of IN was observed in the presence of Mut 101 and CX05168. Reduction of aberrant IN multimerization is observed in the presence of Rev and Mut 101 or CX05168. Blot is a representation of three independent crosslinking experiments.*

3.3.2 Determining integrase multimerization through an AlphaScreen multimerization assay

To validate the crosslinking IN multimerization findings, a secondary assay was conducted using the AlphaScreen multimerization assay. The assay was optimised followed by concentration gradient experiments with increasing Mut 101, CX05168 and Rev concentrations. An increase in the Mut 101, CX05168 and Rev concentration yielded an increase in IN multimerization (Figure 3.10). Mut 101 required low concentrations for aberrant multimerization to occur compared to CX05168 and Rev that required an increase in concentration to observe aberrant multimerization. RAL at 10μM was used as a control and no IN multimerization was induced as expected (results not shown).

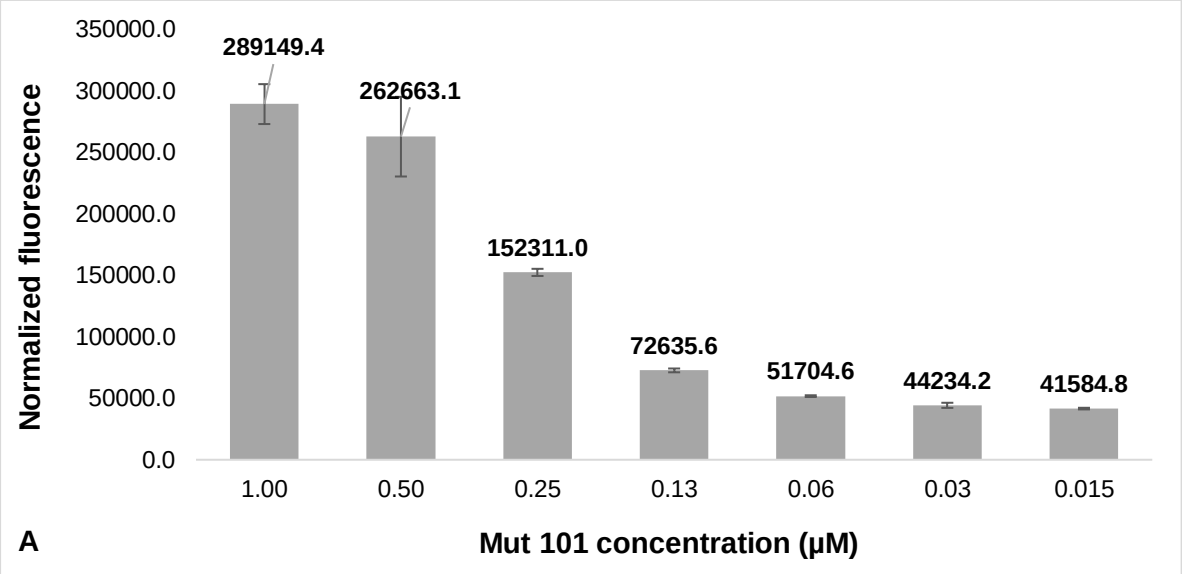


Figure 3.10 continued

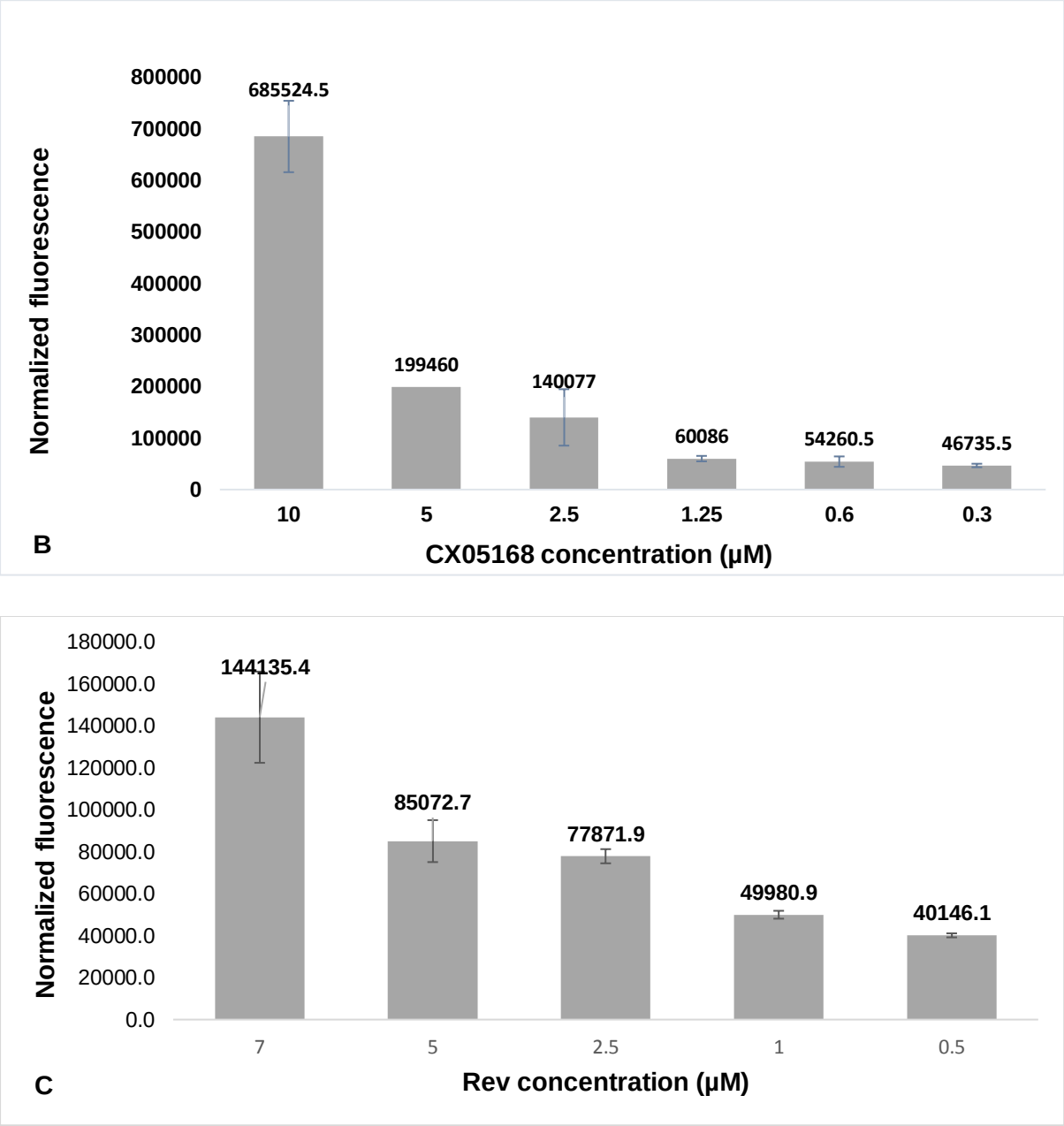


Figure 3.10: Graphs depicting the normalized fluorescence intensity of the interaction between integrase (IN) molecules induced by A) Mut 101 B) CX05168 and C) HIV-1 Rev at a concentration gradient: *Results obtained from AlphaScreen experiments indicated that IN multimerization occurred in a concentration dependent manner. The error-bars represent the standard deviation of the average of three independent experiments comprising duplicates of each reaction (n=6).*

The normalized fluorescent signal yielded were used to calculate the percentage multimerization induced by Mut 101, CX05168, and Rev. When directly comparing IN multimerization induced by Mut 101, CX05168 and Rev at 1µM, it is apparent that Mut 101 promoted the highest percentage multimerization of IN followed by CX05168 then Rev (p < 0.005, Figure 3.11). Mut 101 at 1µM induced 593.4% IN multimerization compared to 1µM CX05168 and 1µM Rev that induced 44.1% and 19.8% IN multimerization, respectively.

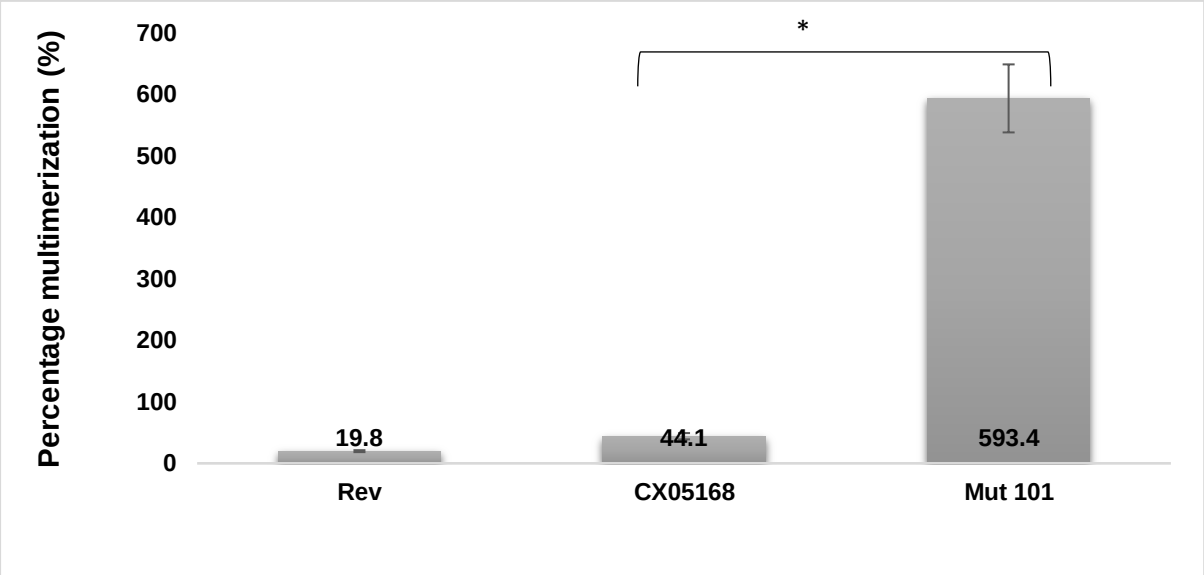


Figure 3.11: Comparing the percentage integrase (IN) multimerization induced by 1µM Mut 101, CX05168 and HIV-1 Rev quantified using an AlphaScreen multimerization assay. Mut 101 (593.4%) promote significantly higher IN multimerization than CX05168. *The asterisk * denote a significant multimerization difference induced by Mut 101 and CX05168. The error-bars represent the standard deviation of the average of three independent experiments comprising duplicates of each reaction (n=6).*

The multimerization of IN was quantified in the presence of both Rev and Mut 101 and Rev and CX05168 using the AlphaScreen multimerization assay. Rev and either Mut 101 or CX05168 were incubated simultaneously with FLAG-tagged IN and His-tagged IN. When comparing Mut 101 induced IN multimerization to IN multimerization induced by both Mut 101 and Rev, it is apparent that IN multimerization was significantly reduced when Rev was added (p < 0.005, Figure 3.12). Similarly, in the presence of Rev, IN multimerization promoted by CX05168 is significantly reduced (p < 0.005). However, when comparing IN multimerization

induced by Rev (83.2%) to Rev in combination with Mut 101 (254.3%) or CX05168 (200.8%), a significant increase in IN multimerization is observed ($p < 0.005$).

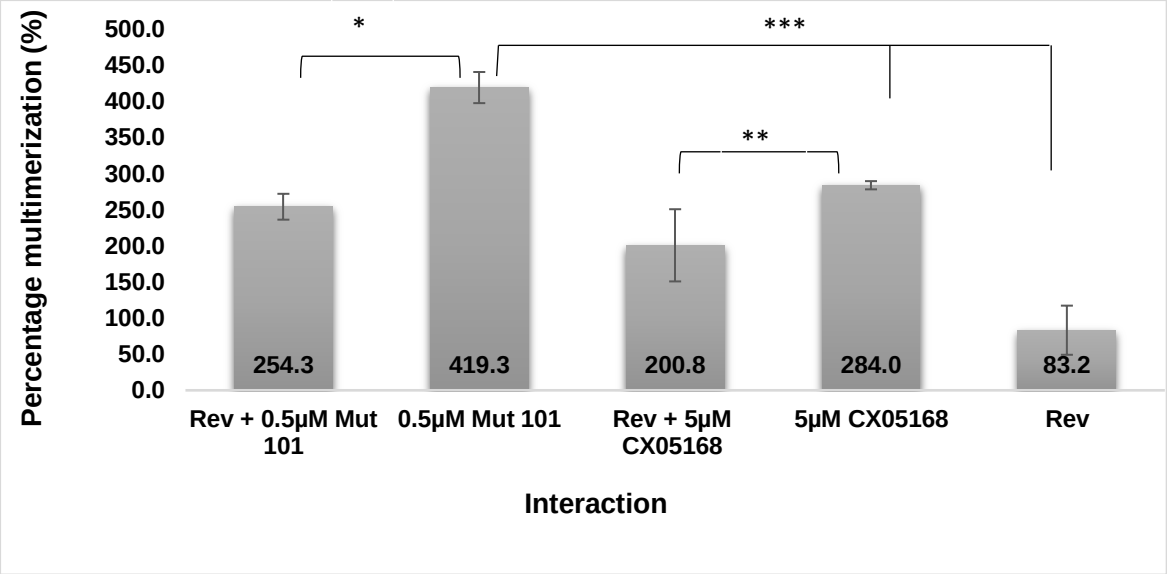


Figure 3.12: Quantification of integrase (IN) multimerization in the presence of both HIV-1 Rev and Mut 101 or CX05168 using an AlphaScreen multimerization assay. *Rev appears to significantly reduce IN multimerization in the presence of Mut 101 (*) or CX05168 (**). However, IN multimerization induced by Rev significantly increases in the presence of Mut 101 or CX05168 when comparing it to the multimerization of IN induced by Rev only (Denoted by ***). The error-bars represent the standard deviation of the average of three independent experiments comprising duplicates of each reaction (n=6).*

3.3.3 Evaluating the size of integrase molecules using dynamic light scattering experiments

In addition to the crosslinking IN multimerization studies and AlphaScreen multimerization experiments, DLS was used to evaluate the effect of ALLINIs in the presence of Rev on aberrant IN multimerization. DLS quantifies the size of large IN particles formed in the presence of Mut 101, CX05168 and HIV-1 Rev. The number distribution was used to determine the size of the molecules expressed by the weighted mean hydrodynamic size of the particle (Z–average, diameter.nm (d.nm)). Monomer IN subunits were undetectable due to their small size, below 1nm, which correlated with the results reported by Feng and co-workers, 2016.[189] DLS Buffer and Mut 101 or CX051368 dissolved in DLS Buffer were recorded below 1nm. Rev monomers alone was also undetectable and recorded a signal

below 1nm due to their small size. However, an equilibrium shift in the size of IN was observed in the presence of Mut 101, CX05168 and Rev. Figure 3.13 represents the equilibrium shift of IN in the presence of Mut 101, Mut 101 with Rev, CX05168, CX05168 with Rev and Rev only. IN with Rev recorded a signal at 34.02 d.nm whereas IN with Rev in the presence of Mut 101 and CX05168 significantly shifted the equilibrium to 544.2 d.nm and 787.6 d.nm ($p < 0.005$), respectively. The peak recorded for IN with Mut 101 and IN with CX05168 was at 1088 d.nm and 1039 d.nm, respectively.

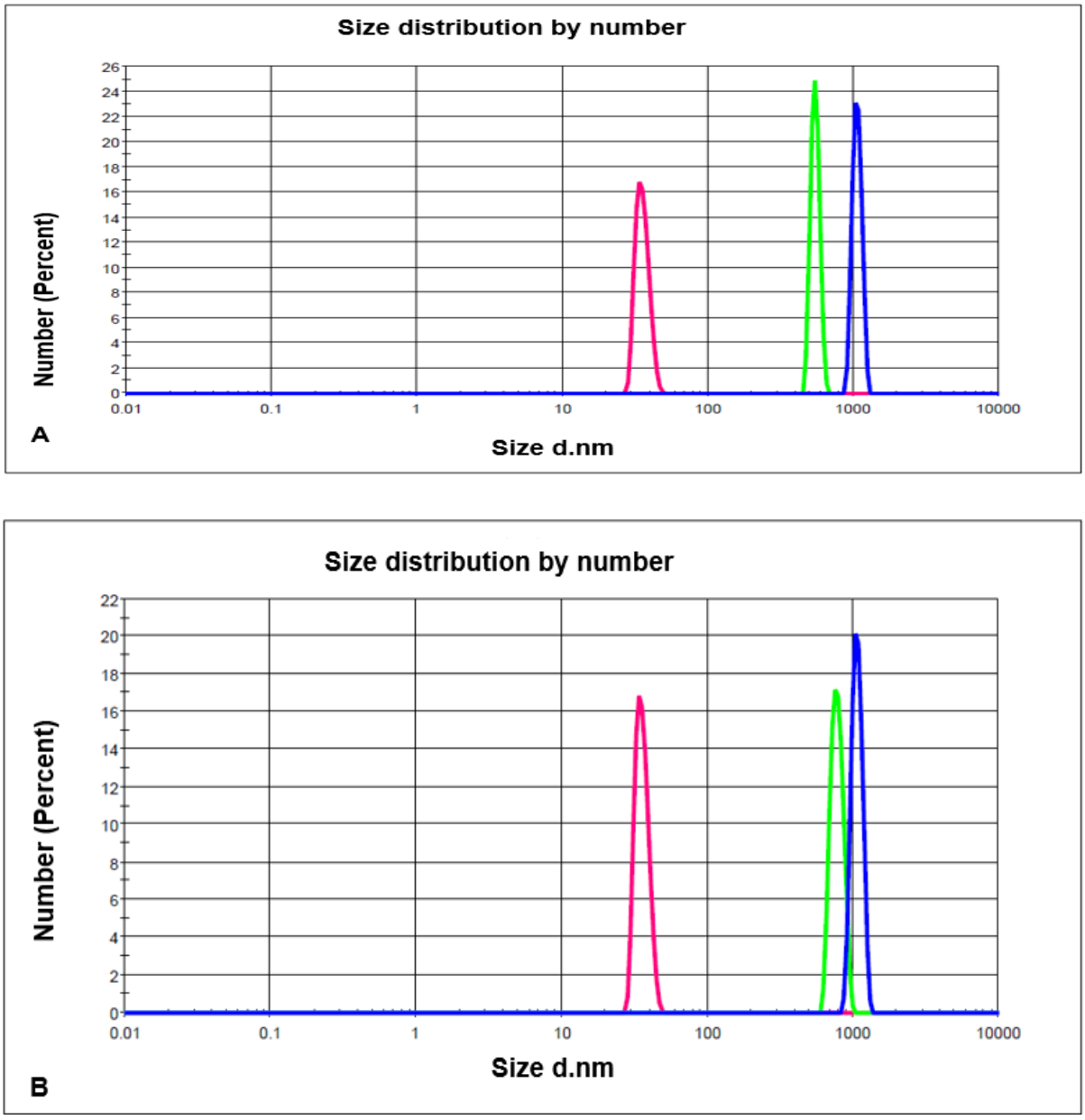


Figure 3.13: Evaluating the effect of A) Mut 101 and B) CX05168 on integrase (IN) multimerization in the absence and presence of HIV-1 Rev through dynamic light scattering analysis (DLS). *The number distribution percentage was used to express the size*

of the particle in diameter nanometer (d.nm). The pink peak denotes the effect of Rev on the size of the IN molecules. The green peak represents the DLS analysis of IN in the presence of Mut 101/CX05168 and Rev. The blue peak represents the effect of Mut 101 or CX05168 on the size of the IN molecules in the absence of Rev.

3.4 DETERMINING THE INTERACTION BETWEEN HIV-1 REV AND INTEGRASE

3.4.1 Calculating the dissociation constant (K_d) of the integrase–Rev interaction in the presence of ALLINIs using an ELISA based method

The interaction between IN and Rev was expressed in terms of its K_d in the absence and presence of Mut 101 and CX05168 (Figure 3.14). The K_d measures the ability of a biochemical complex to reversibly dissociate into smaller molecules. The K_d of the IN-Rev interaction was 461 ± 5.65nM compared to the K_d reported in previous studies of 13nM.[177] An order of addition experiment was conducted to determine if ALLINIs interfere with the binding interaction between Rev and IN. The first order of addition experiment included the addition of ALLINIs at 10μM to the multiwall coated with IN followed by the addition of Rev (IN-ALLINI-Rev interaction). The K_d of IN-Rev in the presence of Mut 101 or CX05168 was subsequently calculated and compared in figure 3.15. The K_d for IN-Mut101-Rev and IN-CX05168-Rev significantly shifted to 850 ± 70.71nM and 1010 ± 127.27nM, respectively, when compared to the K_d of IN-Rev with no ALLINI ($p < 0.005$). In addition, it is evident that the K_d obtained for the IN-CX05168-Rev interaction (1010 ± 127.27nM) was significantly higher than the K_d obtained for IN-Mut101-Rev interaction (850 ± 70.71nM, $p < 0.005$). RAL at 10μM was used as a control and demonstrated no interference between the IN and Rev interaction where the absorbance reading at 620nm correlated with the positive control (IN with Rev). The second order of addition interaction was determined by the addition of Rev to IN coated microwell plates followed by the addition of 10μM ALLINIs (IN-Rev-ALLINI). The IN-Rev-Mut101 and IN-Rev-CX05168 interaction yielded K_d values of 315 ± 21.21nM and 384.5 ± 139.30nM, respectively. No significant K_d shift was observed when comparing the K_d values of IN-Rev without ALLINIs and IN-Rev-ALLINI interactions.

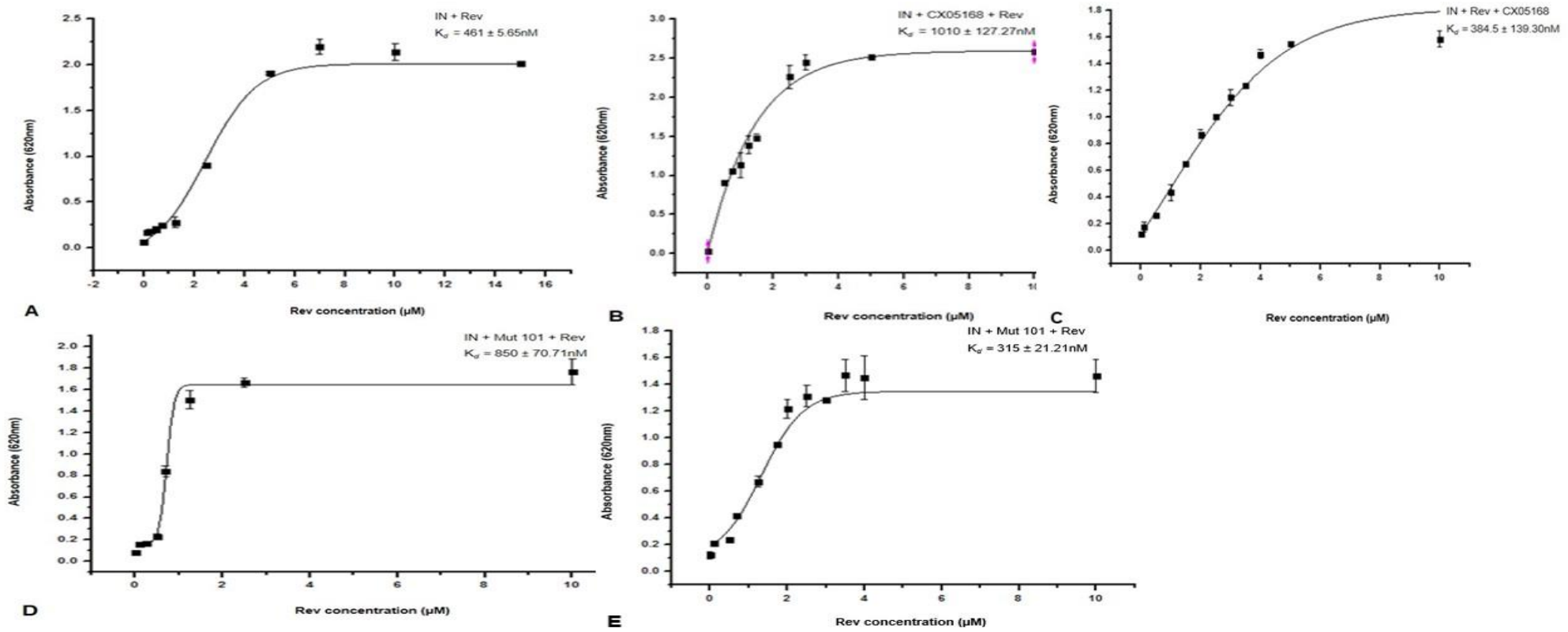


Figure 3.14: The dissociation constant (K_d) plots representing the order of addition interactions between A) integrase (IN) and Rev B: IN-CX05168-Rev C) IN-Rev-CX05168 D) IN-Mut 101-Rev and E) IN-Rev-Mut 101. *The absorbance readings at 620nm versus increasing Rev concentrations obtained from ELISA studies were used to generate the K_d plots of each interaction. The errors bars represent the average values of n=6. The K_d* values for each interaction were calculated using the Lineweaver-Burke equation.

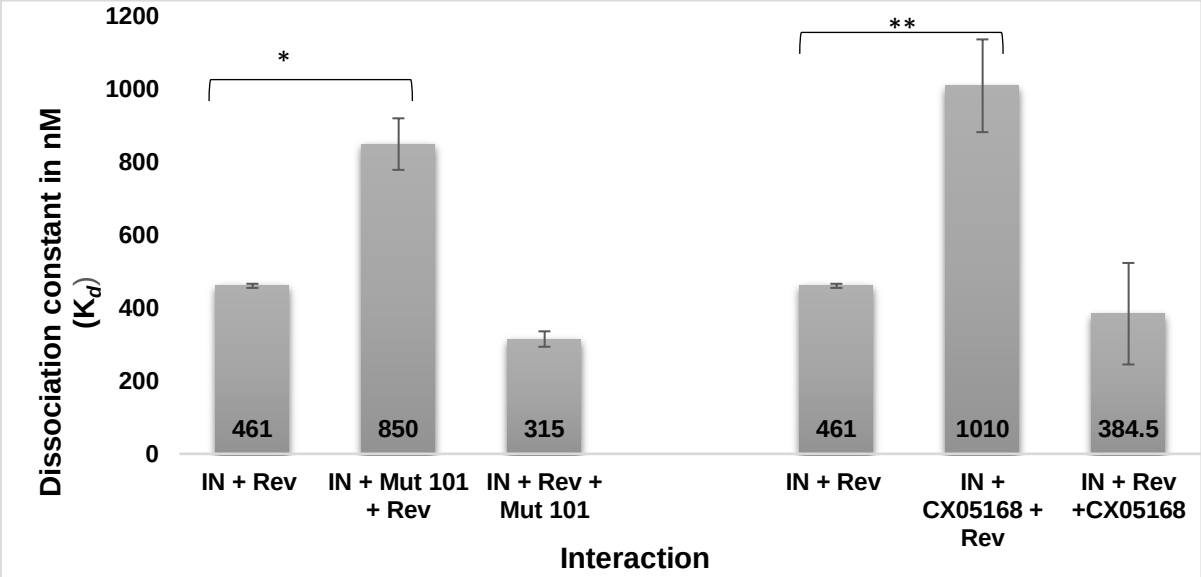
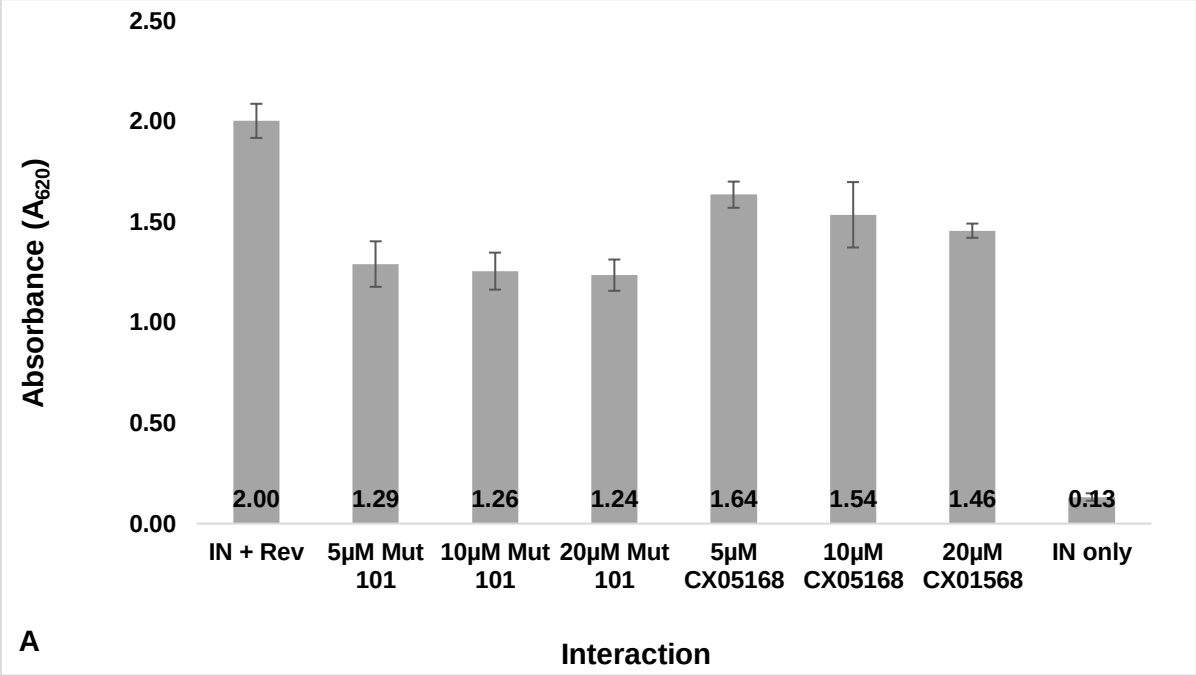


Figure 3.15: Representation of the dissociation constant (K_d) of integrase (IN) and HIV-1 Rev in the absence and presence of Mut 101 and CX05168. *Each interaction represents the order of addition of Rev or ALLINIs. The data set represents the K_d of each interaction in triplicate (n = 6). An increase in K_d shift was observed when comparing the IN + Rev interaction to the IN + Mut 101 + Rev and IN + CX05168 + Rev interaction. The difference in K_d between IN + Rev interaction, IN + Rev + Mut 101 interaction and IN +Rev +CX05168 interaction was not significant.* Indicate that the Kd of the IN + Rev interaction was significant different to IN + Mut 101 +Rev. ** Indicate that the Kd of the IN + Rev interaction was significantly different to the interaction between IN + CX05168 + Rev. The error bars indicate the SD of the mean average of at least three experiments.*

3.4.2 Comparing the percentage reduction of the integrase and Rev interaction between two order of addition reactions

Using the order of addition described in section 3.4.1 (IN-ALLINI-Rev), the percentage reduction of the interaction between IN and Rev was determined in an ALLINI dose dependent manner. The IN-Rev interaction was monitored using an ELISA method and the resulting absorbance readings recorded at 620nm was used to measure the level of interaction between the two proteins. An increase in absorbance values indicated an increase in the interaction between IN and Rev. As such, the positive control contained only IN and Rev while the negative control contained IN only. The IN-Rev was monitored in the presence of Mut 101 and

CX05168 at a concentration gradient (5-, 10-, and 20μM). Although both Mut 101 and CX06158 decreased the IN-Rev interaction ($p < 0.005$), the reduction was not dose dependent ($p > 0.05$, Figure 3.16 A) according to pairwise T-test analysis. The reduction of the IN-Rev attributed to Mut 101 and CX05168 was expressed in terms of the percentage reduction calculated using the absorbance values obtained (Figure 3.16 B). The percentage reduction showed that Mut 101 exhibited the highest level of IN-Rev reduction at 20 μM (41.02%) while CX05168 exhibited a lower percentage reduction than Mut 101.



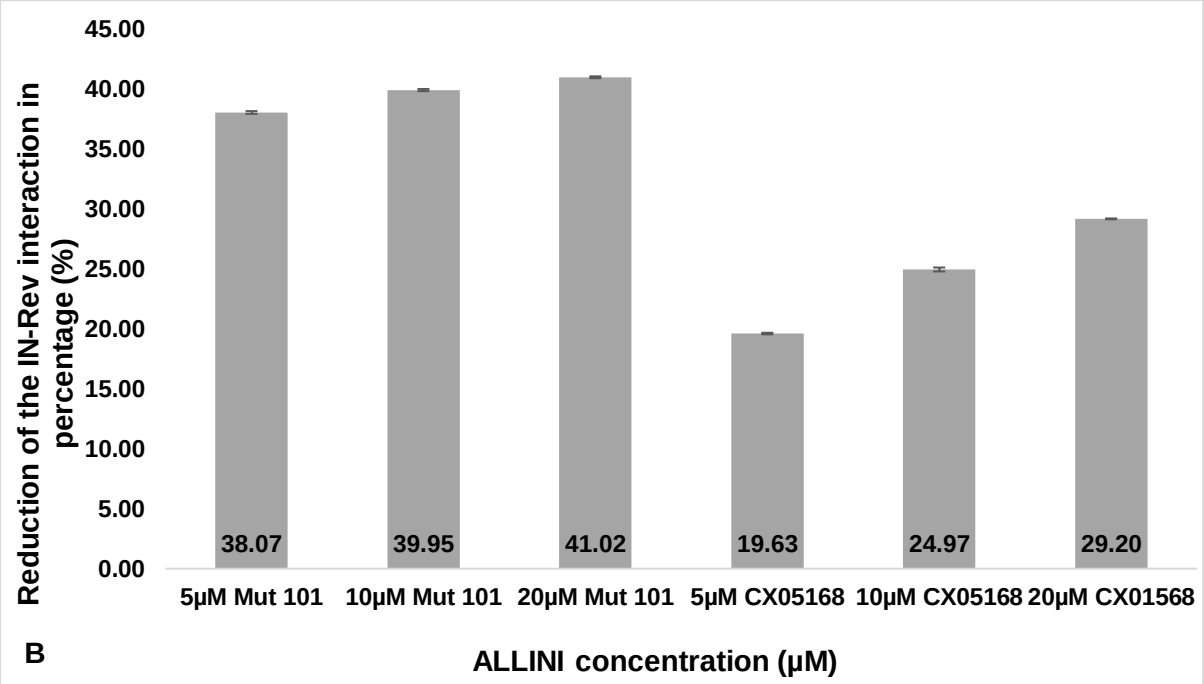


Figure 3.16: A) Bar graphs representing the interaction between IN and Rev in the absence and presence of Mut 101 and CX05168 at a concentration gradient. *The IN-Rev interaction was detected by anti-Rev (NIH Research and Reference Reagents Program, Catalogue number 756) using an ELISA method. The absorbance readings were used to monitor the interaction between IN and Rev in absence and presence of Mut 101 and CX05168.* ***B)*** *The absorbance readings were used to calculate the percentage inhibition of the IN-Rev interaction in the presence of a concentration gradient of Mut 101 and CX05168. The reduction in the IN-Rev interaction attributed to Mut 101 and CX05168 was not dose dependent. The error-bars represent the standard deviation of the average of three independent experiments comprising duplicates of each reaction (n=6).*

Furthermore, a third order of addition interaction was demonstrated by incubating IN with ALLINIs at 5-, 10- and 20μM and subsequently adding the complex to a Rev coated multiwell plate (Rev-IN + ALLINI). The IN-Rev and Rev-IN interactions were considered as the positive controls while IN only and Rev only were deemed as the negative controls. The percentage inhibition of the Rev-IN interaction was calculated using the absorbance values recorded at 620nm. The interactions between Rev, IN and ALLINIs for the Rev-IN + ALLINI order of addition experiment are demonstrated in figure 3.17. The absorbance readings recorded at 620nm represented in figure 3.17 (A) were then used to calculate the percentage reduction in the IN-Rev interaction in the presence of Mut 101 and CX05168. Mut 101 and CX05168 in

conjunction with IN interfered with the binding of IN to Rev. Thus, a significant decrease in the interaction between Rev and IN in the presence of Mut 101 and CX05168, in a dose dependent manner, was observed when compared to the positive control (Rev with IN, $p < 0.005$). When comparing the percentage reduction in Rev-IN interaction caused by Mut 101 at 20μM (88.85 ± 5.5%) and CX05168 at 20μM (83.29% ± 3.4%), it is evident that Mut 101 had a significant larger effect on the interaction than CX05168 ($p < 0.05$).

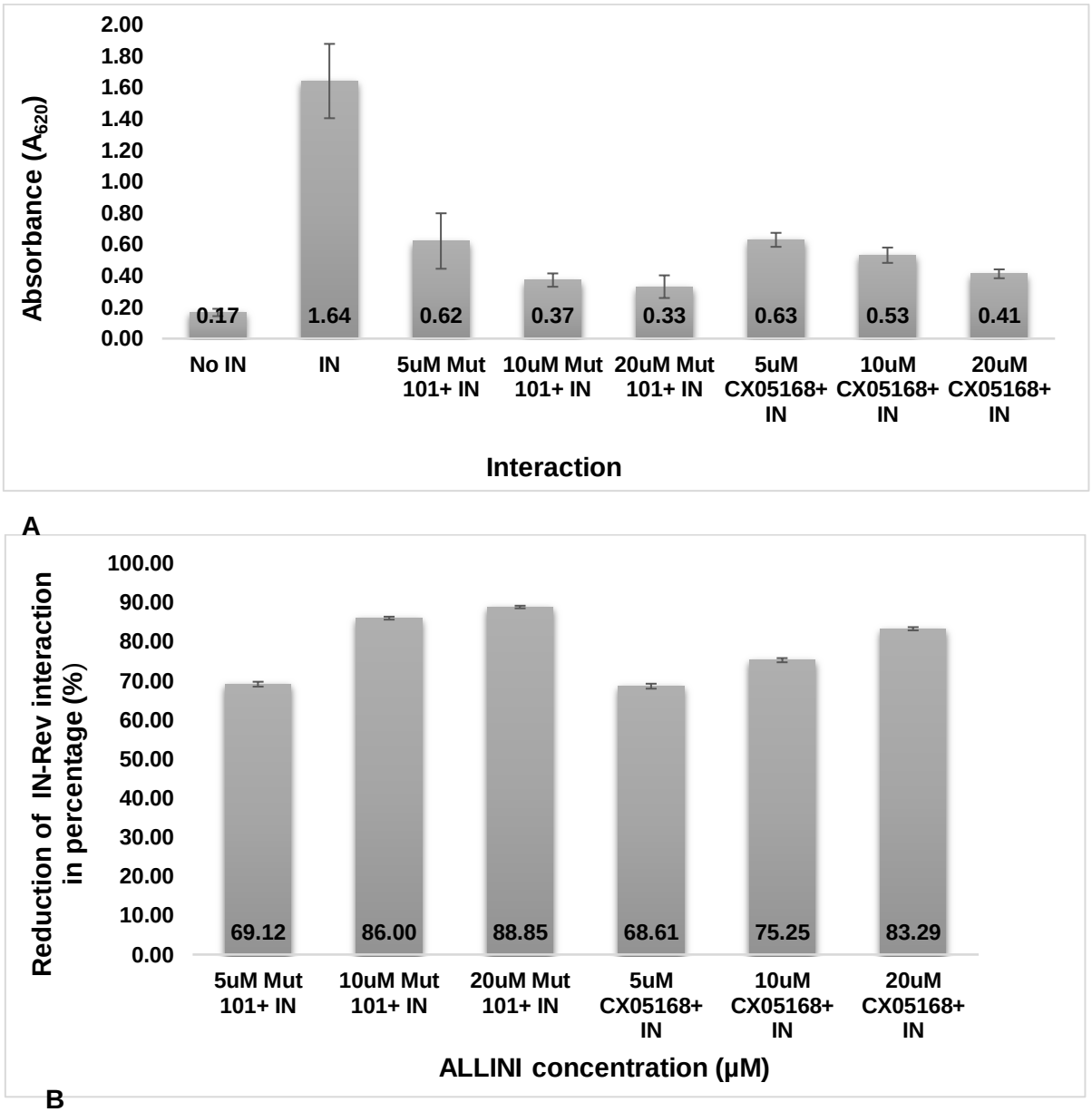


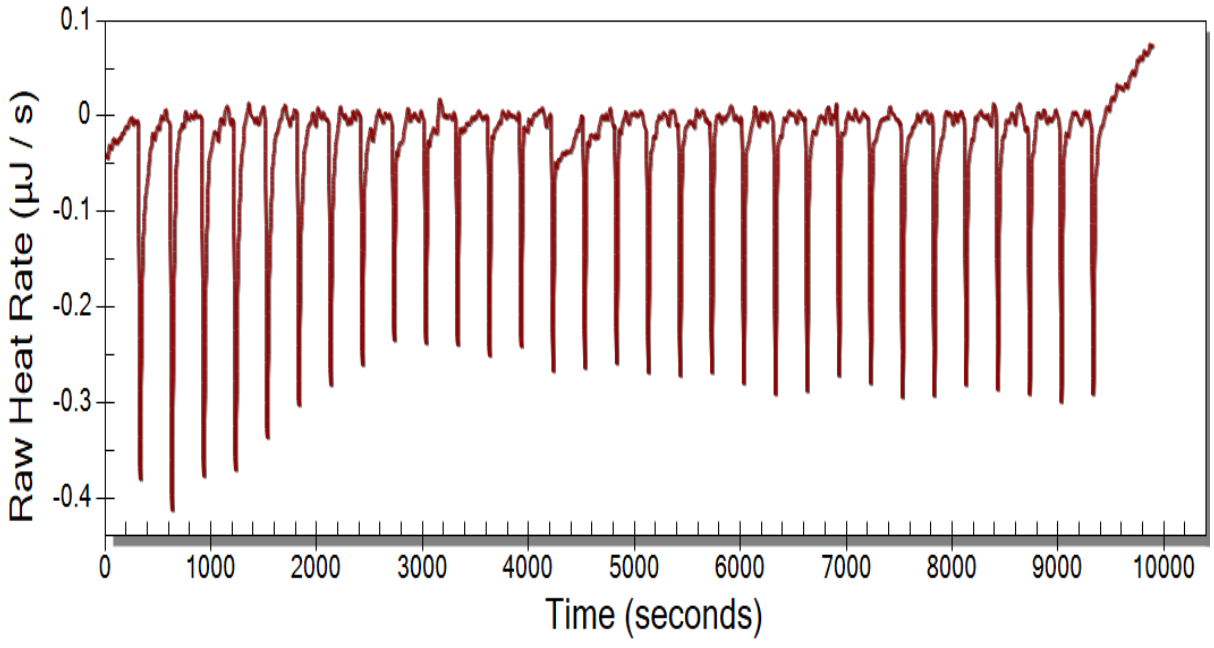
Figure 3.17: Evaluating the effect of Mut 101 and CX05168 on the integrase (IN)-Rev interaction in a dose dependant manner*. The interaction between IN and Rev was detected using anti-IN (NIH Research and Reference Reagents Program, Catalogue number 756) through an ELISA method. IN was incubated with Mut 101 and CX05168 at increasing*

concentrations before adding the complex to the Rev coated 96-well plate. The reduction of the IN-Rev interaction was directly proportional to the concentration of Mut 101 and CX05168. ***B)*** *The percentage reduction of the IN-Rev interaction in the presence of Mut 101 and CX05168. Mut 101 conferred the highest percentage reduction of the IN-Rev interaction at 20µM (88.85% + 5.5%) followed by CX05168 at 20µM (83.29% ± 3.4%). The error-bars represent the standard deviation of the average of three independent experiments comprising duplicates of each reaction (n=6).*

3.4.3 Characterization of the HIV-1 integrase interaction with Rev through isothermal titration calorimetry

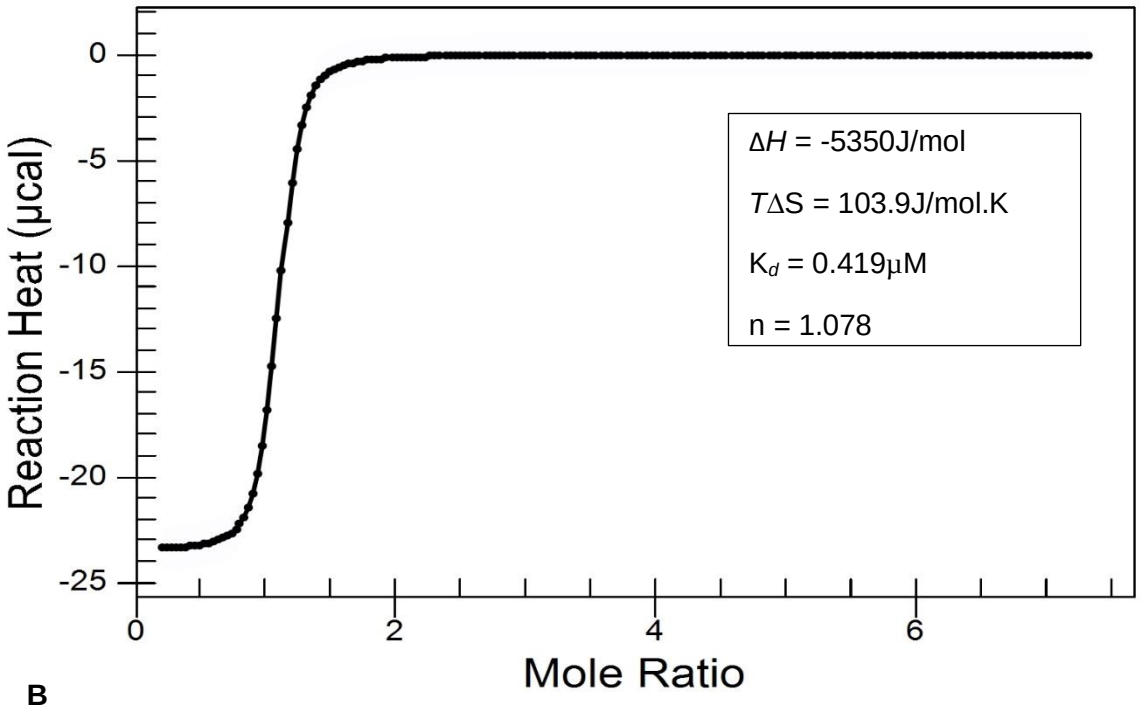
3.4.3.1 The thermodynamic properties of the HIV-1 integrase-Rev interaction

The IN-Rev interaction was observed through ITC experiments. The raw heat rate graphs generated throughout ITC experiments were used to theoretically fit the graphs using the independent model with a blank (constant, Figure 3.18). The thermodynamic properties of the interactions were subsequently calculated. The fitted thermogram of the IN-Rev interaction elicits an exothermic reaction with a favourable enthalpy (ΔH -5350 J/mol) and a temperature entropy change ($T\Delta S$) of 103.9 J/mol.K. The K_d of the IN-Rev interaction was calculated at 419nM while the stoichiometry (n) = 1. The free Gibbs energy was calculated at ΔG = -5453.9J/mol indicating that the reaction is enthalpically driven.



A

Figure 3.18 continued



B

Figure 3.18: The isothermal titration calorimeter (ITC) thermograms of the HIV-1 integrase (IN) and Rev interaction. A) *The raw heat graph of the IN-Rev interaction where 300µM Rev was titrated into 10µM IN. The raw heat rate measured in µJ/seconds were monitored over time (seconds).* ***B)*** *The binding curve was independently fitted using the raw heat thermogram. The independently fitted graph represented the reaction heat of the injectant (µcal) associated with the Mole ratio.*

3.4.3.2 The effect of Mut 101 and CX05168 on the HIV-1 integrase and Rev interaction

To determine whether ALLINIs had an affect on the IN-Rev interaction, the experiment was repeated in the presence of Mut 101 and CX05168. Before the experiment was conducted, IN was incubated with Mut 101 or CX05168 for one hour at room temperature. The experiment was then further conducted using the same conditions used when determining the IN-Rev interaction. The isotherms of IN-Mut 101-Rev and IN-CX05168-Rev demonstrated that the IN-Rev interactions were perturbed in the presence of the ALLINIs (Figure 3.19). As a result, the independent model generated poorly fitted curves and therefore the thermodynamic properties of the reactions could not be determined accurately.

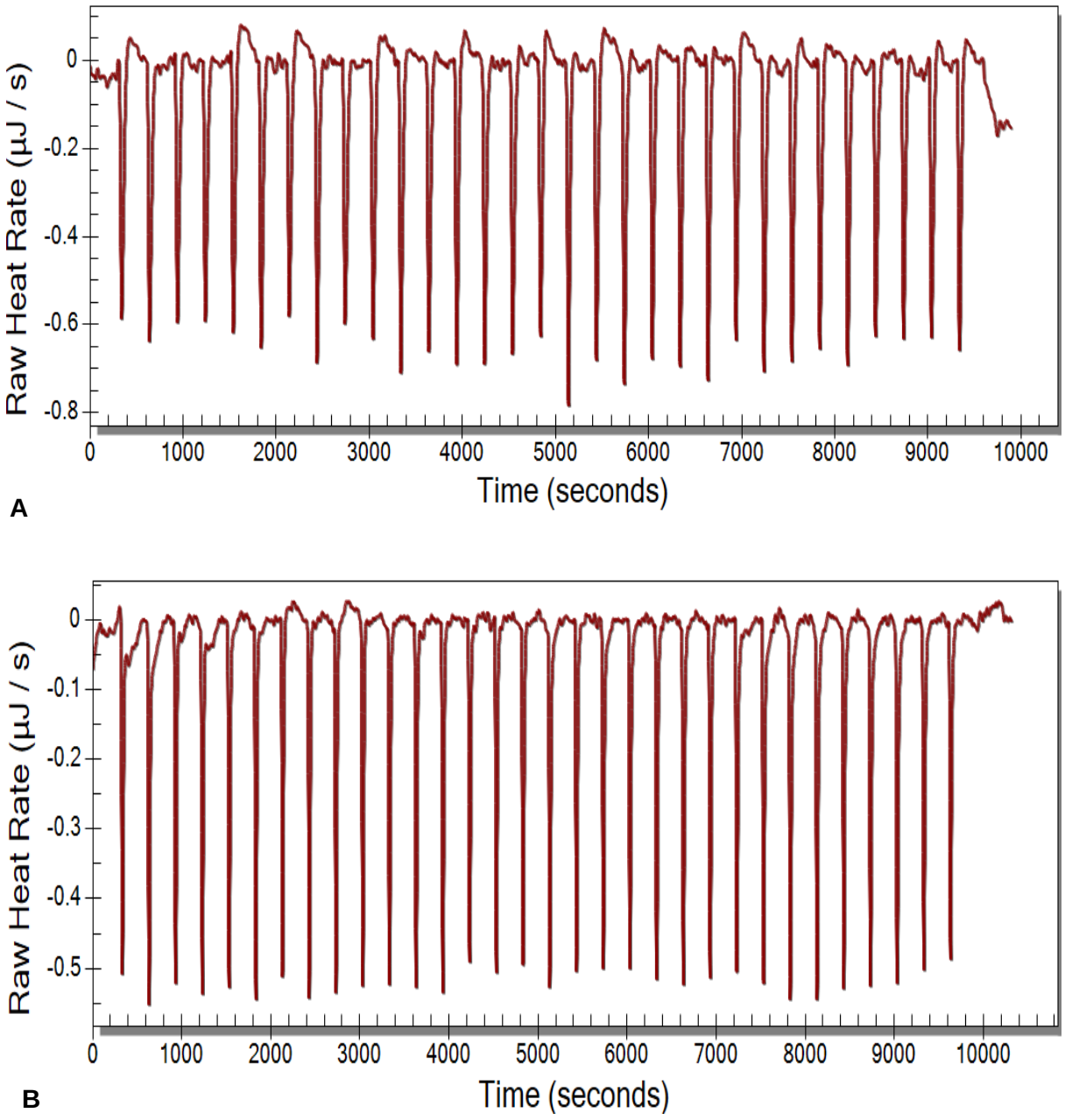


Figure 3.19: The raw heat graphs of the interaction between HIV-1 integrase (IN) and Rev in the presence of A) Mut 101 and B) CX05168. *The thermographs represents the raw heat rate (µJ/seconds) over time (seconds).*

The resultant sample containing IN, Mut 101, CX05168, and the injected Rev was collected from the ITC sample cell and subjected for further fluorescence spectroscopy analysis. By analysing the fluorescence intensity graph (Figure 3.20), it is evident that the IN samples containing ALLINIs and Rev were quenched however, the samples containing both Rev and

ALLINIs demonstrated an increase in quenching when comparing it to the IN sample containing the injected Rev only. The curves for IN-Mut 101-Rev and IN-CX05168-Rev were almost identical with maximal intensity peaks of 8.65 and 8.78, respectively, compared to the maximal intensity peak of IN alone at 19.30. A slight hyperchromic change on the shoulder of the peak was also observed for samples containing IN, Mut 101 or CX05168, and Rev. The maximal intensity peak of IN with the injected Rev was recorded at 15.07. Mut 101 and CX05168 were analysed in isolation and negligible fluorescence was detected.

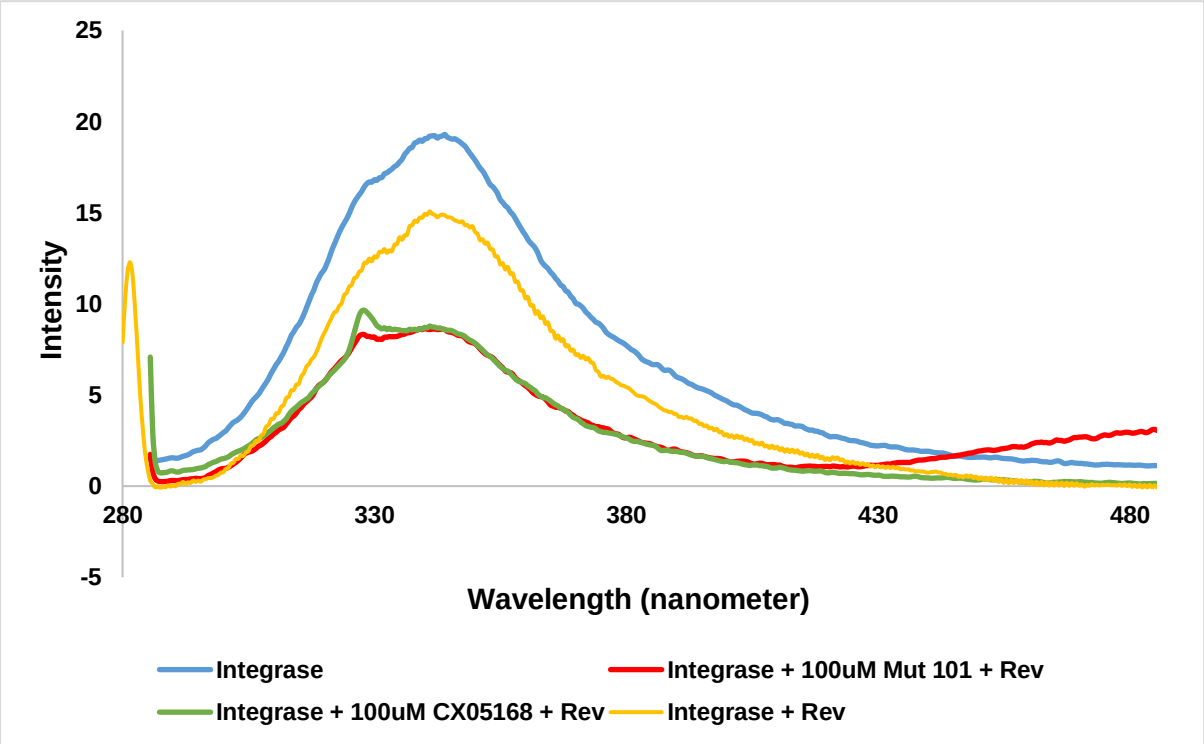


Figure 3.20: The fluorescence intensity peaks obtained when analysing HIV-1 integrase (IN) samples containing injected Rev in the absence and presence of ALLINIs. *The samples were collected from the sample cell of the Nano ITC instrument and the change in fluorescence intensity was determined using the FF-6300 Spectrafluorometer. It is evident that the samples containing Rev and Rev with ALLINIs quenched the fluorescence spectra of IN*

CHAPTER 4

Discussion

In addition to mediating the nuclear export of spliced and unspliced mRNA, HIV-1 Rev plays a vital role in the HIV integration step. A role that involves the inhibition of the integration step through IN multimerization to prevent super-infection of the virus and the production of defective virions. Rev binds to IN at the LEDGF interface located on IN and subsequently dissociates the IN-LEDGF complex forming IN-Rev and LEDGF-Rev complexes. The formation of the IN-Rev complexes subsequently inhibit the integration process. Likewise, the latest class of INI, ALLINIs, bind to the LEDGF interface on IN consequently promoting IN multimerization in the early stage of HIV replication and defective virion production in the late stage of HIIV replication. Since ALLINIs and Rev bind to the LEDGF interface on IN and inhibit the integration step in a similar manner, this study aimed to investigate if ALLINIs interfere with the IN-Rev interaction. *In vitro* selection studies selecting Mut 101 and CX05168 aimed to monitor the emergence resistance mutations in the HIV-1 *IN* gene against primary subtype C FV 3 and FV 26 virus. CX05168 failed to inhibit HIV-1 subtype C viral replication at its reported EC_{50}. Results indicate that the primary subtype C FV 3 and FV 26 isolates was not as susceptible to CX05168 as subtype B virus. Viral breakthrough was observed during Mut 101 selection against both FV 3 and FV 26 isolates. *In vitro* phenotypic inhibition studies showed that the viral breakthrough isolates affected the infectivity ability of the virus as well as the susceptibility of the selected isolates against Mut 101. Genotypic analysis identified polymorphisms in drug naïve FV 3 and FV 26 isolates as well as resistance mutations in isolates where viral breakthrough was observed that might have impacted the efficacy of Mut 101 against these isolates. Furthermore, order of addition experiments were conducted using an ELISA method to determine how the IN-Rev interaction was affected before or after ALLINIs were added to the IN-Rev complex. Results indicate that ALLINIs only affect the IN-Rev interaction before Rev is bound to IN. Two possible mechanisms that affects the IN-Rev interaction have been described. Firstly, multimerization of IN explains the interference of the IN-Rev interaction when the Rev-IN + ALLINI order of addition was tested. Secondly, when the IN-ALLINI-Rev order of addition was tested, the shift in IN-Rev K_d was probably due to the ALLINIs masking the sites on IN to which Rev binds. ITC studies provided a confirmatory experiment that described the thermodynamics of the IN-Rev interaction and corroborated the K_d of IN-Rev obtained through ELISA studies. Since both Rev and ALLINIs induce multimerization of IN in order to inhibit integration, Rev and Mut 101 or CX05168 was tested concurrently through AlphaScreen multimerization studies, DLS and crosslinking studies to

determine how multimerization would be affected in the presence of both Rev and ALLINIs Results corroborate documented literature exhibiting aberrant IN multimerization induced by ALLINIs[189] while Rev did not induce aberrant IN multimerization. In addition, Rev appears to reverse the aberrant multimerization induced by ALLINIs. It can be assumed that Rev and ALLINIs induces multimerization using two distinct pathways. This study ultimately suggests that when Rev and ALLINIs are combined, the mechanisms of interaction as well as multimerization is altered.

4.1 CX05168 IS LESS ACTIVE AGAINST HIV-1 SUBTYPE C PRIMARY FV ISOLATE

CX05168, a 2-quinolin-3-yl acetic acid derivative, forms part of the LEDGIN series of ALLINIs that blocks HIV replication. Studies conducted by Christ et al, 2012 described the mechanism of action of CX05168 against HIV-1.[168] Co-crystal structures indicated that CX05168 does not alter the active site of IN which infers that LEDGINS restrict the oligomeric flexibility of IN consequently perturbing the productive formation of the intasome. Further experimental data indicate that LEDGINS induce an equilibrium shift of the IN oligomerization state that results in inactive IN multimers. As such, the multimeric form of IN required for the binding of vDNA to the IN intasome is no longer viable for HIV-1 replication to ensue. In this study, antiviral activity of CX05168 was tested against primary HIV-1 subtype C FV 3 and FV 26 isolates. A significant increase in EC_{50} was observed when compared to previously reported antiviral activity against subtype B isolates NL4-3, HXB2D, IIIB and BAL using an MT4 cell line as well as PBMCs, to subtype C FV 3 and FV 26 isolates (Section 3.1.2.1).[165] Antiviral activity in HIV subtype C has not been reported as yet. CX05045, one of the initial LEDGINs that were designed which is structurally similar to CX05168, was tested against various HIV-1 clades (A, A1, AG, AE, B, BF, C and D).[168] The $FCIC_{50}$ values reported demonstrated that CX05045 retained antiviral activity against these clades which included several subtype C isolates. Some inhibitory variability was observed within the subtype C clade where EC_{50} values increased or decreased 2-3 fold.[168] This result correlates with the data observed in this study where CX05168 demonstrated an EC_{50} that is 1.8 fold higher against the FV 3 isolate than the reported EC_{50} of 2.35µM against the HIV-1 subtype B NL4-3.[168] *In vitro* selection studies were conducted to determine resistant mutations selected by CX05168. However, due to the inability of CX05168 to suppress HIV replication at lower concentrations against FV 3 and FV 26 isolates (Figure 3.1), viral breakthrough was not observed for the duration of the *in vitro* selection experiment and hence selection with CX05168 was aborted. Resistant mutation

studies by Christ et al showed that mutations emerged in the *IN* gene when under CX05168 pressure against subtype B NL4-3.[165] These mutations include the A128T and E170G located in the LEDGF/p75-IN pocket and is believed to be major resistance pathways of ALLINIs. HIV-1 NL4-3 harbouring these mutations are fully resistant to CX05168.

Interestingly, the mutations emerged after 39 passages at a concentration 25 fold the EC_{50} concentration of CX05168 (2.35µM). The resistance data for this has not been shown. This suggest that the current study may have required a CX05168 concentration 25 fold its EC_{50} against FV 3 and FV 26 (~100 and ~1000uM, respectively). Studies by Harrison A 2014, demonstrated that CX05168 exhibited a 50% cytotoxicity concentration (CC_{50}) value of approximately 71.15 ± 2.33µM in PBMCs.[190] Therefore, cytotoxicity of CX05168 in primary cells in *in vitro* selection studies selecting CX05168 was a concern. To investigate whether natural occurring polymorphisms within the primary isolates were responsible for the shift in EC_{50}, the *IN* gene of untreated FV 3 and FV 26 isolates were genotyped. Polymorphisms were detected in the *IN* gene in untreated FV 3 and FV 26 isolates (Table 3.1). The mutations identified have been reported previously as natural polymorphisms.[191] All polymorphisms identified against both FV 3 and FV 26 isolates in genotypic analysis were detected in the Stanford mutation database using the Detailed IN mutation query tool (https://hivdb.stanford.edu/). All polymorphisms with the exception of IN FV 26 G163E were considered as non-major or minor mutations. However, the G163 mutation detected in the Stanford mutation database was substituted with Arg (R) instead of Glu (E). G163R in the previously reported studies conferred resistance against INSTIs, RAL, EVG and DTG. Although substitutions at position A124 are not considered major or minor mutations against INSTIs, studies have demonstrated that A124T substitutions do indeed confer resistance against ALLINIs such as GS-A.[161,161,172] The quinolone core of the ALLINI is positioned against an IN pocket formed by a helix consisting of A124 and T126 residues. In addition, IN residues at position 124 and 125, located in the IN-LEDGF binding pocket, have demonstrated to be highly polymorphic and therefore polymorphic variants at these positions are likely to impact the efficacy of the ALLINIs.[192] As such, the Thr and Arg substitution at position 124 for FV 3 and FV 26, respectively, could delineate the shift in EC_{50} for CX05168 against FV 3 and FV 26. Residue G163 is not directly involved in the formation of the hydrophobic pocket of IN for LEDGF binding but the residue is located in the CCD binding region of IN and is involved in the IN-LEDGF interaction.[151,152] Ceccherini-Silberstein have reported that position G163 located on the *IN* gene exhibited a variation frequency of up to 25%. Since G163 has a propensity to mutate, it is possible that a substitution at G163 could affect the binding of CX05168 to IN consequently further increasing the EC_{50} against FV 26. The EC_{50} fold

difference of CX06268 between FV 3 and FV 26 could be attributed to the additional G163E polymorphism detected in FV 26.

Developed countries have predominantly discovered antiretroviral drugs, thus extensive research is conducted on the characterization of antivirals against subtype B, the predominant circulating subtype in these countries. Consequently, there is limited knowledge available on resistance and characterization of antivirals, specifically ALLINIs, against HIV-1 subtype C, the subtype responsible for over 50% of new infections worldwide.

A concurrent study conducted in our laboratory used surface plasmon resonance (SPR) and hydrogen exchange experiments to analyse the interaction between South African subtype C IN (primary HIV-1 isolate 05ZAFV06 from the FV isolates) and CX05168. Hydrogen exchange results showed a disparity in binding of subtype B and subtype C to CX05168. In addition, SPR results demonstrated a shift in K_d for the interaction between subtype B/C and CX05168. The interaction between subtype C and CX05168 was weaker than the interaction between subtype B and CX05168. The shift in K_d is possibly attributed to the disparity of the binding interaction between the two clades and CX05168. These results would further explain the shift in EC_{50} of CX05168 against HIV-1 subtype B and subtype C reported in this study. Further experiments are required to corroborate the exact mechanism of binding between CX05168 and IN.

4.2 THE CORRELATION BETWEEN THE GENOTYPIC- AND PHENOTYPIC ANALYSIS OF MUT 101 SELECTED ISOLATES

4.2.1 Non-infectious virions produced in the presence of Mut 101

In vitro phenotypic inhibition assays were conducted to determine the phenotypic effects of the isolates where viral breakthrough was observed when carrying out Mut 101 *in vitro* selection studies. When re-infecting the PBMCs with Mut 101 selected viral breakthrough isolates, viral infection with isolates FV 3 p8 and FV 26 p41 could not be established. The failure to infect could be attributed to several parameters: storage of the viral isolates could have affected the efficacy of the isolate; donor variability of PBMCs; or could be due to the fact that Mut 101 may possibly affect viral activity in the late stage of HIV replication. Further investigations will provide better insight into the reason for the failure of infection. It has been reported that Mut 101 inhibits viral replication in both early- and late stages of the replication cycle. In the early stage, integration is inhibited due to an oligomerization shift of IN induced

by Mut 101 consequently impacting the 3' processing and the ST step of IN. The oligomerization shift causes a conformational change of IN thus preventing the interaction between LEDGF and IN required for integration to proceed. A study conducted by Le Rouzic et al demonstrated that the major action of Mut 101 affects post-integration activities by perturbing the maturation process of virions.[167] Since the FV 3 p8 and FV 26 p41 isolates were unable to infect primary cells such as PBMCs, it can be inferred that Mut 101 is highly active in the late stage of HIV replication and that viral particles of these isolates are defective. A study conducted by Fontana and co-workers elucidated the role of IN in the maturation process of the HIV virion.[193] Upon initiation of the maturation process (discussed in section 1.3), vRNA is released and interacts with the nucleocapsid consequently forming the vRNA nucleocapsid (vRNP). IN interacts with vRNP and enables the incorporation of vRNP into the conical capsid subsequently forming a nucleated capsid. The density inside the conical capsid, also referred to as the density core, is comprised of vRNP, RT, IN and other host cell and viral constituents. The newly formed conical capsid completes core morphogenesis thus allowing infectivity. ALLINIs interfere with the IN-vRNA interaction consequently producing reduced, deformed and mislocalized capsids.[162] The density is translucent and an additional spherical density feature (eccentric density) is present between the viral envelope and the core. Through inference, it is likely that Mut 101 uncouples the incorporation of vRNP into the core for capsid formation. As such, the viral capsids are malformed and the infectivity of the virions are reduced.

4.2.2 Substitution at integrase H171 plays a role during the production of defective HIV-1 virions

Genotypic analysis of isolates which could not confer infection, FV 3 p8 and FV 26 p41 isolates, identified IN mutations at position H171 for both isolates. The H171 mutation is frequently associated with aa Thr in subtype B while Leu (FV 3 p8) and Q (FV 26 p41) were observed in this study.[171,172,191] The H171T/Q mutation has been reported as a major resistant pathway against ALLINIs such as BI-D and GS-A.[170,171] The IN H171T mutation is renowned for its interference with the interaction between ALLINIs and IN which consequently increase the activity of HIV-1. However, in our study H171L/Q was detected in isolates which could not confer infection. Fontana et al demonstrated that H171T subverted the defected virions produced in the presence of ALLINIs into fully matured virions.[193] It is possible that non-infectious virions were the cause of the reduction in viral replication in the isolates before viral breakthrough isolates, such as FV 3 p8, occurred (Figure 3.1).This may have led to the

emergence of the H171L mutations detected in the FV 3 p8. The mutation possibly recovered the morphogenesis of the defective virions which resulted in viral breakthrough at FV 3 p8. The concentration of Mut 101 was increased upon viral breakthrough which probably counteracted the activity of H171L and resulted in a subsequent decrease in viral replication after passage 8 (FV 3, Figure 3.1).

4.2.3 Integrase double mutation H171Q/L172I in HIV-1 isolate FV 26 could attribute to the decrease in viral replication

In addition to the H171Q mutation in isolate FV 26 p41, a secondary mutation L172I was identified through genotypic analysis. The double mutation, in the *IN* gene, H171A/L172A has been documented previously by Zheng et al.[194] When determining the effect of the double mutation H171Q/L172A on HIV replication, the following observations were made: 1 – IN lost its ability to bind to vDNA, 2 – IN was unable to bind to LEDGF and 3 – IN harbouring the double mutation was non-infectious. Although IN mutations H171 and L172 were substituted with Gln and Ile, respectively, instead of Ala, it can be inferred that the mutations in this study exert a similar impact thus resulting in a loss of HIV replication. The mechanism of action most likely follows the defective virion production process discussed in section 4.2.1. To support the increase in EC_{50} of Mut 101 against HIV-1 isolate FV 26 p41, molecular docking studies were conducted between mutated IN and Mut 101. Molecular docking studies predicted a discrepancy in binding between Mut 101 and IN containing H171Q/L172I when comparing it to the interaction between Mut 101 and wild type IN. The double mutation results in a weaker interaction between Mut 101 and IN with a loss of two hydrogen bonds between Mut 101 and the essential Thr-174 and Gln-95 located on IN. The observation of a weaker binding between IN H171Q/L172I and Mut 101 is affirmed by the increase in binding energy of the interaction when compared to the wild type IN and Mut 101 interaction (Table 3.3).

4.2.4 Polymorphisms detected in HIV-1 FV drug naïve isolates do not affect the efficacy of Mut 101

To date, the activity and characterization of Mut 101 has only been reported in HIV subtype B. This current study is the first to report the activity of Mut 101 in primary HIV subtype C isolates. Results indicate no significant difference between the EC_{50} of Mut 101 against HIV-1 subtype B reported by Le Rouzic et al and the EC_{50} of Mut 101 against HIV-1 primary isolate

drug naïve FV 26 (Figure 3.4).[167] Since the EC_{50} of drug naïve FV 26 isolate correlated with the EC_{50} reported in literature, it is evident that the polymorphisms present in the drug naïve FV 26 isolate do not affect the efficacy of Mut 101 against the subtype C isolate.[167] This suggests that the interaction between Mut 101 and IN are similar in HIV subtype B and primary HIV subtype C isolates used in this study. Furthermore, *in vitro* phenotypic inhibition studies of Mut 101 against resistant selected isolates exhibited an EC_{50} shift when compared to the EC_{50} of Mut 101 reported in literature (Section 3.1.2.2).[167] Isolate FV 26 p6 demonstrated a reduction in EC_{50} whereas isolate FV 26 p20 evoked an increase in EC_{50} (Discussed further in section 4.2.5 and 4.2.6).

4.2.5 Integrase Q164L mutation decreases the EC_{50} of Mut 101 against in vitro selected isolates

Genotypic analysis detected the IN Q164L mutation in isolate FV 26 p6 that possibly attributed to the decrease in EC_{50} of Mut 101 (Table 3.2). IN mutation Q164A has been reported by Bouyac-Bertoia where the mutation did not have any effect on HIV-1 replication.[195] Furthermore, Busschots et al reported that IN harbouring Q164A compromised the interaction between IN and LEDGF thus making the Q164 residue pivotal for the IN-LEDGF interaction. As mentioned in section 1.3.6, the efficacy of ALLINIs increase in the absence of LEDGF. Taken together, it is reasonable to assume that the emergence of Q164L reduces the interaction between IN and LEDGF thus rendering the mutated isolate more susceptible to ALLINI treatment. During *in vitro* phenotypic inhibition assays of Mut 101 against the HIV-1 isolate harbouring IN Q164L, Mut 101 is more potent in the presence of reduced IN-LEDGF complexes consequently causing a 2.5 fold reduction in the EC_{50} value. Molecular docking studies between Mut 101 and IN harbouring the Q164L predicted that IN Q164L and Mut 101 interacted in a similar manner as wild type IN and Mut 101. An abrogation of one of the hydrogen bonds between the Thr-174 side chain on IN and the ester group on the carboxylic acid of Mut 101 was observed when compared to wild type IN. The quinolone ring of ALLINIs usually extends toward the subunit where a hydrogen bond forms between Thr-174 and Mut 101.[168,170,196] The lack of the second hydrogen bond involving Thr-174 may induce a change in the position of the quinolone ring of Mut 101 which possibly affects the downstream phenotypic traits resulting in a shift in EC_{50} of Mut 101 against the mutated IN isolate.

4.2.6 L172I located on integrase is attributed to an increase in EC_{50} of Mut 101 against in vitro selected isolates

L172I was detected in isolate FV 26 p20 which correlated with an increase in EC_{50} of Mut 101. L172I is located in the loop region of the IN-LEDGF interface important for vDNA binding as well as LEDGF binding.[151] Previous mutagenesis studies demonstrated that a substitution at L172 compromised the interaction between IN and LEDGF.[194] Since Wang et al reported that ALLINIs and LEDGF compete for the same IN interface and IN L172A perturbs the IN-LEDGF interaction, it can be conjectured that L172I identified in this study may compromise the IN-Mut 101 interaction in a similar manner.[159,194] To further support this notion, molecular modelling studies predicted a disparity between the binding of wild type IN and Mut 101 and IN containing L172I and Mut 101. The mutated IN exhibited a loss of a hydrogen bond between the essential Gln-95 and the nitrogen atom located on Mut 101. An increase in binding energies of the interaction between IN L172I and Mut 101 was observed when compared to the interaction between Mut 101 and wild type IN. This prediction suggests that IN harbouring L172I has a lower affinity for Mut 101 which could result in the increase in EC_{50} as indicated by the results obtained in this study (Section 3.1.2.2).

4.3 HIV-1 REV REVERSES THE MULTIMERIZATION OF INTEGRASE INDUCED BY ALLINIS

As discussed in section 1.2.1, the functionality of IN relies on the equilibrium state of IN. As such, IN multimerization is the latest target for HIV-1 therapeutics. The mechanism of action of ALLINIs have strengthened IN multimerization as a therapeutic target since studies have demonstrated that an oligomerization shift of IN is the primary mechanism of action of ALLINIs.[168,170,196] ALLINIs are known to induce aberrant multimerization of IN which entails the assembly of multiple IN subunits into inactive IN multimers. Consequently, the LEDGF-IN interaction is compromised as well as the formation of the SSC complex. Aberrant multimerization also plays a role in the eccentric condensates of virions developed in the presence of ALLINIs. ALLINIs engage with IN through its hydrophobic pocket formed by the CCD-CCD interface of two IN monomers. This initiates the interaction between inter-subunits of IN leading to aberrant multimerization. AlphaScreen multimerization studies, DLS experiments as well as crosslinking studies demonstrated aberrant oligomerization of IN induced by Mut 101 and CX05168 in a dose dependent manner. AlphaScreen multimerization studies shows that Mut 101 is a better multimerizer than CX05168. Dimer stabilization of IN

induced by Mut 101 can be attributed to the interaction between Mut 101 and residues Gln-96 and Lys-173. Interactions at these residues strongly stabilizes IN thus promoting aberrant multimerization.[167] Rev has also been shown to inhibit integration through a shiftide mechanism that induces oligomerization of IN.[160] Hayouka et al demonstrated that Rev induced a shift in the oligomerization state of IN from an active dimer to inactive tetramer to which viral DNA is unable to bind. The mechanism that Rev uses to induce multimerization is not yet well described, however it is evident that Rev does not induce aberrant multimerization. This suggests that Rev and ALLINIs induce multimerization of IN through two distinct mechanisms. LEDGF and ALLINI, BI-D, are known to utilize two distinct mechanisms of action to induce multimerization of IN. LEDGF induces IN multimerization through the NTD of one subunit of IN and the CCD of the second subunit of IN that forms part of a dimer. ALLINI, BI-D, has been demonstrated to promote aberrant multimerization using the CCD-CCD IN subunit pathways.[161] As such, a comparison can be drawn between Rev, LEDGF and ALLINIs. We propose that Rev induces IN multimerization through the NTD-CCD IN subunits in a similar manner as LEDGF. It is also known that aberrant IN multimerization is reversed in the presence of LEDGF. The results in this study indicate that the aberrant IN multimerization is reduced in the presence of Rev. Since aberrant IN multimerization, induced by ALLINIs is reduced in the presence of Rev and LEDGF, we can infer that Rev reverses IN multimerization using the same mechanism. However, the mechanism of IN multimerization induced by Rev requires further investigation to corroborate this theory.

4.4 The order of addition of ALLINIs impact the integrase-Rev interaction

An order of addition based experiment was conducted using an ELISA based method described by Rosenbluh and co-workers.[174] The aim of the experiment was to determine how ALLINIs affect the interaction between IN and Rev before and after the interaction occurs. For this, we calculated and compared the K_d of the IN-Rev before and after Mut 101 and CX05168 were added.

4.4.1 ALLINIs do not interfere with the integrase-Rev interaction once the protein complex has formed

The K_d of IN–Rev was determined in this study and compared to the K_d reported in literature. K_d reported in this study was significantly higher than the K_d reported by Levin et al, (Section

3.4.1).[177] To date, no other K_d values for the IN–Rev interaction has been reported. Levin at al, used a green fluorescent protein (GFP) based ELISA whereas in this study the interaction between IN and Rev was detected using HRP (Section 2.3). The increase in K_d was possibly attributed to a disparity in sensitivity between the two ELISA detection probes. In addition, the K_d of IN–Rev in the presence of Mut 101 and CX05168 was determined. When comparing the K_d of IN-Rev to the K_d of IN-Mut 101-Rev and IN-CX05168-Rev, it is apparent that the K_d of IN-Rev increased in the presence of Mut 101 and CX05168 (Figure 3.15). This suggests that the binding of the ALLINI to IN obstructs the interaction between IN and Rev. To elaborate on the interaction between IN and Rev discussed in section 1.3.7.2, Rev binds to IN through two aa regions, 13-23 and 53 -67, that interact with aa region 118-128 and 66-80 on IN, respectively.[175,177,197] Rev aa regions 13-23 and 53-67 together interact with IN aa region 174-188. Christ et al demonstrated that upon binding of CX05168 to IN residue, A128 located on IN is displaced.[168] As discussed above, IN residue A128 is involved in the interaction between Rev and IN. Therefore, the binding of Rev to IN in the presence of CX05168 is weaker which explains the increase in K_d. Le Rouzic et al, described the conformational changes of IN when interacting with Mut 101.[167] IN structural differences are observed within α-helices comprising IN residues 115-122 and 123-124 as well as the α-helix comprising IN residues 92-98.[167] According to Benyamini et al, these α-helices are essential for the binding of Rev to IN therefore it is plausible to assume that Rev is unable to interact with the modified IN in the presence of Mut 101.[175] As such, when Mut 101 is already bound to IN, Rev is unable to bind efficiently resulting in a weaker interaction consequently increasing the K_d value.

4.4.2 ALLINIs are unable to dissociate the IN-Rev complex

The second order of addition was tested to determine whether Mut 101 and CX05168 will displace Rev once the IN-Rev interaction has occurred (IN-Rev-ALLINI, Figure 3.15). Results show no significant difference between the K_d of IN-Rev and IN-Rev-ALLINI for both Mut 101 and CX05168. This implies that both ALLINIs are unable to dissociate the IN-Rev complex. According to Le Rouzic and co-workers, the carboxylic acid of Mut 101 forms hydrogen bonds with IN mainly at residues Thr-174, His-171, Glu-170 subsequently displacing Ile-89,Pro-90, and Ala-91.[167] As described in section 1.3.7.2, Rev interacts with IN at residues 174-188 consequently masking Thr-174. Since Thr-174 plays a vital role in the in the interaction between Mut 101 and IN, it is possible that the masking of Thr-174 on IN prevents Mut 101 from binding to IN. As such, Mut 101 is therefore unable to intercept the IN-Rev interaction. In a similar manner, Rev masks the sites on IN essential for CX05168 binding. As described in

section 1.3.7.1, co-crystal structures demonstrated by Christ and co-workers have exhibited the core residues of IN that binds to CX05168. The carboxyl moiety of CX05168 binds to the hydrophobic pocket of an IN dimer at the main chains of Glu-170, His-171, Thr-173, Ala-128 located on the backbone of the protein (Figure 1.8). In addition, CX05168 forms hydrophobic interactions with the side chain of Thr-174. It has been described above that Rev occupies Thr-174 and Ala-128 on IN, residues that are pivotal for the interaction between CX05168 and IN. Consequently, it is conjectured that upon Rev interaction with IN, residues such as Thr-174 and Ala-128 on IN are occupied therefore preventing CX05168 from interacting with IN.[165,196] Alluding to the fact that Rev masks essential IN residues required for Mut 101 and CX05168 binding, no interception of the IN-Rev complex occurs thus resulting in no K_d shift of IN-Rev in the IN-Rev-ALLINI order of addition study. Furthermore, a concentration study of both Mut 101 and CX05168 have been conducted to elucidate whether competitive inhibition occurs in the presence of Rev. No significant difference was observed between 5-, 10-, and 20μM Mut 101 and CX051468 (Figure 3.16).

4.4.3 The immobilization of integrase and Rev to a solid-phase influence the interaction between integrase and Rev

The IN-Rev interaction was observed when coating Rev onto the 96-well multiwall plate to which a pre-formed IN-ALLINI complex was added. This order of addition was tested to distinguish the IN-Rev interaction when IN is immobilized (Discussed in section 4.4.2) and when Rev is immobilized (Rev-IN + ALLINIs). The results corroborate the results discussed in section 4.4.1, wherein ALLINIs intercepted the IN-Rev interaction (Figure 3.16). The reduction in the IN-Rev interaction was dose dependent (Figure 3.16) whereas the concentration of the ALLINIs was inconsequential when testing the IN-ALLINI-Rev order of addition (Figure 3.17). The discrepancy between the impact of the dose of ALLINIs in both order of addition experiments could be attributed to the fact that IN was immobilized when observing the IN-ALLINI-Rev order whereas Rev was immobilized when observing the Rev-IN + ALLINI order. When IN was incubated with the ALLINIs at increasing concentrations (5-, 10-, and 20μM), it is likely that the ALLINIs induced multimerization of IN. Since Mut 101 and CX05168 induce IN multimerization as previously reported, the presence of ALLINIs could have rendered inactive IN multimers that were unable to interact with Rev.[167,168] It is possible that the Rev-IN + ALLINI order was more favourable for multimerization of IN since IN is more flexible in solution allowing multimers to form. As such, a notion to elucidate the discrepancy in dose dependence between the IN-Rev-ALLINI order and the Rev-IN + ALLINI was postulated.

Discussion

Maxisorp 96-well microplates were used in the ELISA order of addition experiments to which either IN or Rev were coated. The adsorbent polystyrene surface of Maxisorp plate comprise hydrophobic- as well hydrophilic groups. Water molecules compete with the surface of the Maxisorp plate in order to bind the biomolecules through hydrogen bonds. Therefore, hydrophilic groups on the Maxisorp surface are more favourable for the binding of biomolecules.[198] According to the hydrophobicity plot measured by the Kyte and Doolittle formula, the grand average of hydrophobicity (GRAVY) of HIV-1 HXBII IN was calculated at -0.366 using the ProtParam tool on the ExPASy Bioinformatics Resource Portal (http://web.expasy.org/protparam/). A GRAVY score below zero indicate that the protein is likely to be hydrophilic.[199] Therefore, IN is highly favourable for the binding to the Maxisorp surface. The regions responsible for multimerization on IN was demonstrated by Shkriabai and co-workers.[200] Through differential hydrogen exchange, mass spectroscopy foot printing, size exclusion chromatography and DLS studies, the C-terminal of IN was identified as a pivotal segment for ALLINI multimerization. These regions include IN residues 181-202 and 250-280 spanning the CCD as well as CTD.[200] Le Rouzic et al, showed that residues in the CCD of IN are involved in IN multimerization induced by Mut 101. When analysing these IN regions using a hydrophobicity plot generated by ProtScale (ExPASy Bioinformatics Resource Portal, http://web.expasy.org/protscale/), it was evident that these regions were comprised of a combination of hydrophobic and hydrophilic groups. When relating this data to the adsorption properties of the Maxisorp surface, it can be inferred that the IN regions responsible for IN multimerization bind to the surface through both hydrogen bonds as well as hydrophobic regions. Therefore, when IN is immobilized onto the Maxisorp surface, it is possible that the regions responsible for IN multimerization are fixed to the surface. Consequently, the IN monomers might be too rigid to interact with each other to efficiently multimerize in the presence of ALLINIs regardless of the ALLINI dose. This would explain the discrepancy between the IN-Rev interaction when IN is immobilized and when Rev is immobilized. When observing the Rev-IN + ALLINI order, Rev is immobilized on to the Maxisorp surface whereas IN with ALLINIs were in solution. The IN molecules in solution are more flexible and therefore able to multimerize more efficiently when incubated with the ALLINIs in a dose dependent manner. In principle, we then infer that the order of addition of the proteins and ALLINIs onto the Maxiwell plates plays a role in the mechanism of which ALLINIs impede the IN-Rev interaction.

4.4.4 Isothermal titration calorimetry studies confirm the interaction between HIV-1 integrase and Rev

ITC confirmed the interaction between IN and Rev and described the thermodynamic properties of the interaction. The K_d (419nM) value of the IN-Rev interaction obtained from ITC experiments correlated with the K_d obtained during the ELISA studies (Figure 3.18, 461nM, p = 0.003). The thermodynamic properties of the IN-Rev interaction has not been described yet, and revealed that the interaction between IN and Rev was an exothermic reaction that is enthalpically driven. The enthalpically driven reaction suggests the presence of polar-, van der Waals- and electrostatic interactions between IN and Rev. The protein structural basis of the IN-Rev interaction was determined by analysing the IN-Rev interaction described by Benyamini and co-workers. The structural model of the IN-Rev has not been defined fully and have only been described through protein docking and structure activity relationship studies using peptide array screening.[175,197] From previous experimental data, Rev dimers minimally interacted with the IN peptide residues 174-188 where the study concluded that Rev prefers a monomeric state for the IN-Rev interaction to occur.[175] This result correlate with the findings of this study where a stoichiometry of 1:1 was calculated. Furthermore, the protein docking studies between IN and Rev elucidated by Benyamini and co-workers demonstrated that hydrophobic interactions occurred between IN residues Leu-68, Gly-70 and Val-72 and Rev residues Leu-13, Val-16, Leu-60 and Leu-64.[175] The hydrophobic interactions observed in the protein docking study was in contrast to the enthalpic reaction observed in the current study. However, Benyamini et al indicated that hydrophobic interactions between IN and Rev were replaced by electrostatic interactions when using a more soluble form of IN harbouring the IN F185K mutation.[175] In the current ITC studies, a recombinant soluble mutant IN was used that was expressed and purified from the pINSD.His.Sol expression vector containing aa substitutions F185K and C280S. These substitutions have demonstrated an improvement in the solubility of the CCD of recombinant IN and does not affect the physiological properties of the enzyme.[201] The disparity between hydrophobic interactions for the IN-Rev interaction observed in wild type IN and electrostatic interactions between IN and Rev observed in soluble mutant IN would explain the enthalpically driven reaction observed in the current ITC experiments. Details of the interaction between the soluble mutant IN and Rev through protein docking was not provided by the study conducted by Benyamini and co-workers. Therefore, further structural analysis of the IN-Rev interaction would support the ITC experimental results and would consequently provide further insight into the mechanism of the interaction.

4.4.5 ALLINIs affect the interaction between HIV-IN and Rev

To further investigate the effect of ALLINIs on the IN-Rev interaction, Mut 101 and CX05168 were incubated with IN before conducting ITC experiments. In the presence of ALLINIs, saturation could not be reached and the data generated could not be fitted using the independent model. As a result, the thermodynamic properties of the IN-Rev interaction could not be calculated and compared to the thermodynamics of the IN-Rev interaction in the absence of ALLINIs (Figure 3.19). It is clear that the presence of ALLINIs interfere with the interaction between IN and Rev. The multimerization studies described in section 3.3 demonstrated that an IN oligomerization shift occurred in the presence of ALLINIs and Rev. Therefore, it is reasonable to assume that Mut 101 and CX05168 promotes multimerization of IN. Consequently, upon the injection of Rev into the sample cell containing IN with Mut 101 or CX05168, Rev is unable to bind to IN. In addition, the resultant ITC samples containing IN, ALLINIs and the titrated Rev were analysed through fluorescence spectroscopy (Figure 3.20). It was evident that the intrinsic fluorescence intensity of IN was quenched by the ALLINIs and Rev. Since it has been proven that IN interacts with Mut 101, CX05168 and Rev, it is plausible to infer that the reduction of the intrinsic fluorescence of the IN molecules in the presence of ALLINIs and Rev is due to static quenching.[167,168,202] As described in figure 1.9, Trp-131 and Trp-132 form essential hydrogen bonds with ALLINIs. The resultant stable complex that forms between the Trp residues of IN and the ALLINIs may lead to a non-fluorescent ground-state that statically quench the reaction.[203] Although further investigation is required to decipher the exact mechanism of the interception of the IN-Rev interaction through ITC experiments, this data suggests that ALLINIs do indeed interfere with the IN-Rev interaction.

.

CHAPTER 5

Future work and Conclusion

5.1 FUTURE WORK

To fully comprehend how Rev is modulated in the presence of ALLINIs, further investigation is required. The following experiments are recommended:

1) Verify phenotypic effects of the IN mutants identified
   Site directed mutagenesis of the aa substitutions identified in the *IN* gene in this current study as well as possible mutations identified in the *rev* gene. Developing a functional assay to investigate the effect the aa substitutions in IN and possibly Rev. A thorough assessment of site directed mutagenesis findings and the phenotypic results from this study would provide insight on the mechanism of action of the resistant mutations observed.
2) Since Rev inhibits HIV replication in the early stage of replication and ALLINIs inhibit replication in the late stage, it would be interesting to observe how ALLINIs modulate Rev in both stages of the replication cycle. This can be achieved through various virology methods: Investigating the morphology of virion particles produced in the presence of both ALLINIs and Rev; Co-immunoprecipitation studies of IN and Rev in the presence of ALLINIs at different time points post-infection.

3) Identifying the mechanism of action used by Rev to induce IN multimerization
   A notion describing Rev's reversal of aberrant multimerization induced by ALLINIs has been reported in this study. Previous literature has defined the mechanism of IN multimerization induced ALLINIs, however the exact mechanism of action involving multimerization of IN induced by Rev is not well defined. A clear description of the manner in which Rev induces IN multimerization will validate the notion that Rev reverses aberrant IN multimerization (described in section 4.5). As such, Rev peptide mapping will identify the regions involved in IN multimerization.

4) Include LEDGF to the current IN, Rev and ALLINI interaction studies as well as multimerization studies
   It would be interesting to observe the interaction between IN, Rev and LEDGF in the presence of ALLINIs. Future studies may include the addition of LEDGF to the experiments to observe the interaction between IN and LEDGF in the presence of both Rev and ALLINIs.

5.2 CONCLUSION

In conclusion, this study delineated the behaviour of HIV-1 Rev in the presence of ALLINIs through three objectives: 1 – To date, limited data on ALLINI resistance against HIV-1 subtype C isolates is available. Therefore, *in vitro* resistant selection studies were conducted to identify resistant mutations in the *IN* gene as well as the *rev gene* against Mut 101 and CX05168. Resistance mutations in the *rev* gene would implicate that ALLINIs have a direct interaction with the Rev protein. However, due to continuous challenges encountered, genotypic analysis of the *rev* gene was unsuccessful. Genotypic analysis of the *IN* gene revealed several mutations against Mut 101. Most of these mutations have been previously observed in HIV-1 subtype B isolates against other quinolone derived ALLINIs. Phenotypic analysis of the mutations in this study demonstrated a change in efficacy of Mut 101 against HIV-1 subtype C isolates harbouring the mutations. Unsuccessful *in vitro* resistance selection studies using CX05168 led to *in vitro* phenotypic inhibition studies to determine the EC_{50} of CX051468 against HIV-1 subtype C isolates. This study is the first to report that the EC_{50} of CX05168 significantly increases against HIV-1 subtype C isolates tested in this study thus suggesting an alternative binding mode of CX05168 to HIV-1 IN subtype compared to HIV-1 subtype B. 2 – Since Rev, Mut 101 and CX05168 induce an oligomerization shift of IN, this objective aimed to elucidate the state of IN multimerization in the presence of both Rev and Mut101 or CX05168. This study postulated a possible mechanism of action where Rev reverses the aberrant multimerization induced by ALLINIs. The third objective described the IN-Rev interaction in the presence of Mut 101 and CX05168. Results indicated that the interaction between IN and Rev is intercepted by ALLINIs in an order of addition manner. ALLINIs are only able to perturb the IN-Rev interaction before the interaction occurs and not through dissociation of the interaction. ITC studies supported these findings and provided novel thermodynamic properties of the IN-Rev interaction. Taken together, the functions of Rev and ALLINIs are indeed compromised when both Rev and ALLINIs are present. The findings in this study provides insight into the mechanism of ALLINIs in the presence of viral proteins that are involved in the integration process. More specifically the results show that ALLINIs interfere with the interaction between IN and Rev which could consequently influence the regulation of integration. The perturbance of integration regulation could be an additional mechanism of action of ALLINIs. As such, this data may assist in the development of future HIV antiretroviral drugs.

1. Barré-Sinoussi, F. *et al.* Isolation of a T-lymphotropic retrovirus from a patient at risk for acquired immune deficiency syndrome (AIDS). *Science* **220,** 868–871 (1983).
2. Durack, D. Opportunistic infections and Kaposi's sarcoma in homosexual men. *N Engl J Med* **305,** 1465–1467 (1981).
3. Gallo, R. C. *et al.* Frequent detection and isolation of cytopathic retroviruses (HTLV-III) from patients with AIDS and at risk for AIDS. *Science* **224,** 500–503 (1984).
4. Gelderblom, H. R. Assembly and morphology of HIV: potential effect of structure on viral function. *AIDS Lond. Engl.* **5,** 617–637 (1991).
5. Smith, J. A. & Daniel, R. Following the path of the virus: the exploitation of host DNA repair mechanisms by retroviruses. *ACS Chem. Biol.* **1,** 217–226 (2006).
6. Lytle, C. D. *et al.* Filtration sizes of human immunodeficiency virus type 1 and surrogate viruses used to test barrier materials. *Appl. Environ. Microbiol.* **58,** 747–749 (1992).
7. Ozel, M., Pauli, G. & Gelderblom, H. R. The organization of the envelope projections on the surface of HIV. *Arch. Virol.* **100,** 255–266 (1988).
8. Hallenberger, S., Moulard, M., Sordel, M., Klenk, H. D. & Garten, W. The role of eukaryotic subtilisin-like endoproteases for the activation of human immunodeficiency virus glycoproteins in natural host cells. *J. Virol.* **71,** 1036–1045 (1997).
9. van der Loeff, M. F. S. *et al.* Sixteen years of HIV surveillance in a West African research clinic reveals divergent epidemic trends of HIV-1 and HIV-2. *Int. J. Epidemiol.* **35,** 1322–1328 (2006).
10. Hamel, D. J. *et al.* Twenty years of prospective molecular epidemiology in Senegal: changes in HIV diversity. *AIDS Res. Hum. Retroviruses* **23,** 1189–1196 (2007).
11. Gelderblom, D. H. R., Özel, M. & Pauli, G. Morphogenesis and morphology of HIV structure-function relations. *Arch. Virol.* **106,** 1–13 (1989).
12. Abrahams, S. Evaluation of the NIH Clinical Collection to identify potential HIV-1 integrase inhibitors. (Faculty of Health Sciences, University of the Witwatersrand, Johannesburg, 2014).
13. Göttlinger, H. G., Sodroski, J. G. & Haseltine, W. A. Role of capsid precursor processing and myristoylation in morphogenesis and infectivity of human immunodeficiency virus type 1. *Proc. Natl. Acad. Sci. U. S. A.* **86,** 5781–5785 (1989).
14. Bernstein, H. B. *et al.* Oligomerization of the hydrophobic heptad repeat of gp41. *J. Virol.* **69,** 2745–2750 (1995).
15. Strebel, K. *et al.* The HIV 'A' (sor) gene product is essential for virus infectivity. *Nature* **328,** 728–730 (1987).

16. Sherman, M. P. & Greene, W. C. Slipping through the door: HIV entry into the nucleus. *Microbes Infect. Inst. Pasteur* **4,** 67–73 (2002).
17. Jacks, T. *et al.* Characterization of ribosomal frameshifting in HIV-1 gag-pol expression. *Nature* **331,** 280–283 (1988).
18. Ruben, S. *et al.* Structural and functional characterization of human immunodeficiency virus tat protein. *J. Virol.* **63,** 1–8 (1989).
19. Zapp, M. L. & Green, M. R. Sequence-specific RNA binding by the HIV-1 Rev protein. *Nature* **342,** 714–716 (1989).
20. Malim, M. H., Hauber, J., Le, S. Y., Maizel, J. V. & Cullen, B. R. The HIV-1 rev trans-activator acts through a structured target sequence to activate nuclear export of unspliced viral mRNA. *Nature* **338,** 254–257 (1989).
21. Felber, B. K., Drysdale, C. M. & Pavlakis, G. N. Feedback regulation of human immunodeficiency virus type 1 expression by the Rev protein. *J. Virol.* **64,** 3734–3741 (1990).
22. Levin, A. *et al.* Novel regulation of HIV-1 replication and pathogenicity: Rev inhibition of integration. *Protein Eng. Des. Sel.* **22,** 753–763 (2009).
23. Garcia, J. V. & Miller, A. D. Downregulation of cell surface CD4 by nef. *Res. Virol.* **143,** 52–55 (1992).
24. Luria, S., Chambers, I. & Berg, P. Expression of the type 1 human immunodeficiency virus Nef protein in T cells prevents antigen receptor-mediated induction of interleukin 2 mRNA. *Proc. Natl. Acad. Sci. U. S. A.* **88,** 5326–5330 (1991).
25. Miller, M. D., Warmerdam, M. T., Gaston, I., Greene, W. C. & Feinberg, M. B. The human immunodeficiency virus-1 nef gene product: a positive factor for viral infection and replication in primary lymphocytes and macrophages. *J. Exp. Med.* **179,** 101–113 (1994).
26. Stanley, B. J. *et al.* Structural insight into the human immunodeficiency virus Vif SOCS box and its role in human E3 ubiquitin ligase assembly. *J. Virol.* **82,** 8656–8663 (2008).
27. Heinzinger, N. K. *et al.* The Vpr protein of human immunodeficiency virus type 1 influences nuclear localization of viral nucleic acids in nondividing host cells. *Proc. Natl. Acad. Sci. U. S. A.* **91,** 7311–7315 (1994).
28. Willey, R. L., Maldarelli, F., Martin, M. A. & Strebel, K. Human immunodeficiency virus type 1 Vpu protein induces rapid degradation of CD4. *J. Virol.* **66,** 7193–7200 (1992).
29. Klimkait, T., Strebel, K., Hoggan, M. D., Martin, M. A. & Orenstein, J. M. The human immunodeficiency virus type 1-specific protein vpu is required for efficient virus maturation and release. *J. Virol.* **64,** 621–629 (1990).

30. Clapham, P. R. & McKnight, Á. HIV-1 receptors and cell tropism. *Br. Med. Bull.* **58,** 43–59 (2001).
31. Haase, A. T. Population biology of HIV-1 infection: viral and CD4+ T cell demographics and dynamics in lymphatic tissues. *Annu. Rev. Immunol.* **17,** 625–656 (1999).
32. Alkhatib, G. *et al.* CC CKR5: a RANTES, MIP-1alpha, MIP-1beta receptor as a fusion cofactor for macrophage-tropic HIV-1. *Science* **272,** 1955–1958 (1996).
33. Doranz, B. J. *et al.* A dual-tropic primary HIV-1 isolate that uses fusin and the beta-chemokine receptors CKR-5, CKR-3, and CKR-2b as fusion cofactors. *Cell* **85,** 1149–1158 (1996).
34. Deng, H. *et al.* Identification of a major co-receptor for primary isolates of HIV-1. *Nature* **381,** 661–666 (1996).
35. Feng, Y., Broder, C. C., Kennedy, P. E. & Berger, E. A. HIV-1 entry cofactor: functional cDNA cloning of a seven-transmembrane, G protein-coupled receptor. *Science* **272,** 872–877 (1996).
36. Wyatt, R. *et al.* The antigenic structure of the HIV gp120 envelope glycoprotein. *Nature* **393,** 705–711 (1998).
37. Liu, J., Bartesaghi, A., Borgnia, M. J., Sapiro, G. & Subramaniam, S. Molecular architecture of native HIV-1 gp 120 trimers. *Nature* **455,** 109–113 (2008).
38. Goto, T., Nakai, M. & Ikuta, K. The life-cycle of human immunodeficiency virus type 1. *Micron Oxf. Engl. 1993* **29,** 123–138 (1998).
39. Haseltine, W. A. Molecular biology of the human immunodeficiency virus type 1. *FASEB J.* **5,** 2349–2360 (1991).
40. Raghavendra, N. K. *et al.* Identification of host proteins associated with HIV-1 preintegration complexes isolated from infected CD4+ cells. *Retrovirology* **7,** 66 (2010).
41. Hamamoto, S., Nishitsuji, H., Amagasa, T., Kannagi, M. & Masuda, T. Identification of a novel human immunodeficiency virus type 1 integrase interactor, gemin2, that facilitates efficient viral cDNA synthesis in vivo. *J. Virol.* **80,** 5670–5677 (2006).
42. Cereseto, A. *et al.* Acetylation of HIV-1 integrase by p300 regulates viral integration. *EMBO J.* **24,** 3070–3081 (2005).
43. Farnet, C. M. & Bushman, F. D. HIV-1 cDNA integration: requirement of HMG I(Y) protein for function of preintegration complexes in vitro. *Cell* **88,** 483–492 (1997).
44. Parissi, V. *et al.* Functional interactions of human immunodeficiency virus type 1 integrase with human and yeast HSP60. *J. Virol.* **75,** 11344–11353 (2001).

45. Violot, S. *et al.* The human polycomb group EED protein interacts with the integrase of human immunodeficiency virus type 1. *J. Virol.* **77,** 12507–12522 (2003).
46. Ao, Z. *et al.* Interaction of human immunodeficiency virus type 1 integrase with cellular nuclear import receptor importin 7 and its impact on viral replication. *J. Biol. Chem.* **282,** 13456–13467 (2007).
47. Kalpana, G. V., Marmon, S., Wang, W., Crabtree, G. R. & Goff, S. P. Binding and stimulation of HIV-1 integrase by a human homolog of yeast transcription factor SNF5. *Science* **266,** 2002–2006 (1994).
48. Cherepanov, P. *et al.* HIV-1 integrase forms stable tetramers and associates with LEDGF/p75 protein in human cells. *J. Biol. Chem.* **278,** 372–381 (2003).
49. Willetts, K. E. *et al.* DNA repair enzyme uracil DNA glycosylase is specifically incorporated into human immunodeficiency virus type 1 viral particles through a Vpr-independent mechanism. *J. Virol.* **73,** 1682–1688 (1999).
50. Bushman, F. D. & Craigie, R. Activities of human immunodeficiency virus (HIV) integration protein in vitro: specific cleavage and integration of HIV DNA. *Proc. Natl. Acad. Sci. U. S. A.* **88,** 1339–1343 (1991).
51. Karn, J. & Stoltzfus, C. M. Transcriptional and posttranscriptional regulation of hiv-1 gene expression. *Cold Spring Harb. Perspect. Med.* **2,** (2012).
52. Mak, T. W. & Saunders, M. E. *The immune response: basic and clinical principles*. (Elsevier/Academic, 2006).
53. Zhu, P. *et al.* Electron tomography analysis of envelope glycoprotein trimers on HIV and simian immunodeficiency virus virions. *Proc. Natl. Acad. Sci. U. S. A.* **100,** 15812–15817 (2003).
54. Lee, S.-K., Potempa, M. & Swanstrom, R. The Choreography of HIV-1 Proteolytic Processing and Virion Assembly. *J. Biol. Chem.* **287,** 40867–40874 (2012).
55. Sundquist, W. I. & Kräusslich, H.-G. HIV-1 assembly, budding, and maturation. *Cold Spring Harb. Perspect. Med.* **2,** (2012).
56. Kolegraff, K., Bostik, P. & Ansari, A. A. Characterization and role of lentivirus-associated host proteins. *Exp. Biol. Med. Maywood NJ* **231,** 252–263 (2006).
57. Reeves, J. D. & Piefer, A. J. Emerging drug targets for antiretroviral therapy. *Drugs* **65,** 1747–1766 (2005).
58. Lutzke, R. A. & Plasterk, R. H. HIV integrase: a target for drug discovery. *Genes Funct.* **1,** 289–307 (1997).

59. De Clercq, E. Anti-HIV drugs: 25 compounds approved within 25 years after the discovery of HIV. *Int. J. Antimicrob. Agents* **33,** 307–320 (2009).
60. Pauwels, R. New non-nucleoside reverse transcriptase inhibitors (NNRTIs) in development for the treatment of HIV infections. *Curr. Opin. Pharmacol.* **4,** 437–446 (2004).
61. Broder, S. The development of antiretroviral therapy and its impact on the HIV-1/AIDS pandemic. *Antiviral Res.* **85,** 1–18 (2010).
62. Yarchoan, R. *et al.* Administration of 3'-azido-3'-deoxythymidine, an inhibitor of HTLV-III/LAV replication, to patients with aids or AIDS-related complex. *The Lancet* **327,** 575–580 (1986).
63. Goody, R. S., Müller, B. & Restle, T. Factors contributing to the inhibition of HIV reverse transcriptase by chain-terminating nucleotides in vitro and in vivo. *FEBS Lett.* **291,** 1–5 (1991).
64. HIV and AIDS Activities - Antiretroviral drugs used in the treatment of HIV infection. Available at: http://www.fda.gov/ForConsumers/byAudience/ForPatientAdvocates/HIVandAIDSActivities/ucm118915.htm. (Accessed: 16th July 2013)
65. Tantillo, C. *et al.* Locations of anti-AIDS drug binding sites and resistance mutations in the three-dimensional structure of HIV-1 reverse transcriptase: implications for mechanisms of drug inhibition and resistance. *J. Mol. Biol.* **243,** 369–387 (1994).
66. Spence, R. A., Kati, W. M., Anderson, K. S. & Johnson, K. A. Mechanism of inhibition of HIV-1 reverse transcriptase by non nucleoside inhibitors. *Science* **267,** 988–993 (1995).
67. Lee, W. A. *et al.* Selective intracellular activation of a novel pro-drug of the human immunodeficiency virus reverse transcriptase inhibitor tenofovir leads to preferential distribution and accumulation in lymphatic tissue. *Antimicrob. Agents Chemother.* **49,** 1898–1906 (2005).
68. Esnouf, R. *et al.* Mechanism of inhibition of HIV-1 reverse transcriptase by non-nucleoside inhibitors. *Nat. Struct. Mol. Biol.* **2,** 303–308 (1995).
69. De Clercq, E. The role of non-nucleoside reverse transcriptase inhibitors (NNRTIs) in the therapy of HIV-1 infection. *Antiviral Res.* **38,** 153–179 (1998).
70. Yee, K. L. *et al.* Evaluation of Doravirine pharmacokinetics when switching from efavirenz to doravirine in healthy subjects. *Antimicrob. Agents Chemother.* **61,** e01757-16 (2017).
71. Wensing, A. M. J., van Maarseveen, N. M. & Nijhuis, M. Fifteen years of HIV protease inhibitors: raising the barrier to resistance. *Antiviral Res.* **85,** 59–74 (2010).

72. Kharasch, E. D. *et al.* Mechanism of ritonavir changes in methadone pharmacokinetics and pharmacodynamics: I. Evidence against CYP3A mediation of methadone clearance. *Clin. Pharmacol. Ther.* **84,** 497–505 (2008).
73. Castonguay, L. A. *et al.* Binding of 2-aryl-4-(piperidin-1-yl)butanamines and 1,3,4-trisubstituted pyrrolidines to human CCR5: a molecular modeling-guided mutagenesis study of the binding pocket. *Biochemistry (Mosc.)* **42,** 1544–1550 (2003).
74. Lieberman-Blum, S. S., Fung, H. B. & Bandres, J. C. Maraviroc: a CCR5-receptor antagonist for the treatment of HIV-1 infection. *Clin. Ther.* **30,** 1228–1250 (2008).
75. Bai, Y. *et al.* Covalent fusion inhibitors targeting HIV-1 gp41 deep pocket. *Amino Acids* **44,** 701–713 (2013).
76. Weissenhorn, W., Dessen, A., Harrison, S. C., Skehel, J. J. & Wiley, D. C. Atomic structure of the ectodomain from HIV-1 gp41. *Nature* **387,** 426–430 (1997).
77. Chan, D. C., Fass, D., Berger, J. M. & Kim, P. S. Core structure of gp41 from the HIV envelope glycoprotein. *Cell* **89,** 263–273 (1997).
78. d'Angelo, J., Mouscadet, J. F., Desmaele, D., Zouhiri, F. & Leh, H. HIV-1 integrase: the next target for AIDS therapy? *Pathol. Biol.* **49,** 237–246 (2001).
79. Summa, V. *et al.* Discovery of Raltegravir, a potent, selective orally bioavailable HIV-integrase inhibitor for the treatment of HIV-AIDS infection. *J. Med. Chem.* **51,** 5843–5855 (2008).
80. HIV and AIDS activities - FDA approval of Isentress (raltegravir). Available at: http://www.fda.gov/ForConsumers/ByAudience/ForPatientAdvocates/HIVandAIDSActivities/ucm124040.htm. (Accessed: 17th July 2013)
81. Serrao, E., Odde, S., Ramkumar, K. & Neamati, N. Raltegravir, elvitegravir, and metoogravir: the birth of. *Retrovirology* **6,** 25 (2009).
82. Elion, R. *et al.* The single-tablet regimen Elvitegravir/Cobicistat/Emtricitabine/Tenofovir Disoproxil Fumarate (EVG/COBI/FTC/TDF; 'QUAD') maintains a high rate of virologic suppression, and Cobicistat (COBI) is an effective pharmacoenhancer through 48 weeks. (2010).
83. Xu, L. *et al.* Cobicistat (GS-9350): A potent and selective inhibitor of human CYP3A as a novel pharmacoenhancer. *ACS Med. Chem. Lett.* **1,** 209–213 (2010).
84. Cohen, C. *et al.* Randomized, phase 2 evaluation of two single-tablet regimens elvitegravir/cobicistat/emtricitabine/tenofovir disoproxil fumarate versus efavirenz/emtricitabine/tenofovir disoproxil fumarate for the initial treatment of HIV infection: *AIDS* **25,** F7–F12 (2011).

85. Tsiang, M. *et al.* Antiviral activity of Bictegravir (GS-9883), a novel potent hiv-1 integrase strand transfer inhibitor with an improved resistance profile. *Antimicrob. Agents Chemother.* **60,** 7086–7097 (2016).
86. U.S. Food and Drug Administration Approves Gilead's Biktarvy® (Bictegravir, Emtricitabine, Tenofovir Alafenamide) for treatment of HIV-1 Infection | Gilead. Available at: http://www.gilead.com/news/press-releases/2018/2/us-food-and-drug-administration-approves-gileads-biktarvy-bictegravir-emtricitabine-tenofovir-alafenamide-for-treatment-of-hiv1-infection. (Accessed: 9th July 2018)
87. Witmer, M. & Danovich, R. Selection and analysis of HIV-1 integrase strand transfer inhibitor resistant mutant viruses. *Methods* **47,** 277–282 (2009).
88. O'Neil, P. K. Mutation and selection: shaping the HIV-1 genome. (The University of Utah, 2003).
89. Mansky, L. M. HIV mutagenesis and the evolution of antiretroviral drug resistance. *Drug Resist. Updat. Rev. Comment. Antimicrob. Anticancer Chemother.* **5,** 219–223 (2002).
90. Abram, M. E., Ferris, A. L., Shao, W., Alvord, W. G. & Hughes, S. H. Nature, position, and frequency of mutations made in a single cycle of HIV-1 replication. *J. Virol.* **84,** 9864–9878 (2010).
91. Palella, F. J., Jr *et al.* The association of HIV susceptibility testing with survival among HIV-infected patients receiving antiretroviral therapy: a cohort study. *Ann. Intern. Med.* **151,** 73–84 (2009).
92. Garone, D. B. *et al.* High rate of virological re-suppression among patients failing second-line antiretroviral therapy following enhanced adherence support: A model of care in Khayelitsha, South Africa. *South. Afr. J. HIV Med.* **14,** 170–176 (2013).
93. Hewer Raymond, Kriel Frederiek H & Coates Judy. *Drug Discovery in Africa - Impacts of Genomics, Natural Products, Traditional Medicines, Insights*. (2012).
94. Clavel, F. & Hance, A. J. HIV Drug Resistance. *N. Engl. J. Med.* **350,** 1023–1035 (2004).
95. Paraschiv, S. *et al.* Nucleoside reverse transcriptase inhibitor resistance mutations in subtype F1 strains isolated from heavily treated adolescents in Romania. *Int. J. Infect. Dis.* **13,** 81–89 (2009).
96. Brun-Vézinet, F. *et al.* Clinically relevant interpretation of genotype for resistance to abacavir. *AIDS Lond. Engl.* **17,** 1795–1802 (2003).
97. Petropoulos, C. J. *et al.* A novel phenotypic drug susceptibility assay for human immunodeficiency virus type 1. *Antimicrob. Agents Chemother.* **44,** 920–928 (2000).

98. Lanier, E. R. *et al.* Antiviral efficacy of abacavir in antiretroviral therapy-experienced adults harbouring HIV-1 with specific patterns of resistance to nucleoside reverse transcriptase inhibitors. *Antivir. Ther.* **9,** 37–45 (2004).
99. Sluis-Cremer, N., Temiz, N. A. & Bahar, I. Conformational changes in HIV-1 reverse transcriptase induced by nonnucleoside reverse transcriptase inhibitor binding. *Curr. HIV Res.* **2,** 323–332 (2004).
100. Vingerhoets, J. *et al.* TMC125 displays a high genetic barrier to the development of resistance: evidence from in vitro selection experiments. *J. Virol.* **79,** 12773–12782 (2005).
101. Rhee, S.-Y. *et al.* Natural variation of HIV-1 group M integrase: Implications for a new class of antiretroviral inhibitors. *Retrovirology* **5,** 74 (2008).
102. Bacheler, L. *et al.* Genotypic correlates of phenotypic resistance to efavirenz in virus isolates from patients failing nonnucleoside reverse transcriptase inhibitor therapy. *J. Virol.* **75,** 4999–5008 (2001).
103. Knoll, B. M., Vento, S. & Temesgen, Z. Etravirine. *Drugs Today Barc. Spain 1998* **44,** 23–33 (2008).
104. Rimsky, L. *et al.* Genotypic and phenotypic characterization of HIV-1 isolates obtained from patients on rilpivirine therapy experiencing virologic failure in the phase 3 ECHO and THRIVE studies: 48-week analysis. *J. Acquir. Immune Defic. Syndr. 1999* **59,** 39–46 (2012).
105. Kim, R. & Baxter, J. D. Protease inhibitor resistance update: where are we now? *AIDS Patient Care STDs* **22,** 267–277 (2008).
106. Sista, P. R. *et al.* Characterization of determinants of genotypic and phenotypic resistance to enfuvirtide in baseline and on-treatment HIV-1 isolates. *AIDS Lond. Engl.* **18,** 1787–1794 (2004).
107. Menzo, S. *et al.* Genotype and phenotype patterns of human immunodeficiency virus type 1 resistance to enfuvirtide during long-term treatment. *Antimicrob. Agents Chemother.* **48,** 3253–3259 (2004).
108. Deeks, S. G. *et al.* Interruption of Enfuvirtide in HIV-1-Infected Adults with Incomplete Viral Suppression on an Enfuvirtide-Based Regimen. *J. Infect. Dis.* **195,** 387–391 (2007).
109. Trkola, A. *et al.* HIV-1 escape from a small molecule, CCR5-specific entry inhibitor does not involve CXCR4 use. *Proc. Natl. Acad. Sci. U. S. A.* **99,** 395–400 (2002).

110. Kuhmann, S. E. *et al.* Genetic and phenotypic analyses of human immunodeficiency virus type 1 escape from a small-molecule CCR5 inhibitor. *J. Virol.* **78,** 2790–2807 (2004).
111. Moore, J. P. & Kuritzkes, D. R. A pièce de resistance: how HIV-1 escapes small molecule CCR5 inhibitors. *Curr. Opin. HIV AIDS* **4,** 118–124 (2009).
112. Rice, P. A. & Baker, T. A. Comparative architecture of transposase and integrase complexes. *Nat. Struct. Mol. Biol.* **8,** 302–307 (2001).
113. Engelman, A., Bushman, F. D. & Craigie, R. Identification of discrete functional domains of HIV-1 integrase and their organization within an active multimeric complex. *EMBO J.* **12,** 3269–3275 (1993).
114. Engelman, A. & Craigie, R. Identification of conserved amino acid residues critical for human immunodeficiency virus type 1 integrase function in vitro. *J. Virol.* **66,** 6361–6369 (1992).
115. van Gent, D. C., Vink, C., Groeneger, A. A. & Plasterk, R. H. Complementation between HIV integrase proteins mutated in different domains. *EMBO J.* **12,** 3261–3267 (1993).
116. Valkov, E. *et al.* Functional and structural characterization of the integrase from the prototype foamy virus. *Nucleic Acids Res.* **37,** 243–255 (2009).
117. Esposito, D. & Craigie, R. HIV integrase structure and function. *Adv. Virus Res.* **52,** 319–333 (1999).
118. Kulkosky, J., Jones, K. S., Katz, R. A., Mack, J. P. & Skalka, A. M. Residues critical for retroviral integrative recombination in a region that is highly conserved among retroviral/retrotransposon integrases and bacterial insertion sequence transposases. *Mol. Cell. Biol.* **12,** 2331–2338 (1992).
119. Polard, P. & Chandler, M. Bacterial transposases and retroviral integrases. *Mol. Microbiol.* **15,** 13–23 (1995).
120. Rowland, S. J., Sherratt, D. J., Stark, W. M. & Boocock, M. R. Tn552 transposase purification and in vitro activities. *EMBO J.* **14,** 196–205 (1995).
121. McColl, D. J. & Chen, X. Strand transfer inhibitors of HIV-1 integrase: Bringing IN a new era of antiretroviral therapy. *Antiviral Res.* **85,** 101–118 (2010).
122. Delelis, O., Carayon, K., Saïb, A., Deprez, E. & Mouscadet, J.-F. Integrase and integration: biochemical activities of HIV-1 integrase. *Retrovirology* **5,** 114 (2008).
123. Emiliani, S. *et al.* Integrase mutants defective for interaction with LEDGF/p75 are impaired in chromosome tethering and HIV-1 replication. *J. Biol. Chem.* **280,** 25517–25523 (2005).

124. Yoder, K. E. & Bushman, F. D. Repair of Gaps in Retroviral DNA Integration Intermediates. *J. Virol.* **74,** 11191–11200 (2000).
125. Brin, E., Yi, J., Skalka, A. & Leis, J. Modeling the late steps in HIV-1 retroviral integrase-catalyzed DNA integration. *J Biol Chem* **275,** 39287 (2000).
126. Engelman, A., Mizuuchi, K. & Craigie, R. HIV-1 DNA integration: mechanism of viral DNA cleavage and DNA strand transfer. *Cell* **67,** 1211–1221 (1991).
127. Hare, S. *et al.* Structural basis for functional tetramerization of lentiviral integrase. *PLoS Pathog* **5,** e1000515 (2009).
128. DeAnda, F. *et al.* Dolutegravir interactions with HIV-1 integrase-DNA: structural rationale for drug resistance and dissociation kinetics. *PLOS ONE* **8,** e77448 (2013).
129. Cherepanov, P. *et al.* High-level expression of active HIV-1 integrase from a synthetic gene in human cells. *FASEB J.* **14,** 1389–1399 (2000).
130. Hare, S. *et al.* Molecular mechanisms of retroviral integrase inhibition and the evolution of viral resistance. *Proc. Natl. Acad. Sci.* **107,** 20057–20062 (2010).
131. Hare, S., Gupta, S. S., Valkov, E., Engelman, A. & Cherepanov, P. Retroviral intasome assembly and inhibition of DNA strand transfer. *Nature* **464,** 232–236 (2010).
132. Al-Mawsawi, L. Q., Christ, F., Dayam, R., Debyser, Z. & Neamati, N. Inhibitory profile of a LEDGF/p75 peptide against HIV-1 integrase: Insight into integrase–DNA complex formation and catalysis. *FEBS Lett.* **582,** 1425–1430 (2008).
133. Hayouka, Z. *et al.* Inhibiting HIV-1 integrase by shifting its oligomerization equilibrium. *Proc. Natl. Acad. Sci.* **104,** 8316–8321 (2007).
134. Kessl, J. J. *et al.* An allosteric mechanism for inhibiting HIV-1 integrase with a small molecule. *Mol. Pharmacol.* **76,** 824–832 (2009).
135. Agrawal, A. *et al.* Probing chelation motifs in HIV integrase inhibitors. *Proc. Natl. Acad. Sci.* **109,** 2251–2256 (2012).
136. Gallien, S. *et al.* Emerging integrase inhibitor resistance mutations in raltegravir-treated HIV-1-infected patients with low-level viremia. *AIDS Lond. Engl.* **25,** 665–669 (2011).
137. Baldanti, F., Paulucci, S., Gulminetti, R., Brandolini, G. & Maserati, R. Early emergence of Raltegravir resistance mutations in patients receiving HAART salvage regimens.
138. Fikkert, V. *et al.* Multiple mutations in human immunodeficiency virus-1 integrase confer resistance to the clinical trial drug S-1360. *AIDS Lond. Engl.* **18,** 2019–2028 (2004).
139. Roquebert, B. *et al.* Selection of the Q148R integrase inhibitor resistance mutation in a failing raltegravir containing regimen. *AIDS Lond. Engl.* **22,** 2045–2046 (2008).

140. Malet, I. *et al.* Mutations associated with failure of raltegravir treatment affect integrase sensitivity to the inhibitor in vitro. *Antimicrob. Agents Chemother.* **52,** 1351–1358 (2008).
141. Fransen, S. *et al.* Loss of raltegravir susceptibility by human immunodeficiency virus type 1 is conferred via multiple non overlapping genetic pathways. *J. Virol.* **83,** 11440–11446 (2009).
142. Delelis, O. *et al.* The G140S mutation in HIV integrases from raltegravir-resistant patients rescues catalytic defect due to the resistance Q148H mutation. *Nucleic Acids Res.* **37,** 1193–1201 (2008).
143. Blanco, J.-L., Varghese, V., Rhee, S.-Y., Gatell, J. M. & Shafer, R. W. HIV-1 integrase inhibitor resistance and its clinical implications. *J. Infect. Dis.* **203,** 1204–1214 (2011).
144. Fransen, S., Gupta, S., Frantzell, A., Petropoulos, C. J. & Huang, W. Substitutions at amino acid positions 143, 148, and 155 of HIV-1 integrase define distinct genetic barriers to raltegravir resistance in vivo. *J. Virol.* **86,** 7249–7255 (2012).
145. Geretti, A. M., Armenia, D. & Ceccherini-Silberstein, F. Emerging patterns and implications of HIV-1 integrase inhibitor resistance. *Curr. Opin. Infect. Dis.* **25,** 677–686 (2012).
146. Ramanathan, D. S., Mathias, A. A., German, P. & Kearney, B. P. Clinical Pharmacokinetic and Pharmacodynamic Profile of the HIV Integrase Inhibitor Elvitegravir. *Clin. Pharmacokinet.* **50,** 229–244 (2011).
147. Goethals, O. *et al.* Resistance Mutations in human immunodeficiency virus type 1 integrase selected with elvitegravir confer reduced susceptibility to a wide range of integrase inhibitors. *J. Virol.* **82,** 10366–10374 (2008).
148. Garrido, C. *et al.* Resistance associated mutations to dolutegravir (S/GSK1349572) in HIV-infected patients--impact of HIV subtypes and prior raltegravir experience. *Antiviral Res.* **90,** 164–167 (2011).
149. Quashie, P. K. *et al.* Characterization of the R263K mutation in HIV-1 integrase that confers low-level resistance to the second-generation integrase strand transfer inhibitor dolutegravir. *J. Virol.* **86,** 2696–2705 (2012).
150. Mesplede, T. *et al.* Viral fitness cost prevents HIV-1 from evading dolutegravir drug pressure. *Retrovirology* **10,** 22 (2013).
151. Cherepanov, P., Ambrosio, A. L. B., Rahman, S., Ellenberger, T. & Engelman, A. Structural basis for the recognition between HIV-1 integrase and transcriptional coactivator p75. *Proc. Natl. Acad. Sci. U. S. A.* **102,** 17308–17313 (2005).

152. Busschots, K. *et al.* Identification of the LEDGF/p75 Binding Site in HIV-1 Integrase. *J. Mol. Biol.* **365,** 1480–1492 (2007).
153. Maertens, G. *et al.* LEDGF/p75 is essential for nuclear and chromosomal targeting of HIV-1 integrase in human cells. *J. Biol. Chem.* **278,** 33528–33539 (2003).
154. Hare, S. *et al.* A Novel Co-Crystal Structure Affords the Design of Gain-of-Function Lentiviral Integrase Mutants in the Presence of Modified PSIP1/LEDGF/p75. *PLOS Pathog.* **5,** e1000259 (2009).
155. McKee, C. J. *et al.* Dynamic modulation of hiv-1 integrase structure and function by cellular lens epithelium-derived growth factor (ledgf) Protein. *J. Biol. Chem.* **283,** 31802–31812 (2008).
156. Llano, M., Delgado, S., Vanegas, M. & Poeschla, E. M. Lens epithelium-derived growth factor/p75 prevents proteasomal degradation of hiv-1 integrase. *J. Biol. Chem.* **279,** 55570–55577 (2004).
157. Schrijvers, R. *et al.* LEDGF/p75-independent HIV-1 replication demonstrates a role for HRP-2 and remains sensitive to inhibition by LEDGINs. *PLoS Pathog.* **8,** e1002558 (2012).
158. Shun, M.-C. *et al.* LEDGF/p75 functions downstream from preintegration complex formation to effect gene-specific HIV-1 integration. *Genes Dev.* **21,** 1767–1778 (2007).
159. Wang, H. *et al.* HRP2 determines the efficiency and specificity of HIV-1 integration in LEDGF/p75 knockout cells but does not contribute to the antiviral activity of a potent LEDGF/p75-binding site integrase inhibitor. *Nucleic Acids Res.* **40,** 11518–11530 (2012).
160. Hayouka, Z., Levin, A., Loyter, A. & Friedler, A. Peptide inhibitors of the HIV-1 integrase protein. *Bull. Isr. Chem. Soc. Issue No 25* 20–28 (2010).
161. Jurado, K. A. *et al.* Allosteric integrase inhibitor potency is determined through the inhibition of HIV-1 particle maturation. *Proc. Natl. Acad. Sci.* **110,** 8690–8695 (2013).
162. Kessl, J. J. *et al.* HIV-1 integrase binds the viral RNA genome and is essential during virion morphogenesis. *Cell* **166,** 1257–1268.e12 (2016).
163. Du, L. *et al.* D77, one benzoic acid derivative, functions as a novel anti-HIV-1 inhibitor targeting the interaction between integrase and cellular LEDGF/p75. *Biochem. Biophys. Res. Commun.* **375,** 139–144 (2008).
164. De Luca, L. *et al.* Pharmacophore-based discovery of small-molecule inhibitors of protein-protein interactions between HIV-1 integrase and cellular cofactor LEDGF/p75. *ChemMedChem* **4,** 1311–1316 (2009).

165. Christ, F. *et al.* Rational design of small-molecule inhibitors of the LEDGF/p75-integrase interaction and HIV replication. *Nat. Chem. Biol.* **6,** 442–448 (2010).
166. Hou, Y. *et al.* Screening for antiviral inhibitors of the HIV integrase-LEDGF/p75 interaction using the AlphaScreen luminescent proximity assay. *J. Biomol. Screen.* **13,** 406–414 (2008).
167. Le Rouzic, E. *et al.* Dual inhibition of HIV-1 replication by integrase-LEDGF allosteric inhibitors is predominant at the post-integration stage. *Retrovirology* **10,** 144 (2013).
168. Christ, F. *et al.* Small-molecule inhibitors of the LEDGF/p75 binding site of integrase block HIV replication and modulate integrase multimerization. *Antimicrob. Agents Chemother.* **56,** 4365–4374 (2012).
169. Feng, L. *et al.* The A128T resistance mutation reveals aberrant protein multimerization as the primary mechanism of action of allosteric HIV-1 integrase inhibitors. *J. Biol. Chem.* **288,** 15813–15820 (2013).
170. Tsiang, M. *et al.* New class of HIV-1 integrase (IN) inhibitors with a dual mode of action. *J. Biol. Chem.* **287,** 21189–21203 (2012).
171. Slaughter, A. *et al.* The mechanism of H171T resistance reveals the importance of N δ-protonated His171 for the binding of allosteric inhibitor BI-D to HIV-1 integrase. *Retrovirology* **11,** 100 (2014).
172. Gupta, K. *et al.* Structural basis for inhibitor-induced aggregation of hiv integrase. *PLoS Biol.* **14,** e1002584 (2016).
173. Pollard, V. W. & Malim, M. H. The HIV-1 rev protein. *Annu. Rev. Microbiol.* **52,** 491–532 (1998).
174. Rosenbluh, J. *et al.* Interaction between HIV-1 Rev and integrase proteins: A basis for the development of anti-hiv peptides. *J. Biol. Chem.* **282,** 15743–15753 (2007).
175. Benyamini, H., Loyter, A. & Friedler, A. A structural model of the HIV-1 Rev-integrase complex: The molecular basis of integrase regulation by Rev. *Biochem. Biophys. Res. Commun.* **416,** 252–257 (2011).
176. Levin, A. *et al.* Peptides Derived from HIV-1 integrase that bind rev stimulate viral genome integration. *PLoS ONE* **4,** e4155 (2009).
177. Levin, A., Rosenbluh, J., Hayouka, Z., Friedler, A. & Loyter, A. Integration of HIV-1 DNA is regulated by interplay between viral rev and cellular LEDGF/p75 proteins. *Mol. Med.* **16,** 34 (2010).

178. Grewe, B. & Uberla, K. The human immunodeficiency virus type 1 Rev protein: menage a trois during the early phase of the lentiviral replication cycle. *J. Gen. Virol.* **91,** 1893–1897 (2010).
179. Mphahlele, M. K. In vitro selection and characterisation of human immunodeficiency virus type-1 subtype C integrase strand transfer inhibitor resistant mutants. (Faculty of Health Sciences, University of the Witwatersrand, 2015).
180. Margot, N. A. *et al.* In vitro resistance selections using elvitegravir, raltegravir, and two metabolites of elvitegravir M1 and M4. *Antiviral Res.* **93,** 288–296 (2012).
181. Connell, B. J. In vitro selection of CD4-independent HIV-1 subtype C: relevance for HIV pathogenesis and therapeutic intervention. (2008).
182. Ramakrishnan, R. *et al.* Evaluations of HIV type 1 rev gene diversity and functional domains following perinatal transmission. *AIDS Res. Hum. Retroviruses* **21,** 1035–1045 (2005).
183. Fish, M. Q. Development of an HIV-1 integrase enzyme strand transfer assay. (2011).
184. Beaudet, L. *et al.* AlphaLISA immunoassays: the no-wash alternative to ELISAs for research and drug discovery. *Nat. Methods* **5,** (2008).
185. Alegria-Schaffer, A. General protein-protein cross-linking. *Methods Enzymol.* **539,** 81–87 (2014).
186. Lorber, B., Fischer, F., Bailly, M., Roy, H. & Kern, D. Protein analysis by dynamic light scattering: Methods and techniques for students. *Biochem. Mol. Biol. Educ.* **40,** 372–382 (2012).
187. Kessl, J. J., Sharma, A. & Kvaratskhelia, M. Methods for the analyses of inhibitor-induced aberrant multimerization of HIV-1 integrase. in *HIV Protocols* (eds. Prasad, V. R. & Kalpana, G. V.) **1354,** 149–164 (Springer New York, 2016).
188. Davey, N. E. *et al.* The HIV mutation browser: a resource for human immunodeficiency virus mutagenesis and polymorphism data. *PLOS Comput. Biol.* **10,** e1003951 (2014).
189. Feng, L. *et al.* The competitive interplay between allostreic integrase inhibitors HIV‐1 integrase inhibitor BI/D and LEDGF/p75 during the early stage of HIV‐1 replication adversely affects inhibitor potency. *Am. Chem. Soc.* **11,** 1313–1321 (2016).
190. Harrison, A. Identification and evaluation of inhibitors targeting the HIV-1 integrase-LEDGF/p75 interaction. (University of the Witwatersrand, 2014).
191. Dimonte, S., Babakir-Mina, M., Aquaro, S. & Perno, C.-F. Natural polymorphisms of HIV-1 subtype-C integrase coding region in a large group of ARV-naïve infected individuals. *Infection* **41,** 1097–1102 (2013).

192. Engelman, A., Kessl, J. J. & Kvaratskhelia, M. Allosteric inhibition of HIV-1 integrase activity. *Curr. Opin. Chem. Biol.* **17,** 339–345 (2013).
193. Fontana, J. *et al.* Distribution and redistribution of HIV-1 nucleocapsid protein in immature, mature, and integrase-inhibited virions: a role for integrase in maturation. *J. Virol.* **89,** 9765–9780 (2015).
194. Zheng, Y., Ao, Z., Jayappa, K. D. & Yao, X. Characterization of the HIV-1 integrase chromatin- and LEDGF/p75-binding abilities by mutagenic analysis within the catalytic core domain of integrase. *Virol. J.* **7,** 68 (2010).
195. Bouyac-Bertoia, M. *et al.* HIV-1 infection requires a functional integrase NLS. *Mol. Cell* **7,** 1025–1035 (2001).
196. Kessl, J. J. *et al.* Multimode, cooperative mechanism of action of allosteric hiv-1 integrase inhibitors. *J. Biol. Chem.* **287,** 16801–16811 (2012).
197. Gabizon, R. *et al.* Structure–activity relationship studies using peptide arrays: the example of HIV-1 Rev–integrase interaction. *Med Chem Commun* **4,** 252–259 (2013).
198. Esser, P. Principles in adsorption to polystyrene. *Thermo Sci. Nunc Bull.* 1–5 (1988).
199. Kyte, J. & Doolittle, R. F. A simple method for displaying the hydropathic character of a protein. *J. Mol. Biol.* **157,** 105–132 (1982).
200. Shkriabai, N. *et al.* A critical role of the C-terminal segment for allosteric inhibitor-induced aberrant multimerization of HIV-1 integrase. *J. Biol. Chem.* **289,** 26430–26440 (2014).
201. Jenkins, T. M., Engelman, A., Ghirlando, R. & Craigie, R. A soluble active mutant of HIV-1 integrase: involvement of both the core and carboxyl-terminal domains in multimerization. *J. Biol. Chem.* **271,** 7712–7718 (1996).
202. Levin, A. *et al.* A novel role for the viral Rev protein in promoting resistance to superinfection by human immunodeficiency virus type 1. *J. Gen. Virol.* **91,** 1503–1513 (2010).
203. Principles of Fluorescence Spectroscopy | Joseph R. Lakowicz | Springer. Available at: http://www.springer.com/la/book/9780387312781. (Accessed: 1st November 2017)

Human Research Ethics Committee (Medical) 50 years 1966 – 2016

Research Office Secretariat: Faculty of Health Sciences, Phillip Tobias Building, 3rd Floor, Office 3U1, 29 Princess of Wales Terrace, Parktown, 2193 Tel: +27 (0)11-717-1252/1234/2656/2705
Private Bag 3, Wits 2050, email: zanele.ndlovu@wits.ac.za
Office email: hrec-medical.researchoffice@wits.ac.za
Website: www.wits.ac.za/research/about-our-research/ethics-and-research-integrity/

Ref: W-CJ-170606-3 06/06/2017

TO WHOM IT MAY CONCERN:

Waiver: This certifies that the following research does not require clearance from the Human Research Ethics Committee (Medical).

Investigator: Ms Shaakira Abrahams (student no. 500916).

Project title: The role of HIV-1 Rev during allosteric inhibition of integrase.

Reason: This laboratory study entails the expression and purification of recombinant HIV-1 proteins integrase and Rev as well as LEDGF/p75 for use in direct biochemical inhibitory enzyme assays. There are no human participants.

Professor Peter Cleaton-Jones

Chair: Human Research Ethics Committee (Medical)

UNIVERSITY OF THE WITWATERSRAND
PROF PE CLEATON-JONES
HREC (MEDICAL)
2017 -06- 06
JOHANNESBURG

Copy – HREC (Medical) Secretariat: Zanele Ndlovu, Rhulani Mkansi, Lebo Moeng.